



Senior Design Project

Rocket Launched Aircraft

AE4790 Fall 2023

Group 12-23-05

**Jack Friedle
Matthew Guscar
Alexander Jarrett**

Acknowledgement

We are deeply grateful to Dr. Kepsong Ro, our senior design team mentor, for his invaluable guidance and support throughout this project. His mentorship played a pivotal role in helping us realize the project's full potential. Our sincere gratitude extends to Alex Foradori, whose 3D printing expertise and dedication to printer optimization were instrumental in achieving the highest quality parts. Finally we would like to thank Scott Guscar for his use of tools and assistance in the aircrafts assembly.

Disclaimer

This project report was written by students at Western Michigan University to fulfill an engineering curriculum requirement. Western Michigan University makes no representation that the material contained in this report is error-free or complete in all respects. Persons or organizations who choose to use this material do so at their own risk.



Abstract

Long range aerial surveillance has become increasingly important in the past few years especially with recent conflicts around the globe. An in-depth analysis was conducted to assess the advantages between traditional quadcopters and a rocket launched remotely controlled aircraft equipped with data-collecting systems, such as cameras and environmental sensors. Safety, financial viability, and logistical considerations took precedence in this assessment. Combining the vertical launch capabilities of a rocket with the versatility of remotely controlled flight has the potential to transform the aerospace domain, opening avenues for applications in surveillance, research, and defense. This evaluation serves as a blueprint for the development and manufacturing of a rocket-launched, remote-controlled aircraft.



Table of Contents

Acknowledgement.....	2
Disclaimer.....	3
Abstract.....	4
Table of Contents.....	5
List of Figures.....	8
List of Tables.....	10
Background.....	11
Design Requirements Overview.....	11
1. Rocket Launch Specifications.....	11
2. Glider Design Constraints.....	12
3. Deployment Dynamics.....	12
4. Data Gathering Objectives.....	12
5. Autonomous Flight Capabilities.....	13
Benchmarking.....	13
Conclusion.....	14
Milestone Chart.....	15
ROCKET DESIGN.....	16
1. Conceptual Design.....	16
1.1. Rocket Goals.....	16
1.2. General Requirements.....	17
1.3. Rocket Requirements.....	18
1.4. Design Configurations Considered.....	18
1.5. Final Conceptual Design.....	23
2. Preliminary Design.....	25
2.1. Design Methodology.....	25
2.2. Rocket Body Sizing.....	25
2.3. Nose Cone Sizing and Design.....	26
2.4. Fin Sizing and Design.....	27
2.5. Internal Components.....	27
2.6. Rocket Motor Decision Process.....	29
3. Detailed Design.....	29
4. Electronic Components.....	31
5. Performance Characteristics.....	31
5.1. Rocket CFD.....	31
5.2. OpenRocket.....	37
5.3. MATLAB Calculations.....	39
6. Manufacturing Plan.....	41



6.1. Materials Considered.....	41
6.2. Material Analysis.....	42
6.3. Process Selection.....	43
6.4. Component Manufacturing.....	43
6.5. Cost Breakdown.....	51
6.6. Milestone Chart.....	52
7. Testing Plan.....	52
7.1. Testing Objectives.....	52
7.2. Testing Schedule.....	53
AIRCRAFT DESIGN.....	54
1. Conceptual Design.....	54
1.1. Aircraft goals.....	54
1.2. General Requirements.....	54
1.3. Aircraft Requirements.....	55
1.4. Configurations Considered, Concept Weighting , and Selection Process.....	55
1.5. Final Conceptual Design.....	59
2. Preliminary Design.....	61
2.1. Design Methodology.....	61
2.2. Fuselage Sizing.....	62
2.3. Wing Design and Sizing.....	64
2.4. Tail Design and Sizing.....	65
2.5. Control surface sizing.....	66
2.6. Airfoil Selection.....	66
3. Detailed Design.....	70
3.1. Dimensional Parameters.....	70
3.2. Drawing Package.....	70
4. Electronic Components.....	75
4.1. Video Transmission.....	75
4.2. Pixhawk.....	78
4.3. Digital Spectrum Modulation Transmitter and Receiver.....	78
4.4. Glider Data Gathering Components.....	79
5. Performance Characteristics.....	81
5.1. Stability Analysis.....	81
5.2. Estimated drag.....	84
5.3. Turn Radius.....	85
5.4. Stall speed.....	86
6. Manufacturing Plan.....	87
6.1. Materials Considered.....	87



6.2. Material Analysis.....	88
6.3. Process selection.....	89
6.4. Component Manufacturing Process.....	89
6.5. Cost Breakdown.....	91
6.6. Milestone Chart.....	92
7. Testing Plan.....	93
7.1. Testing Objectives.....	93
7.2. Testing Schedule.....	93
7.3. Propulsion Testing.....	94
7.4. Spring Testing.....	96
7.5. Structural Testing.....	98
7.6. Video Transmission Testing.....	99
7.7. Arduino Testing.....	100
7.8. Flight Testing.....	102
Results.....	103
Conclusions.....	104
References.....	105
Appendix.....	105
Appendix A: MATLAB Code To Calculate Launch.....	106
Appendix B: Aircraft Assembly Photos.....	109
Appendix C: Aircraft Stability Derivatives With Rudder Deflection of 3 Degrees.....	112
Appendix D: Rocket Assembly.....	116
Appendix E: Openrocket Charts and CFD Images.....	121
Appendix F: Data Gathering Arduino Code.....	125
Appendix G: MATLAB Code for Glider Ejection.....	127
Appendix PUT HERE:Resumes.....	130



List of Figures

Figure (A): Comparison between a cluster motor and singular motor.....	19
Figure (B): Rectangular rocket fin.....	20
Figure (C): Swept rocket fins.....	20
Figure (D): Tapered swept rocket fins.....	20
Figure (E): Clipped delta rocket fins.....	21
Figure (F): Trapezoidal fins.....	21
Figure (G): Elliptical rocket fins.....	21
Figure (AP): Final rocket conceptual design.....	24
Figure (H): Planar CFD main rocket project image.....	33
Figure (I): Trace CFD main rocket project.....	34
Figure (J): Rectangular fin planar CFD.....	35
Figure (K): Rectangular fin trace CFD.....	35
Figure (L): Parabolic nose cone planar CFD.....	36
Figure (M): Parabolic nose cone trace CFD.....	36
Figure (N): OpenRocket model.....	37
Figure (AQ): OpenRocket simulation.....	38
Figure (O): Plate Design.....	44
Figure (AR): Motor guide design.....	44
Figure (P): Nose cone design.....	45
Figure (AS): Nose cone shoulder design.....	46
Figure (Q): Rocket body tubes.....	47
Figure (R): Nose cone, plates, motor guides, and shoulder results.....	48
Figure (S): Fin manufacturing and assembly.....	49
Figure (T): Final rocket build.....	50
Figure (U): Aircraft conceptual sketch side view.....	59
Figure (V): Aircraft conceptual sketch top view.....	60
Figure (W): Aircraft design process.....	61
Figure (X): Fuselage cross section shapes.....	62
Figure (Y): Front cross sectional view.....	63
Figure (Z): Side cross sectional view.....	63
Figure (AA): Main wing section.....	64
Figure (AB): Coefficient of moment vs coefficient of lift.....	67
Figure (AC): Coefficient of lift/ coefficient of drag vs coefficient of moment.....	68
Figure (AD): Coefficient of moment vs angle of attack.....	69
Figure (AE): Video transmission wiring diagram.....	77
Figure (AQ): Data Gathering Wiring Diagram.....	80
Figure (AF): Coefficient of moment vs alpha graph.....	81



Figure (AG): Longitudinal root locus plot.....	83
Figure (AH): Lateral root locus plot.....	84
Figure (AI): Testing Process.....	93
Figure (AJ): ecalc thrust data.....	95
Figure (AK): Thrust testing setup.....	96
Figure (AL): Main wing drag force vs coefficient of moment.....	97
Figure (AM): Spring testing.....	98
Figure (AN): Carbon fiber spar testing.....	99
Figure (AO): Camera field of view.....	100
Figure (AP).....	103



List of Tables

Table 1: Rocket General Requirements.....	17
Table 2: Rocket Requirements.....	18
Table 3: Rocket motor FOM.....	19
Table 4: Rocket Fin FOM.....	22
Table 5: OpenRocket simulation data.....	38
Table 6: MATLAB Code Graphs.....	41
Table 7: Rocket costs.....	51
Table 8: Rocket construction milestone chart.....	52
Table 9: FAA rules for recreational flyers.....	54
Table 10: Aircraft Requirements.....	55
Table 11: Wing position FOM.....	56
Table 12: Tail configuration FOM.....	57
Table 13: Required aircraft tail area.....	65
Table 14: Required coefficient of lift.....	66
Table 15: Wing configurations with airfoils.....	69
Table 16: Aircraft wing dimensions.....	70
Table 17: RunCam 2 specifications.....	75
Table 18: Video transmitter specifications.....	76
Table 19: Video receiver specifications.....	76
Table 20: Video frequency chart.....	77
Table 21: Pixhawk Sensors.....	78
Table 22: Material Selection Figure of Merit.....	89
Table 23: Aircraft cost breakdown.....	91
Table 24: Aircraft construction milestone chart.....	92
Table 25: Aircraft testing milestone chart.....	93
Table 26: Thrust data.....	96

Background

The senior design project at Western Michigan University aims to develop a novel aerospace prototype that merges the dynamics of rocketry with the finesse of gliding. Traditionally, the university's rocketry projects have involved launching rockets to significant altitudes with payloads designed for controlled descent. Building on these experiences, the current project intends to create a rocket that launches to an altitude of 400 feet and then deploys an autonomous glider.

The project is motivated by the educational objective to give students hands-on experience in designing, building, and testing complex aerospace systems within the limitations of academic environments and regulatory frameworks. It operates within the practical constraints imposed by funding, the certification limits with the National Association of Rocketry (NAR), and the Federal Aviation Administration (FAA) regulations.

The project challenges include accommodating the glider within the spatial confines of the rocket, ensuring reliable deployment at the correct altitude, and achieving autonomous flight to a predetermined location. The scope encompasses rigorous design and simulation, innovative manufacturing, and comprehensive testing to validate the design under real-world conditions.

Ultimately, the project's success will be measured not only by its academic merits but also by its potential applicability in various fields, including environmental monitoring and data collection, where the combined capabilities of a rocket and glider could offer substantial benefits.

Design Requirements Overview

1. Rocket Launch Specifications

The rocket component of the project is tasked with a critical initial operation – achieving a minimum altitude of 400 feet. This launch altitude serves as a baseline for the mission, ensuring that the glider is sufficiently aloft to initiate its autonomous flight sequence. To meet this requirement, the rocket must be designed with an appropriate propulsion system, aerodynamic stability, and structural integrity to withstand the stresses of rapid ascent. It should also incorporate a reliable ignition and launch tracking system, ensuring that it follows a predictable trajectory to the specified altitude.



2. Glider Design Constraints

The design of the glider must adhere to strict spatial constraints to ensure it fits within the rocket's fuselage. This requirement necessitates a compact and efficient structure for the glider, with an emphasis on collapsible or foldable components, especially the wings and tail sections. The design must optimize the internal volume of the rocket tube, allowing for the stowage and securement of the glider without compromising its aerodynamic profile or the deployment mechanism. Materials chosen for the glider should balance lightness with strength, and the design should accommodate the necessary sensors and control systems without excessive spatial demands. Careful attention must be given to the design of the deployment system, ensuring that it can smoothly transition the glider from its contained state to full flight configuration before it reaches 300 feet. This aspect of the design is essential for a successful transition from rocket ascent to the glider's autonomous flight phase.

3. Deployment Dynamics

The deployment mechanism of the glider is critically pivotal to the mission's success. This system must be engineered to ensure a reliable deployment sequence, commencing the glider's transition to flight before the rocket descends below 300 feet. The intricacies of the deployment involve a sequence of carefully timed events: the triggering of the mechanism, the unfurling or unfolding of the glider components, and the stabilization of the glider's flight path post-deployment. The system must be robust to withstand the forces experienced during rocket ascent and agile enough to deploy without malfunction. Given the rapid decrease in altitude post-apogee, the deployment system must actuate within a narrow time frame, necessitating a design that is both sensitive to altitude cues and resilient to the physical stresses of high-speed flight. Moreover, the design should minimize the risk of entanglement or interference with the rocket structure upon deployment, ensuring that the glider can enter its glide phase with unimpeded control surfaces and aerodynamic integrity.

4. Data Gathering Objectives

The design must incorporate a comprehensive suite of data gathering instruments to measure the critical aspects of the mission. A high priority is placed on the accurate capture of g-forces experienced during the launch, which involves the rocket's rapid ascent phase, the subsequent glider deployment, the stabilized glide phase, and the final landing sequence. These measurements are essential for assessing the structural and operational integrity of both rocket and glider under dynamic flight conditions. Collecting all this data will help determine the viability of putting an aircraft inside a rocket.

In addition to acceleration data, atmospheric pressure readings are required to determine altitude and to monitor the glider's vertical trajectory during descent. Atmospheric temperature data is also crucial, as it can significantly alter air density and, consequently, the

glider's performance. These environmental metrics are vital for calibrating flight control systems to the changing conditions and validating predictive models of the glider's behavior.

The autonomy of the glider's flight poses another layer of data gathering needs. The system must not only navigate a predetermined flight path but also respond to real-time environmental data to reach the targeted landing area accurately. Therefore, data gathering will extend beyond physical sensors to include navigational data, which will inform the autonomous flight control system, ensuring the glider can execute its mission with precision and adapt to unforeseen aerial phenomena or operational anomalies.

5. Autonomous Flight Capabilities

For the autonomous flight capabilities, the glider design must integrate a flight control system capable of executing a predefined flight pattern and navigating towards a set destination without human intervention. The system should utilize a combination of onboard sensors, pre-flight programming, and possibly real-time communication with ground control to adapt its flight path to the changing conditions of the atmosphere and the physical dynamics of the glider's airframe.

This flight control system must include an algorithm for dynamic stabilization, a GPS module for location tracking, and a data logging feature to record the flight path and conditions. It will rely on inputs from the atmospheric pressure and temperature sensors for altitude and weather condition adjustments, as well as an accelerometer to monitor and manage the glider's orientation and acceleration.

To ensure successful autonomous operation, the glider should be capable of conducting self-checks prior to deployment and must have fail-safe protocols to handle a range of contingencies, such as communication loss or sensor malfunctions. The software driving autonomous flight should also be tested and verified to handle the tasks of waypoint navigation, obstacle avoidance, and controlled descent for landing. In addition, the system must adhere to FAA regulations for unmanned vehicles, both in terms of the software's operational capabilities and the communication protocols used during flight.

Benchmarking

In this section, we conduct a thorough benchmarking analysis to evaluate the performance and applicability of our rocket-launched aircraft. By comparing our design with prevalent data-gathering devices, we aim to understand its relative strengths, weaknesses, and potential market positioning. These devices include quadcopters, weather balloons, the Switchblade drone, and other similar technologies.



Quadcopters: Quadcopters are popular for various applications, including data gathering, due to their ease of use, maneuverability, and relatively low cost. When benchmarking against quadcopters, we will consider factors such as flight time, range, stability, and payload capacity. Comparing our design with quadcopters will help us understand how our rocket-launched glider performs in terms of mobility, ease of use, and overall data-gathering capabilities.

Weather Balloons: Weather balloons are commonly used for atmospheric data collection and have the advantage of being relatively inexpensive and easy to deploy. However, they lack maneuverability and are subject to wind conditions. When benchmarking against weather balloons, we will focus on factors such as altitude achieved, duration of data collection, and the accuracy and resolution of the gathered data. This comparison will help us evaluate the advantages and limitations of our rocket-launched glider as an alternative to traditional weather balloons.

Switchblade Drone: The Switchblade drone is a small, tactical aerial vehicle designed for reconnaissance and surveillance. It has the advantage of being highly portable and can be launched from a variety of platforms. When benchmarking against the Switchblade drone, we will consider factors such as range, endurance, payload capacity, and the ability to operate in various environments. Comparing our design with the Switchblade drone will help us understand how our rocket-launched glider performs in terms of versatility, deployability, and data-gathering capabilities.

Other data gathering devices: We will also benchmark our rocket-launched glider against other data-gathering devices, such as fixed-wing drones, high-altitude platforms, and satellite systems. This will provide a comprehensive view of the competitive landscape and help us identify the unique selling points of our design.

Conclusion

The benchmarking process has provided valuable insights into the competitive landscape of data-gathering devices. Our rocket-launched glider showcases distinctive attributes in terms of deployment altitude, flight dynamics, and payload versatility. These findings not only affirm the unique value proposition of our design but also guide potential future enhancements and market opportunities.



ROCKET DESIGN

1. Conceptual Design

In the conceptual design phase of the rocket project, we meticulously evaluated the project goals and transformed them into specific design parameters, including the development of a figure of merit table to assess various solutions. This analysis led to the finalization of the

Device	Range (km)	Endurance (Hours)	Payload Capacity	Max Altitude	Deployability	Data Collection Capabilities	Mobility	Cost
Rocket-launched Glider	1-10	0.1-0.5	TBD	750	High	Imagery, video, and sensor data, Atmospheric data, temperature, etc.	High	TBD
Switchblade Drone	10-100	0.5-1	0.5-1	3000	High	Imagery, video, and sensor data	High	High
Weather Balloon	N/A	1-2	1-2	30,000	Low	Atmospheric data, temperature, etc.	Low	Low
Quadcopter	0.5-5	0.1-0.5	0.5-2	500	High	Imagery, video, and sensor data	High	Low
Fixed-Wing Drones	50-200	0.5-1	1-5	5,000	Moderate	Imagery, video, and sensor data	High	High
High-altitude Platforms	N/A	10-100	10-100	20,000	Low	Telecommunication, imagery, video	Low	High
Satellite Systems	N/A	Years	10-500	>100,000	Extremely Low	Imagery, video, and sensor data	Fixed	Very High

most efficient rocket configuration, known as D3, which is designed to reach an altitude of 400 feet and features a lightweight structure with adequate space for a glider, sensors, and a battery. This design ensures retrievability and complies with regulations to prevent classification as a missile, adheres to rocket motor legality, and is adaptable to launch location and weather conditions. A notable element of the design is the use of trapezoidal fins, chosen for their stability and control benefits, which complement the single-unit design incorporating smaller rocket motors in the nose cone for efficient nose cone ejection and safe deployment of both the glider and a parachute, ensuring a controlled descent and effective heat mitigation.



1.1. Rocket Goals

The primary objectives for the rocket design were centered around achieving a balance of performance, safety, and regulatory compliance. These goals guided the entire design and development process, ensuring that the final product would not only meet but exceed the expectations set forth at the project's inception. The following are the key goals for the rocket:

1. **Reach 400 ft Altitude:** The rocket is engineered to achieve a minimum altitude of 400 feet, a benchmark that tests the limits of its propulsion and aerodynamic capabilities while staying within the safety and regulatory boundaries.
2. **Lightweight Design:** Emphasis was placed on minimizing the overall weight of the rocket. A lighter structure improves the efficiency of the rocket, enhancing its altitude capabilities and reducing the load on the propulsion system.
3. **Accommodation for Glider:** The rocket must have a dedicated and secure compartment for housing a glider. This requirement is crucial for the dual functionality of the project, where the rocket serves as a launch vehicle for the glider.
4. **Inclusion of Sensors and Battery:** The design allocates space for essential sensors (such as temperature, barometer, accelerometer, and gyroscope) and a battery. These components are vital for gathering data during the flight and powering the necessary electronics.
5. **Retrievability:** A key goal is to ensure that the rocket can be retrieved post-launch. This involves the successful deployment of a parachute system and maintaining the structural integrity of the rocket upon landing, making it reusable for subsequent launches.
6. **Regulatory Compliance:** The rocket must adhere to all relevant regulations, ensuring it is not classified as a missile. This includes compliance with rocket motor legality, adherence to launch location protocols, and consideration of weather conditions during launch.
7. **Heat Mitigation:** Given the high temperatures experienced during launch and flight, the design incorporates methods to mitigate heat, ensuring the protection of both the rocket's structure and the onboard glider.

These goals collectively define the scope and direction of the rocket project, laying a solid foundation for the subsequent phases of design, development, and testing. Each goal is interlinked, contributing to the overall success and functionality of the rocket.

1.2. General Requirements

General rocket requirements are made from a combination of glider limitations and basic model rocketry safety along with Michigan and Federal law. A summary of this can be found below in table 1.



Rocket General Requirements	
Glider Limitations	Fly at a maximum of 400 feet
	Must be able to eject glider at apogee
Law	Must have no secondary directional control other than stationary fins
	Must have a person of level 2 certification at launch
	Do not interfere with other aircraft

Table 1: Rocket General Requirements

The level two certification requirement comes from the choice of rocket motors. The K class rocket motor being used requires a level 2 model rocketry certification. The rocket motor bundling was done to make this certification level as low as possible as if a single motor was used it is very likely that a level 4 certification would be required.

1.3. Rocket Requirements

Since our project was not sponsored, aircraft requirements were set by our design team and faculty mentor. A summary of these requirements can be found in table 2 below.

Rocket Requirements	
General	The rocket should resemble basic model rockets
Sizing	The rocket must be able to house the glider along with sensors needed to collect data on the rocket's flight
Flight Path	Maintain a constant upward flight path up until the apogee
Propulsion	Motor must be commercially available
	Preferably under M class
	Preferably Cluster Motors
Electronics	Must be able to record pressure
	Must be able to record temperature by the motors
	Must be able to detect Gs and gyroscopic position
Launch	Must be able to launch from a stand with remote launch



Table 2: Rocket Requirements

1.4. Design Configurations Considered

The following section outlines configurations considered for the rocket design. Glider ejection methods, fin shape, nose cone shape, and motor configuration are discussed. To evaluate each of these concepts, and identify the optimal rocket configuration, a figure of merit analysis was conducted.

Motor Configuration

For motor configuration there are two options being a singular motor and a cluster configuration. With a singular motor, it makes for an easier buy and an easier housing in the lower portion of the rocket. A singular motor also makes it easier to maintain a stable flight. Using a single motor is rather simple as only a single igniter is needed and it leaves more space in the motor housing portion of the rocket.

Motor clustering is the use of more than one motor fired at the same time. Clustering adds together thrust level which in turn increases the lifting power of all the motors used. Clustering rocket motors are a good choice for heavy lifting or for rockets that are larger which can be considered when motors above F or G class motors are used. For the most part any rocket motor can be used for clustering. Due to the increase in thrust, rocket motors that have longer burn times will benefit from clustering. Three and four motor clusters are the most commonly implemented. Clusters greater than four tend to not be used as ignition reliability goes down so it is best to stick to four. In terms of ignition, the better the igniters and the increase in power supply, the more reliable the cluster will be. The cluster is arranged in a way to keep the center of thrust as close to the centerline as possible to limit asymmetric thrust in the unlikely event a motor does not ignite. A comparison of cluster and singular motors is shown in the figure below.



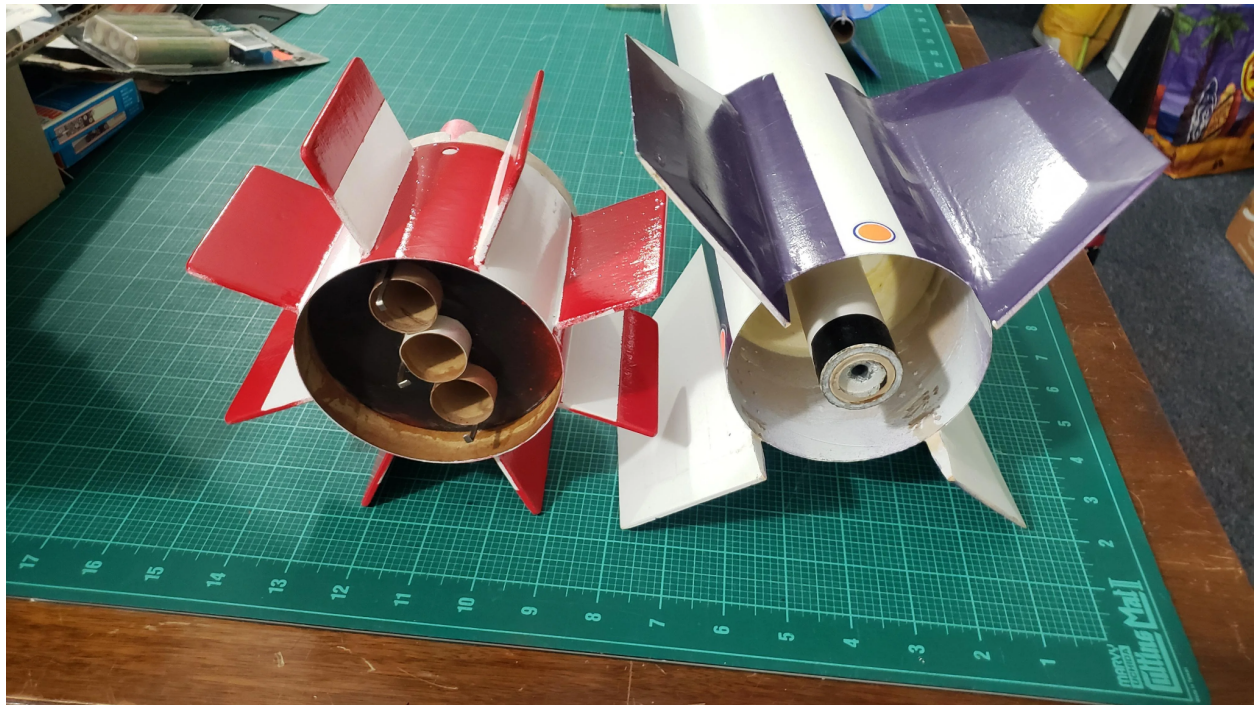


Figure (A): Comparison between a cluster motor and singular motor

All of this information was compiled into table 3 below. From the table it was clear the Clustering of the motors was the best option for the design as it had the highest score.

Figure of Merit	Factor	Singular	Cluster
Lift	0.3	3	5
Stability	0.2	4	3
Availability	0.4	3	4
cost	0.1	2	2
Total	1	3.1	3.9

Table 3: Rocket motor FOM

Fin Shape



There are six major rocket fin types to consider. The types to consider are rectangular, swept, tapered swept, clipped delta, trapezoidal, and elliptical. Each fin has their own advantages as well as disadvantages. Below each type will be discussed and a figure of merit will be done to decide which fin type is best to use for the rocket.

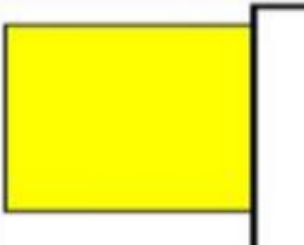


Figure (B): Rectangular rocket fin

Rectangular fins main positive attribute is that they are extremely easy to manufacture. The downside is that they are the least aerodynamic fin out of all six. With the rocket's flight path needing to be maintained and kept constant, it makes rectangular fins possibly the worst of the choices.

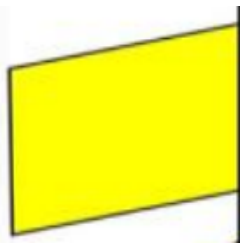


Figure (C): Swept rocket fins

Swept fins are still quite easy to manufacture. The aerodynamics of the swept fins are also slightly better than the rectangular fins as the sweep makes it so the air flow around the fin isn't so abruptly changed.

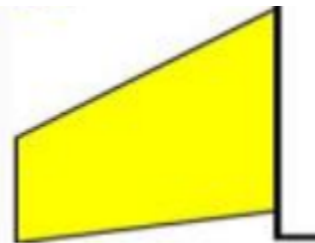


Figure (D): Tapered swept rocket fins

Tapered swept fins move the center of pressure back which makes them a good choice for rockets whose main goal is top speed. The aerodynamics of this fin are slightly better than the regular swept rocket wins.

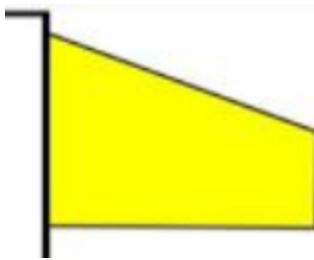


Figure (E): Clipped delta rocket fins

Clipped delta rocket fins have very good aerodynamics and are easier to manufacture compared to swept and tapered swept rocket fins. Clipped delta fins are generally used on low-drag rockets with high performance.

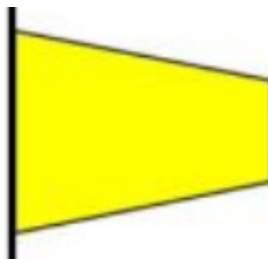


Figure (F): Trapezoidal fins

Trapezoidal rocket fins have very good aerodynamics and are still rather easy to manufacture. The fin moves the center of pressure forward and for rockets carrying payloads this helps keep it behind the center mass.

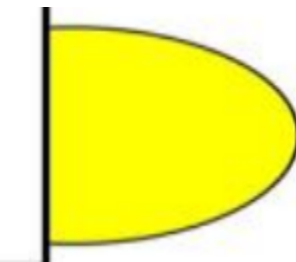


Figure (G): Elliptical rocket fins

Elliptical fins have the best aerodynamics out of all the rocket fins. The main drawback to these fins is that they are the hardest to manufacture and are rather uncommon in use.

All of this information was compiled into table 4 below. From the table it was clear the trapezoidal rocket fins were the best option for the design as it had the highest score.

Figure of Merit	Factor	Rectangular	Swept	Tapered Swept	Clipped Delta	Trapezoidal	Elliptical
Manufacturing	0.5	5	3	2	4	4	1
Aerodynamics	0.3	1	2	4	3	4	5
Relation to Build	0.2	2	4	3	4	5	2
Total	1	2.2	2.9	2.8	3.7	4.2	2.4

Table 4: Rocket Fin FOM

Nose Cone Shape

There are three main types of model rocket nose cones being conical, ogive, and parabolic. Conical nose cones are best for rockets that approach transonic or supersonic speeds which is not a speed the rocket being built can realistically accomplish making this design a bad option. Ogive and parabolic nose cones are both generally used in larger model rockets and the ogive shape is easier to design and manufacture when compared to parabolic. So with that being said, an ogive nose cone seems to be the best option for the build of this rocket.

Glider Ejection Method

There are three methods for the glider ejection that have been created for this project being the multiple ejection charge, spring loaded ejection, and nose cone ejection method. The methods are discussed below with the nose cone ejection method being presented last as it is the final choice in the design.

The multiple ejection charge method essentially puts separation charges between the motor body and top body as well as between the top body and nose cone. There are shock cords attached to all bodies. The hope was, after the motors and nose cone were ejected there would be enough movement where the glider would eject itself from the top body without any physical ejection acting on the glider. The main issue with this is there is no way to accurately predict if the glider would actually have enough movement of the rocket bodies around it to effectively launch it. There is also the problem of complexity of having multiple ejection charges being executed within the rocket simultaneously. The worst drawback is the release of the parachute as with this method there is no good spot for the parachute that doesn't have it clash with the glider. Overall as this is the first method it happens to be the worst but it is not a bad start.



The spring loaded ejection method has the goal of keeping the rocket together with no separations between any parts of the rocket. This is accomplished by having the nose cone being designed to split down the middle by being pulled by electric motors lower in the rocket. The nose cone will stay closed during flight by having hinges that are spring loaded in the direction needed to keep it shut. After the nose cone is opened, a spring below the glider would release and eject the glider as well as the parachute which is stationed below the glider. This is a great method but, it has a major drawback of complexity and reliance on a lot of moving parts that have to be small and lightweight. Finding a spring with the required force to launch the drone and parachute as well as being lightweight was just not possible. This method is much better than the prior method but still not feasible for the rocket goals needed to be met.

The final method is the nose cone ejection method. This method only has the nose cone separate from the main rocket, keeping the lower and upper bodies of the rocket together. For this method the glider and parachute will rest on a plate at the bottom of the upper body of the rocket. This plate will have a cord attached to it which attaches to the nose cone. The nose cone will have multiple small C or D class rocket motors within it to ignite and launch the nose cone off the rocket while pulling the plate that the glider and parachute rest on. This will allow the glider to be ejected along with the parachute. This is a single action making the only hurdle being the ignition timing on the motors in the nose cone which can easily be done with a timer.

1.5. Final Conceptual Design

For the final conceptual design, a combination of the best design configurations discussed above were used. For the glider ejection, the nose cone ejection method was used. An ogive nose cone and trapezoidal fins were decided to be the best options to keep the rocket aerodynamically stable and ensure a constant flight path. As for the rocket motor configuration, the cluster method was chosen as it provides the greatest amount of thrust as well as keeping the certification level needed for the motors the lowest possible. A conception sketch is shown below to give the general idea of where the rocket's final design will end up.



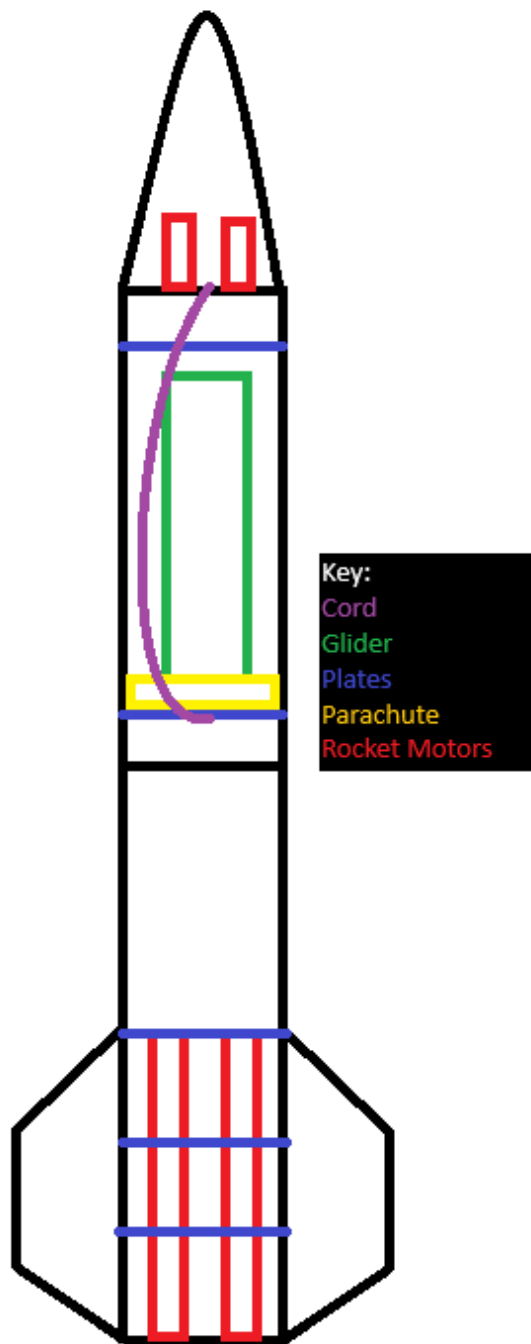


Figure (AP): Final rocket conceptual design

2. Preliminary Design

2.1. Rocket Body Sizing

The sizing of the rocket body is a crucial aspect of our design, significantly influencing the rocket's overall performance, stability, and its capacity to house essential components. To determine the optimal size, we considered a range of factors, ensuring that each aspect of the rocket's functionality and efficiency was addressed.

A primary consideration in the sizing was to provide enough space for the glider. With the glider planned to have a folded diameter of 5.5 inches, the rocket's internal diameter was set at 6 inches. This additional space not only accommodates the glider but also allows for potential variations in size or additional payloads, ensuring versatility in the rocket's use. The dimensions of the rocket body play a pivotal role in maintaining structural integrity and achieving an optimal weight balance. The chosen diameter had to be large enough to house the necessary components without excessively increasing the rocket's surface area, which could impact its aerodynamic efficiency and add unwanted weight.

Aerodynamic efficiency was a key factor in determining the rocket body's dimensions. The length and diameter were carefully calculated to minimize drag and maintain stability during flight. The aspect ratio, the length-to-diameter ratio, was particularly crucial, as it significantly influences the rocket's aerodynamic properties. The rocket body is divided into two main sections - the upper portion for the glider and the lower portion for the motors and sensors. This division is essential not just for functional purposes but also for ease of assembly and maintenance. Each segment is sized to accommodate its respective components comfortably, ensuring smooth operation and ease of access. The sizing of the rocket body also had to align with other design elements such as the nose cone, fins, and recovery system. Compatibility with these components was essential for maintaining the rocket's structural coherence and functional integrity.

Finally, practical aspects such as manufacturability and transportability were also taken into account. The chosen size needed to be feasible for production methods like 3D printing or molding and convenient for transportation to and from the launch site.

In summary, the decision to set the rocket body's internal diameter at 6 inches was a result of a comprehensive analysis, balancing the need for glider accommodation, structural integrity, aerodynamic efficiency, component segregation, compatibility with other design elements, and practical manufacturing and transportation considerations. This dimension



ensures that the rocket is not only functionally effective but also versatile and manageable in various aspects of its construction and use.

2.2. Nose Cone Sizing and Design

In the development of our rocket, the design and sizing of the nose cone were given significant attention due to their impact on the rocket's aerodynamic properties and overall functionality. The nose cone is a critical component, influencing both the flight dynamics and the internal component accommodation.

We opted for a standard ogive-shaped nose cone, a decision based on its proven aerodynamic benefits. The ogive shape is known for reducing drag and improving the stability of the rocket during flight, which is crucial for achieving the desired altitude and maintaining a predictable trajectory. This shape also contributes to the efficiency of the rocket by smoothing the airflow over the body, thus reducing aerodynamic resistance. The size of the nose cone was another vital consideration. After extensive analysis, we determined that a length of 16 inches provided the best balance between aerodynamic efficiency and internal space requirements. This length was chosen to give the most advantageous curve and point, optimizing the rocket's aerodynamic profile without compromising the space needed for internal components.

For the functional integration of the nose cone with the rest of the rocket, we designed the base of the nose cone with five holes. Four of these are allocated for motor attachment, while the fifth hole is designed for a rope hook, essential for the deployment mechanisms. This design ensures not only a secure attachment of the nose cone to the rocket body but also facilitates the necessary functional aspects like motor ignition and parachute deployment.

The material selection for the nose cone was also a critical decision. We prioritized materials that offered the necessary strength to withstand the forces during launch and flight, while also being lightweight to maintain the overall efficiency of the rocket. Additionally, heat resistance was a key factor, considering the high temperatures experienced during flight, particularly at the nose cone.

In conclusion, the design and sizing of the nose cone were meticulously planned to ensure optimal aerodynamic performance, adequate space for internal components, and compatibility with the rocket's overall design. The 16-inch ogive-shaped nose cone with strategically placed holes for motors and deployment mechanisms represents a harmonious blend of functionality, aerodynamics, and structural integrity, contributing significantly to the rocket's performance capabilities.



2.3. Fin Sizing and Design

The design and sizing of the fins for our rocket project played a crucial role in achieving optimal aerodynamic stability and control during flight. After careful consideration and analysis, trapezoidal fins were chosen due to their efficiency in balancing these factors. The dimensions of the fins were meticulously calculated to ensure they effectively contribute to the rocket's aerodynamic performance while adhering to the overall design constraints.

The fins were designed with a base length of 16 inches, a height of 4 inches, and a top length of 6 inches. These dimensions were not chosen arbitrarily; rather, they were the result of a detailed analysis aimed at optimizing the rocket's stability and control. The base length of 16 inches provides a substantial surface area for generating adequate aerodynamic forces, crucial for stabilizing the rocket during ascent. The height of 4 inches was determined to be optimal for ensuring that the fins would not only be effective in controlling the rocket's trajectory but also fit within the structural and spatial confines of the design. Lastly, the top length of 6 inches contributes to the trapezoidal shape, which is known for its effectiveness in reducing drag and improving the aerodynamic efficiency of the rocket.

The trapezoidal shape of the fins was specifically chosen due to its advantageous aerodynamic properties. Compared to other fin shapes, trapezoidal fins offer a good balance between minimizing drag and maximizing stability. This shape also allows for easier manufacturing and integration with the rocket's body, considering the materials and processes involved in the construction.

In conclusion, the fin design, with its specific trapezoidal shape and carefully calculated dimensions, plays a pivotal role in ensuring the rocket's stability and control during its flight. These fins not only contribute to achieving the desired altitude and trajectory but also enhance the overall aerodynamic efficiency of the rocket, ensuring that it meets the stringent performance criteria set for the project.

2.4. Internal Components

In this section, we detail the internal components of the rocket for our Senior Design Project, outlining their arrangement from the bottom to the top of the rocket.

At the base, the rocket is equipped with four rocket motors, carefully selected for their thrust capabilities and reliability. These motors are essential in providing the necessary propulsion to reach the desired altitude of 400 feet. Surrounding these motors are rocket guides, precision-engineered to ensure a stable and direct ascent. They are crucial for maintaining a straight trajectory, minimizing any off-axis movements that could occur during launch.



Above the motors lies a robust bottom plate, serving as a foundational structure. This plate not only secures the motors and guides in place but also withstands the intense forces experienced during lift-off. Just above this plate, there is a compartment designed specifically for the battery. This box safeguards the battery from flight stresses, such as vibrations and temperature changes, while also ensuring optimal placement for maintaining the rocket's center of gravity.

An intermediary plate is positioned further up, creating a distinct separation between the battery compartment and the electronic sensors located above it. This plate adds to the structural integrity and stability of the rocket. The section above this plate houses various electronic sensors and components, including pressure, temperature, accelerometer, and gyroscope sensors. These instruments are key to gathering vital data about the rocket's performance and environmental conditions during flight.

Connecting the lower and upper sections of the rocket is a tube, designed for both strength and aerodynamic efficiency. It ensures a smooth transition between the propulsion system at the bottom and the glider deployment system at the top. The upper section begins with a bottom plate, specifically engineered to hold and support the glider. This plate is an integral part of the deployment system, designed to release the glider at the predetermined altitude.

A rope mechanism is employed to connect this bottom plate to the subsequent plate. This setup is crucial for the controlled and timely release of the glider, synchronized with the rocket's ascent and apogee. Above the glider, there's a protective plate, tasked with shielding the glider from the heat and forces emitted by the nose cone's rocket motors. This protective measure is essential for maintaining the glider's integrity until its deployment.

In the nose cone of the rocket, additional, smaller rocket motors are installed. These motors are primarily responsible for initiating the glider's deployment. They play a critical role in the final phase of the rocket's ascent, ensuring a seamless transition from rocket-powered flight to the glider's deployment.

Capping the rocket is the nose cone, an aerodynamically designed component that minimizes drag and protects the rocket's internal components during flight. It is engineered to detach at the precise moment, facilitating the deployment of the glider housed within the upper section.

Overall, each internal component of the rocket is meticulously designed and placed, contributing significantly to the rocket's performance, safety, and the successful achievement of the project's objectives. The careful consideration in the design and arrangement of these



components reflects a deep understanding of rocketry, ensuring an efficient and harmonious operation.

2.5. Rocket Motor Decision Process

In the development of our rocket, selecting the appropriate motor was a critical step, as it directly impacts the rocket's ability to achieve its target altitude and carry its payload effectively. The motor selection process was guided by two primary requirements: the ability to lift a 15-pound payload and reach an altitude of 400 feet.

After evaluating various options, we decided on a bundled motor approach. This strategy involved using multiple motors to generate the necessary thrust without the need for a single, higher-class motor, which can be more complex and expensive. The bundled approach also offers redundancy, enhancing the reliability of the launch.

We selected a bundle of four motors, ensuring they were evenly spaced to maintain balance and stability during flight. This arrangement optimizes the distribution of thrust and minimizes the risk of asymmetric force application, which could lead to flight instability.

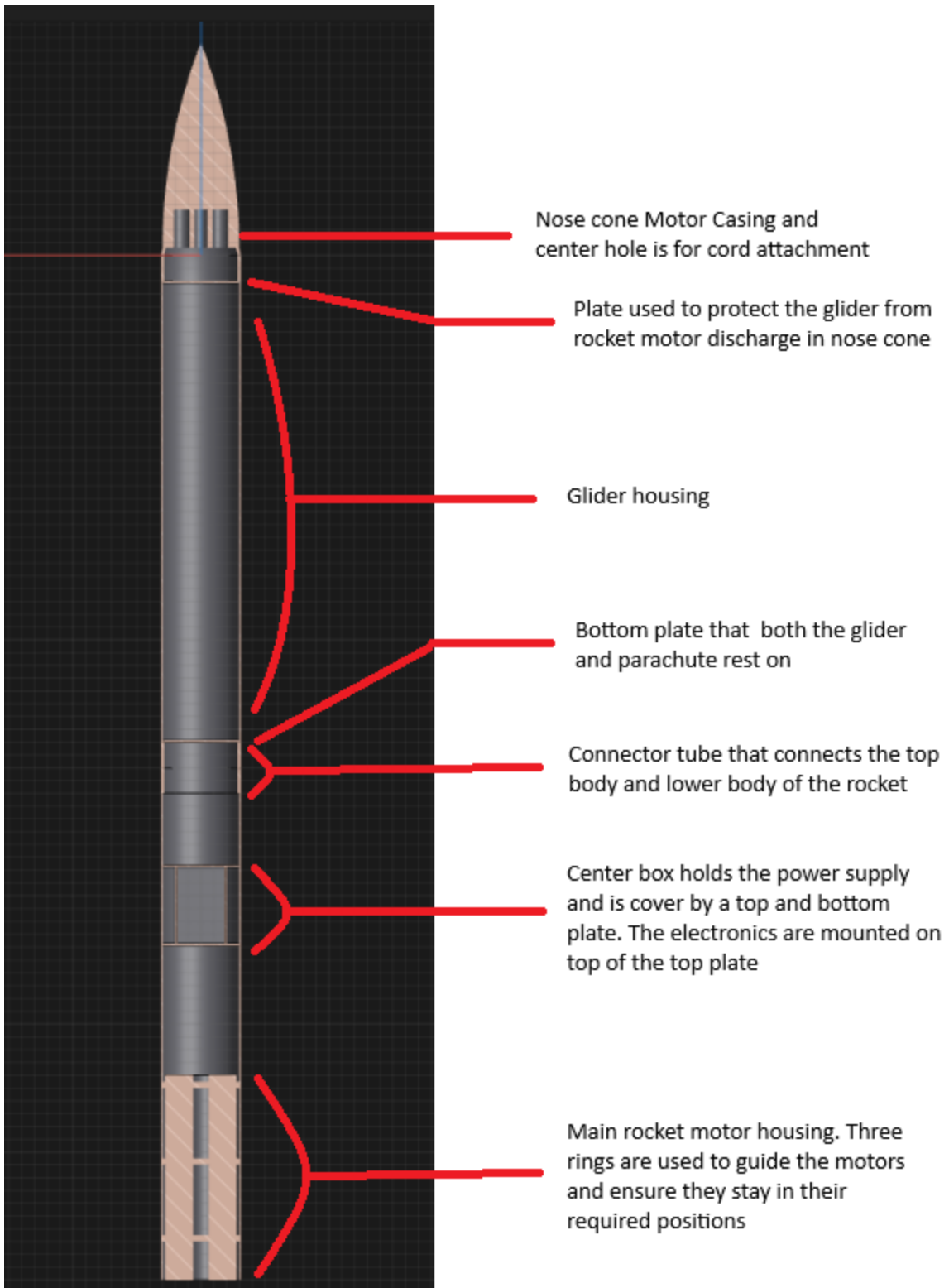
The specific motors chosen for this application were four Aerotech K659R rocket motors. These motors were selected for their proven reliability, suitable thrust profile, and compatibility with the weight and altitude requirements of our project. The Aerotech K659R motors are well-regarded in the rocketry community for their consistent performance and quality, making them an ideal choice for our needs.

This decision to use a bundle of four Aerotech K659R rocket motors strikes a balance between power, cost-effectiveness, and reliability, ensuring that the rocket can meet its performance goals while maintaining a manageable level of complexity and cost. The configuration of these motors within the rocket's design is a key factor in achieving the desired altitude and payload capacity, crucial for the success of the project.

3. Detailed Design

In this section, a 3D slice of the rocket design will be presented and labeled. It is based on all of the components discussed in the preliminary design.





4. Electronic Components

In this section, we will outline the electronic components chosen for the rocket. This includes the microcontroller, sensors, and power supply.

Arduino UNO: This microcontroller is the central processing unit of our rocket. It manages the data collected from various sensors, ensuring robust data processing and control.

Motor Driver: The Studio Grove 12C Motor Driver will be responsible for sending an electrical current to the igniters of the small rocket motors in the nose cone.

Temperature Sensor: Essential for monitoring the internal temperature of the rocket, this sensor provides critical insights into the thermal dynamics affecting the rocket's performance.

Pressure Sensor: This sensor measures atmospheric pressure, a crucial parameter for determining the rocket's altitude. Its readings are key to tracking the ascent and descent phases.

3-Axis Accelerometer: This component measures acceleration in three dimensions, offering valuable data on the dynamic forces and vibrations experienced during the rocket's flight.

3-Axis Gyroscope: Complementing the accelerometer, the gyroscope provides data on the rocket's rotational movement, critical for assessing stability and orientation during flight.

Talentcell Rechargeable Lithium-ion Battery Pack: Powering the electronic suite, this battery pack was chosen for its reliability and consistent power delivery, especially under low-output conditions. Its dual voltage output suits the varying power needs of our components, and its compact design adds minimal weight to the rocket.

5. Performance Characteristics

5.1. Rocket CFD

For the Rocket CFD analysis, a wind tunnel test was simulated. The process of setting up the test as well as executing the test will be discussed. There will also be rocket fin and nose cone comparisons done.

Process

To start the analysis of the process to conduct the CFD wind tunnel test a 3D model of the rocket is needed. The model was designed using the Shapr3D modeling software. The



model for the rocket needs to be solid and in as few parts as possible. This is to lessen the computational load as a personal custom built desktop PC is being used and damaging any component of it could be very costly and detrimental to the project. To get the rocket in as few parts as possible only one fin will be modeled and the rocket body and nose cone will be fused into one object. This makes the meshing of the model as simple as we can get it. This also gives the opportunity to look at the airflow across the rocket body with no fins present as only one side of the rocket will have a fin. This can clearly be seen later in this section. Next in the modeling process the “wind tunnel” must be created. This is simply making a large solid box that will be placed over the rocket. So the rocket will reside within the solid box that will act as a wind tunnel. A problem that occurred was when importing the model, it would either refuse to mesh as the parts were too complex or refuse to upload as facets were not well connected. The fix to this, as weird as it may be, was when modeling the fin, the side in contact with the rocket needed to perfectly conform to the rocket so it had to have a very slight arch to the point in contact with the rocket. The next step in the solution was to copy and rotate the fin to the opposite side of the rocket. We can only assume this is needed because the copy of the fin is treated as a whole, unaugmented object which would make the facets connect to a better degree than the original fin. With these problems now solved, the next step would be to upload the model as an .stl file to the CFD program of choice being Autodesk CFD 2024. After this, the parts must be assigned materials, the wind tunnel box will be assigned as air with the rocket parts being assigned as aluminum or a plastic as the material has little effect on the analysis in this case as it is a test of air flow and not heat transfer. Next would be to label boundary conditions. This front or nose cone side of the wind tunnel box should be set to a velocity of 120m/s as this is the average velocity the rocket will be reaching as discovered in openrocket. The back side of the wind tunnel box should be set to a pressure of 0 to ensure the flow remains in a constant direction. With this done we can now run the solve function as it will automatically mesh the objects and perform an analysis.

Project Rocket CFD

In this section the CFD of the main rocket being used in this project will be looked at. There will be two main results that will be looked at being a flow trace image and a planar model. The planar model will show the complete flow around the rocket while the trace shows specific strands of flow and how they interact with the rocket.

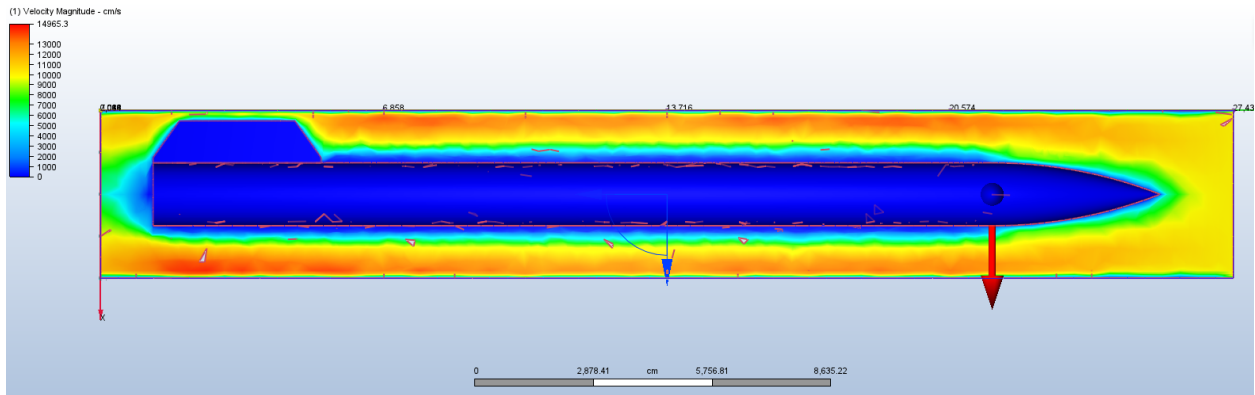
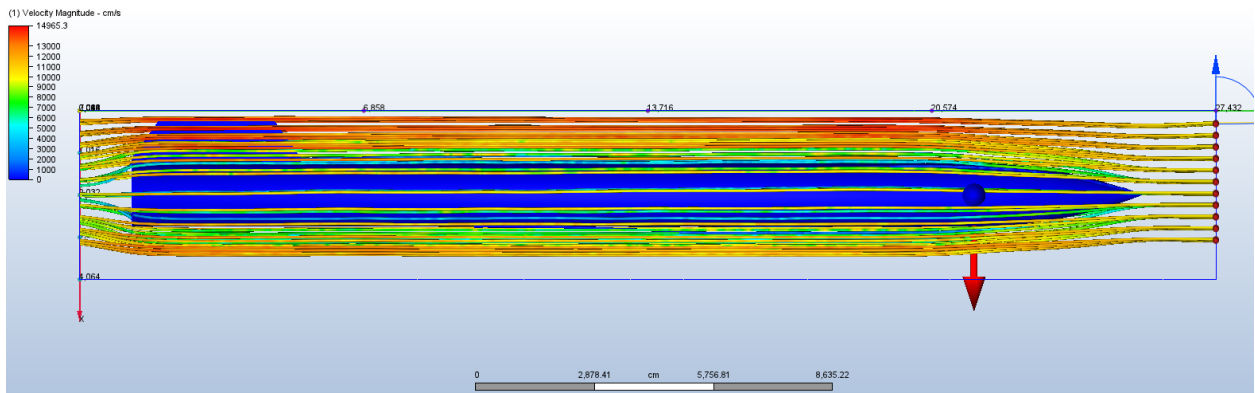


Figure (H): Planar CFD main rocket project image

Shown above in figure (H) is the planar CFD image. This shows the velocity of the air flow as the rocket interacts with the airflow as it makes contact with the rocket. As can be seen, as the flow first interacts with the rocket's nose cone, it slows substantially as would be expected. The nose cone does a very good job at dispersing the air flow evenly keeping the disturbance very close to the rocket's body. When the flow reaches the rocket's fin it makes a gradual arc up the fin staying close to the fin itself, and then making a smooth transition to eventually converge behind the rocket. Overall the results are as expected as there are no major disturbances in the flow which is in line with rockets as they are smaller and have much less of an impact on the direction of the airflow.



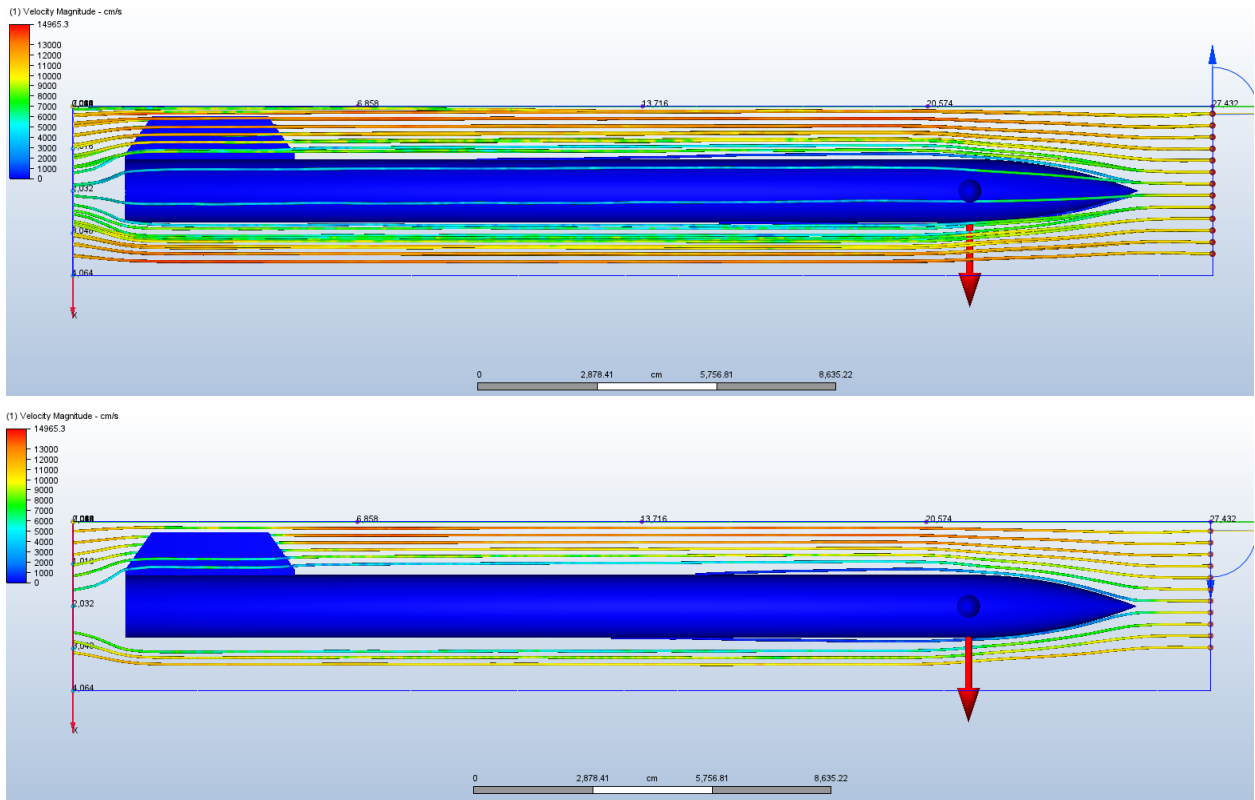


Figure (I): Trace CFD main rocket project

Shown above in Figure (I) is the trace results in the CFD Program. There are three images shown in decreasing order starting from a full trace with the entire rocket body, a partial trace, and a single line trace. The full trace essentially shows the same aspects as the planar CFD analysis does but in strands of air flow. The same is seen with the flow as the nose cone initially separates the flow around the rocket body keeping it close to the body and the flow then reaches the fin and has a smooth transition around the fin to then converge back behind the rocket. The partial shows this as well with the single trace clearly showing the separation of flow when interacting with the rocket fin.

Rectangular Fin CFD Comparison

For this section we will look at a CFD analysis of the rocket with rectangular fins instead of its trapezoidal fins. The purpose of this is to further understand the improvements trapezoidal fins bring to the rocket when compared to the very simple rectangular fin. There will be two images shown being a planar CFD and a trace CFD image and they will be compared to that of the main rocket project images above.



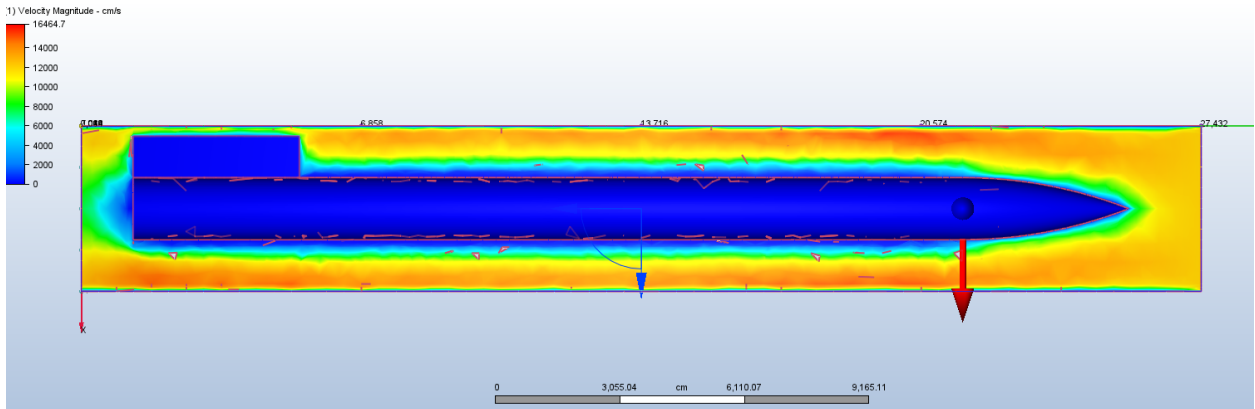


Figure (J): Rectangular fin planar CFD

The image shown above illustrates the planar CFD with a model that boasts rectangular fins instead of the trapezoidal fins being used in the project. First thing to notice is that at the front of the fin where first contact with the airflow is made, it is a blunt impact when compared to the trapezoidal. The airflow does not follow the fin smoothly as it travels along it but would rather split from it. When looking at the trapezoidal it is clear that the airflow follows the fin with minimal flow separation. Secondly, when the airflow reaches the end of the fin, it does not smoothly converge back behind the rocket, or at least as smoothly as the trapezoidal fins make it. The airflow is more disturbed behind the rocket when compared to the trapezoidal fins.

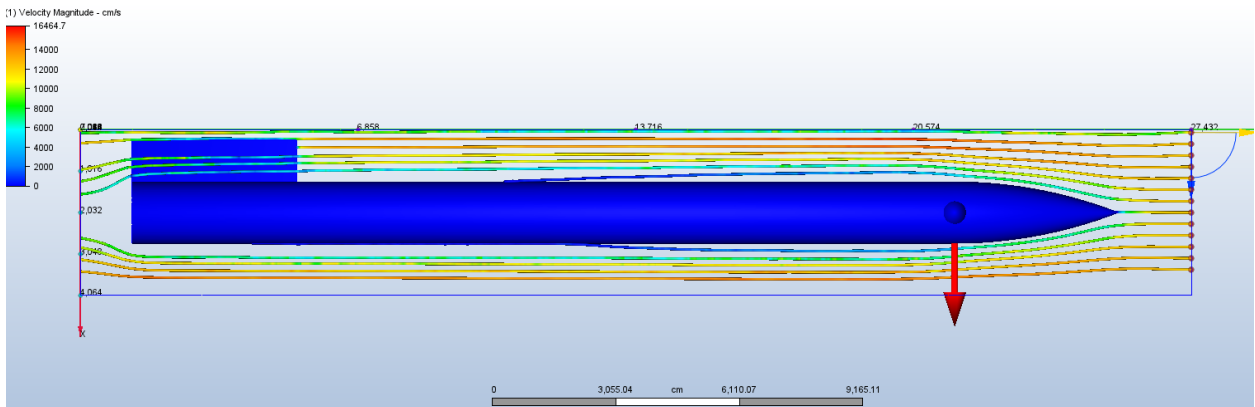


Figure (K): Rectangular fin trace CFD

The image shown above illustrates the trace CFD with the rectangular fin configuration just as the planar CFD shown above. As can be predicted from the planar CFD, the flow does indeed separate more along the side of the fin. This is likely due to the bluntness of the fin when interacting with the airflow as there are no angled surfaces to direct the airflow. The convergence of the airflow can also be seen here to be not as smooth as shown with the

trapezoidal fin configuration. Overall the trapezoidal fins have a clear advantage over the rectangular fins.

Nose Cone CFD Comparison

In this section, a nose cone that is more akin to a parabolic nose cone will be simulated through Autodesk CFD software and compared to the ogive nose cone being used for the project. A parabolic nose cone has a smooth nose when compared to the point achieved when using an ogive or conical nose cone. With this we can expect a greater split in the oncoming airflow than we would see using an ogive nose cone.

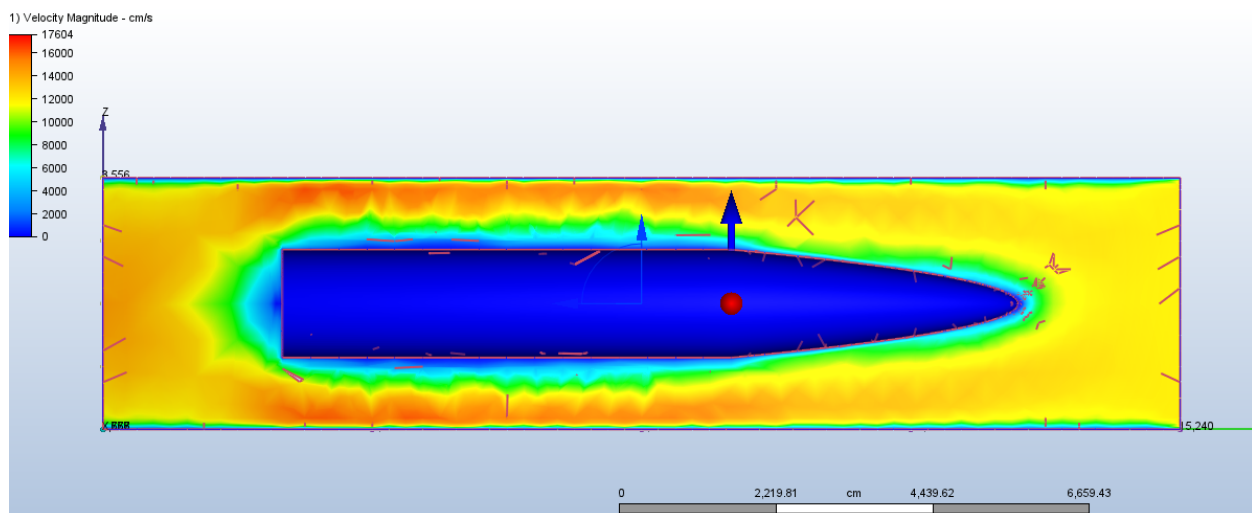


Figure (L): Parabolic nose cone planar CFD

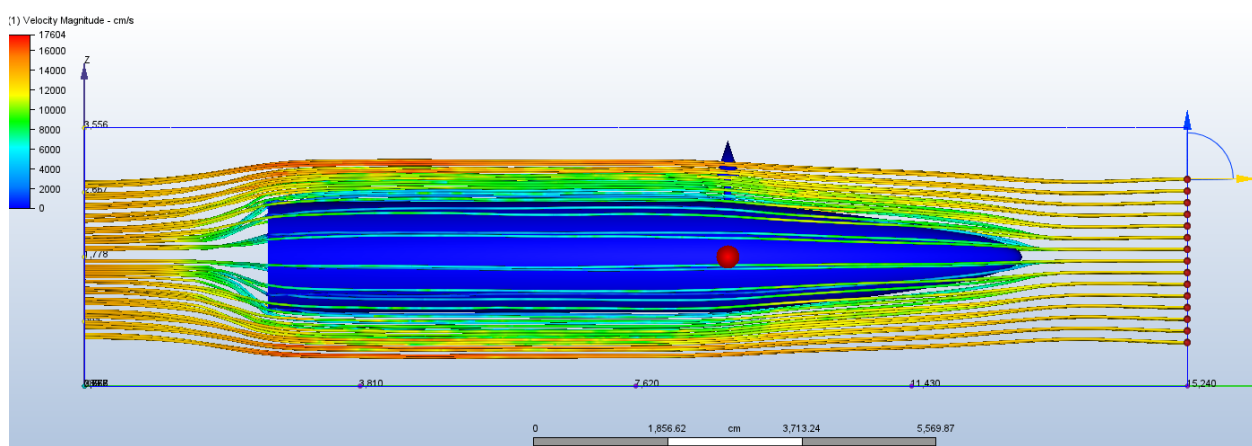


Figure (M): Parabolic nose cone trace CFD

The figures shown above illustrate the parabolic nose cone in both the planar and trace CFD analysis. When looking at the planar CFD image it is clear that the flow separation at the tip of the parabolic nose cone is much more prevalent than the ogive nose cone. It appears it affects the adherence of the airflow to the body of the rocket as well. A shorter body was used in this test to get a better look at the effects of the nose cone. The parabolic nose cone would most certainly perform fine with speeds below transonic but once approaching higher speeds it is clear this cone would suffer.

5.2. OpenRocket

For this section the OpenRocket simulation will be given. OpenRocket is an open source, fully featured model rocket simulator that allows you to design and simulate a rocket before building and launching. The design process is rather simple for OpenRocket, first you would start with the nose cone in which multiple shapes can be chosen from as a sort of template. The sizing of each piece can be edited.

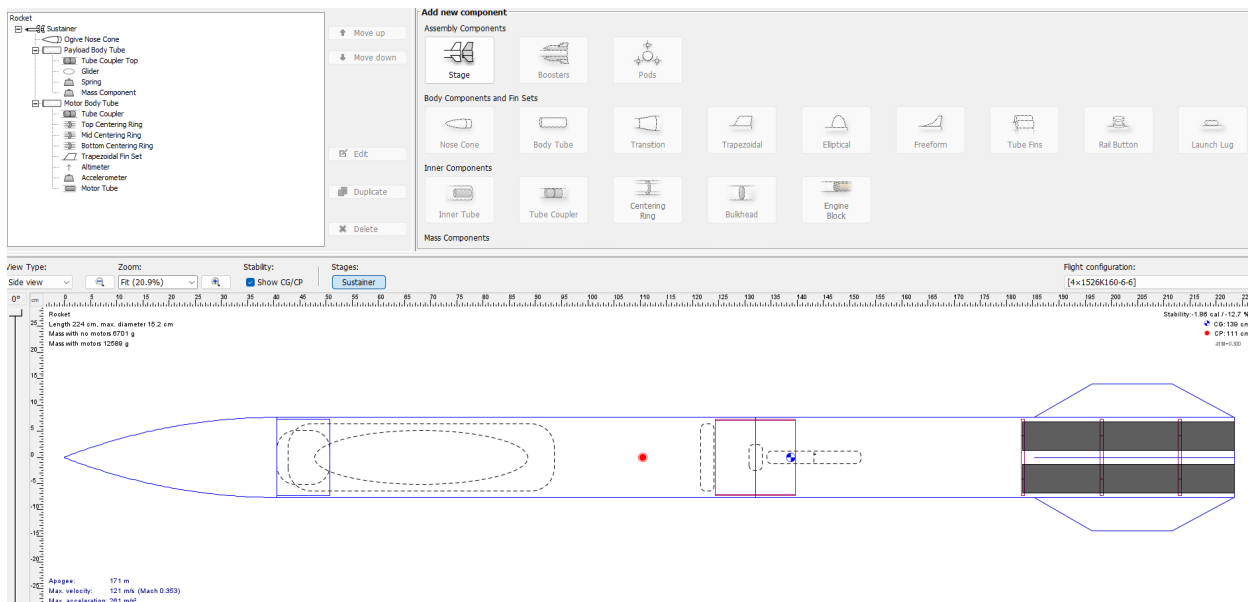


Figure (N): OpenRocket model

Shown above is the model of the rocket made in OpenRocket. There is a cluster motor configuration used with the Aerotech K695R rocket motor. The K695R provides the required thrust with an Isp of around 1500s. A cluster of four of these motors proves to be enough to get the rocket to an apogee of 169 meters or around 554 feet. The apogee in OpenRocket will be greater than that seen in real testing due to added weights as OpenRocket while accurate with calculations, it cannot predict added weights from the build process as well as real time weather conditions.



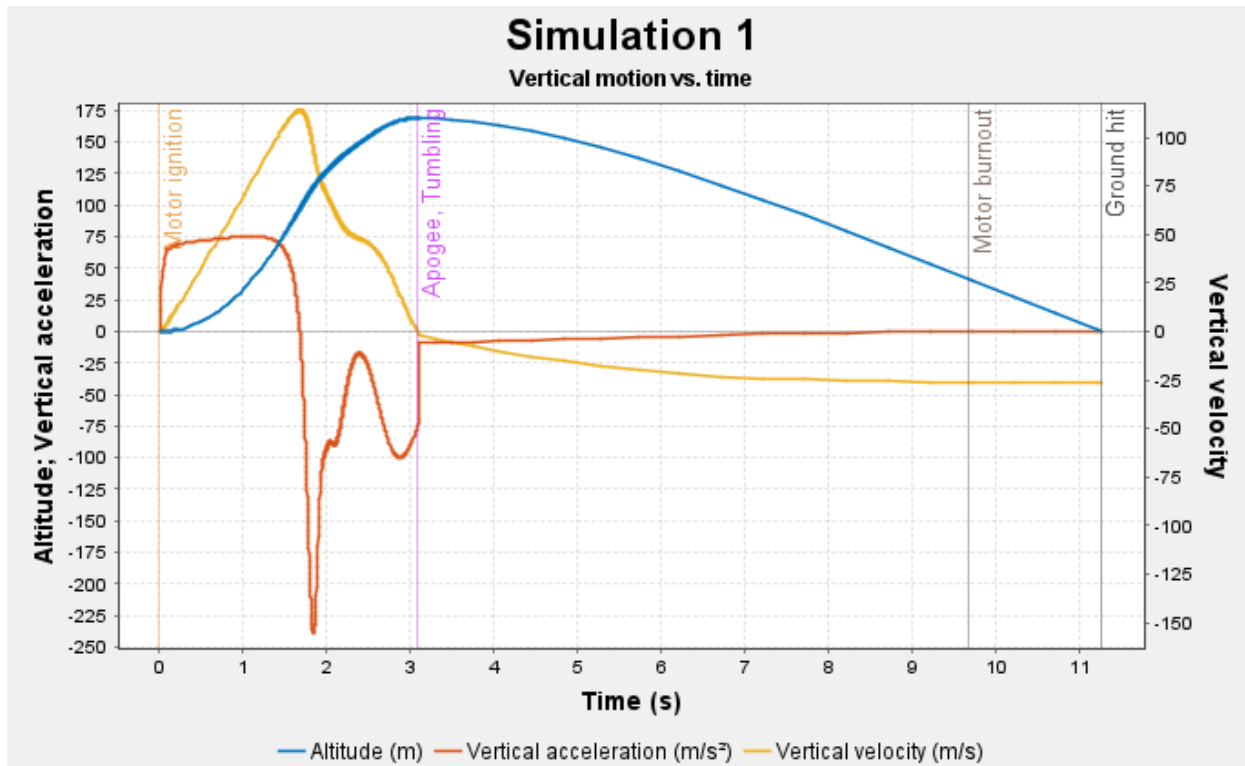


Figure (AQ): OpenRocket simulation

Velocity Off Rod	11.7 m/s
Apogee	169m = 554.462ft
Optimum Delay	-6.59s
Max Velocity	117 m/s = 262 mph
Max Acceleration	241 m/s^2
Time to Apogee	3.09s
Flight Time	11.3s
Ground Hit Velocity	26.2 m/s = 58.6 mph

Table 5: OpenRocket simulation data

The graph and table shown above shows the OpenRocket simulation of the rocket's flight. On launch the acceleration increases dramatically as the rocket's motors are ignited and are achieving their highest thrust. The velocity is steadily increasing which is great to see as it means there are no jumps or uneven flight occurring. The velocity curve is great for showing



possible tumbling which occurs when the rocket starts to wobble and then flip directions sporadically. The altitude curve is excellent as it shows a smooth increase with a slower downfall which is one of the reasons why a goal for the rocket was for it to be light. With the rocket being lightweight, in the unfortunate case of the parachute being stuck or unable to deploy, the rocket will not fall as fast as a heavier rocket would. In this case the rocket would descend at a velocity of 26.2 meters per second or about 58 miles per hour. The apogee is 169 meters or 554 feet which overshoots the 400 feet ceiling. This is to give an ample amount of space or height for the glider to correct itself post-ejection. The rocket will reach a maximum velocity of 117 meters per second or 262 miles per hour which isn't too high or low in terms of rockets with payloads. Especially considering the lower height this rocket aims to reach. Overall the OpenRocket simulation shows a promising launch for the rocket design.

5.3. MATLAB Calculations

The provided Matlab script calculates the velocity, altitude, acceleration, and G-force experienced by the rocket during its flight, employing empirical data, physical principles, and mathematical modeling for simulation. It starts by importing thrust curve data (thrust, motor mass, and time) and sets constants like gravity, drag coefficient, and nose cone diameter. The script extracts and processes the thrust curve data, initializes arrays for time, velocity, altitude, acceleration, and G-force, and sets the initial altitude. In the main simulation loop, it calculates current thrust, adjusts rocket mass for fuel consumption, computes air density using an exponential model, and calculates drag force. Net force is determined by considering gravitational and drag forces, and acceleration is calculated using Newton's second law. G-force is computed by dividing acceleration by gravity. The script updates the rocket's velocity and altitude for each time step, and after the loop, it calculates and displays the maximum altitude and G-force experienced. Finally, it plots the rocket's performance metrics over time, providing a visual representation of the flight dynamics, thereby serving as a crucial tool for analyzing the rocket's performance and validating its design.

The Matlab simulation, using detailed inputs and physics-based modeling, provides valuable insights into the performance of our rocket. The key outputs of the simulation, which include a maximum altitude of 284.5365 meters and a maximum G-force experienced of 18.6054 g's, are critical in assessing the rocket's capabilities and design effectiveness.

The maximum altitude achieved surpasses the initial target of 400 feet (approximately 121.92 meters), indicating that the rocket is capable of achieving and even exceeding its altitude goals. This higher-than-expected altitude is a testament to the effectiveness of the rocket's propulsion system and its aerodynamic design. The altitude achieved also suggests that the rocket has sufficient power and stability to carry its intended payload, including the glider and onboard sensors, to the desired height, providing a promising outlook for its operational capabilities.



The maximum G-force experienced by the rocket, measured at 18.6054 g's, provides an important indicator of the stresses that the rocket and its payload will endure during flight. This value, while significant, is within the tolerable limits for most aerospace materials and electronic components, suggesting that the rocket's structure and its internal systems are well within safe operational thresholds. Moreover, this G-force level is informative for ensuring the safety and integrity of the glider deployment mechanism, which is a critical component of the mission.

The four graphs generated by the script, illustrating the rocket's velocity, altitude, acceleration, and G-force over time, offer a comprehensive view of the flight dynamics. These visualizations not only validate the rocket's design but also provide essential data for further optimizations and adjustments.

In conclusion, the Matlab simulation outputs and the accompanying graphical data collectively demonstrate that the rocket is well-positioned to meet its design objectives. The achieved altitude and experienced G-force are indicative of a robust and capable design, validating the engineering decisions made during the development process.

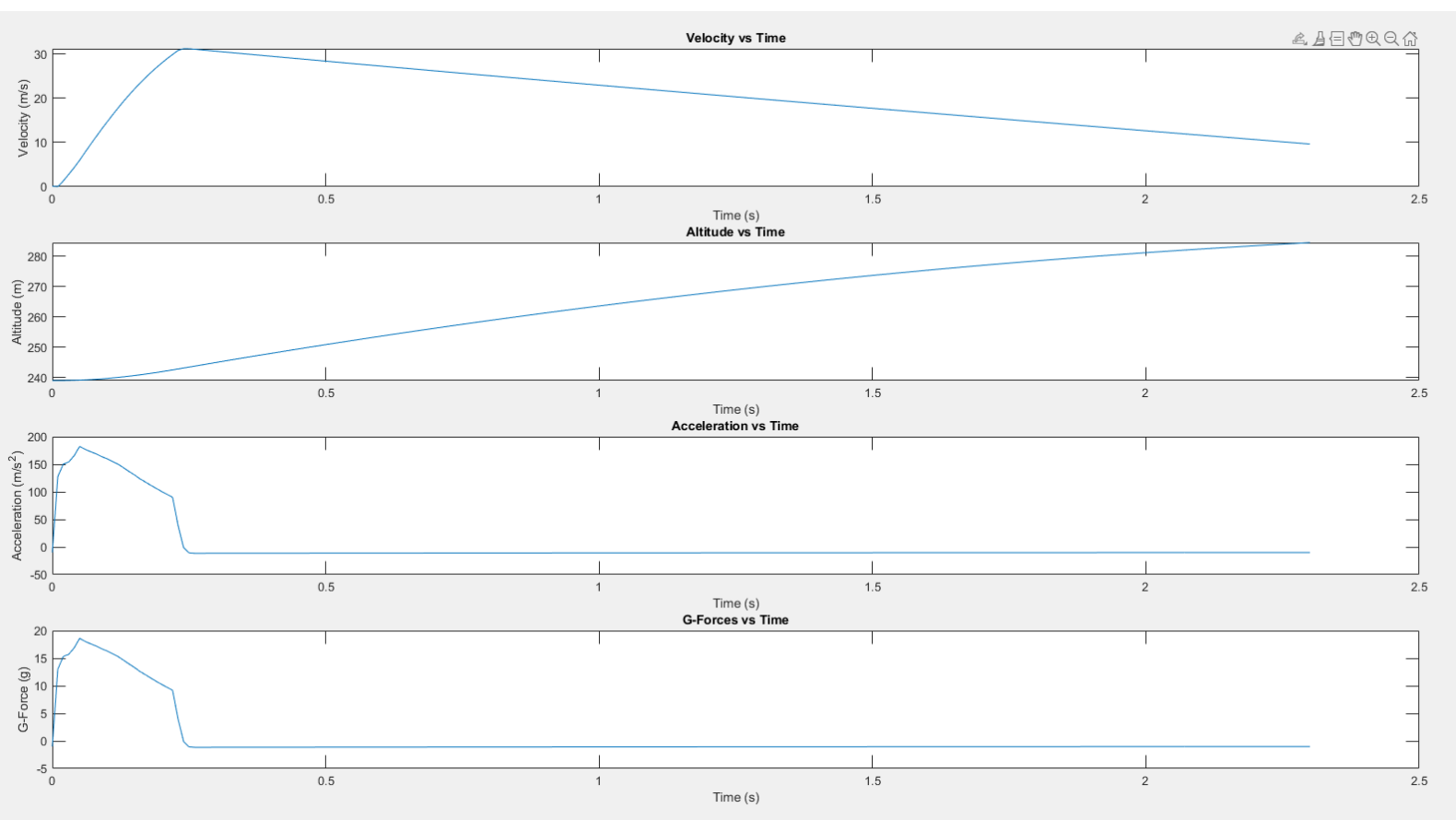


Table 6: MATLAB Code Graphs

6. Manufacturing Plan

6.1. Materials Considered

For the rocket's body and internal components, the team deliberated on various materials, weighing their advantages and limitations. The materials considered were:

Cardboard: Due to its lightweight and cost-effectiveness, cardboard was an initial consideration. However, its susceptibility to moisture and limited durability under stress were concerning.

Carbon Fiber: Known for its high strength-to-weight ratio, carbon fiber was a strong contender. It was particularly favorable for parts that required rigidity and resilience to stress.



PVC (Polyvinyl Chloride): PVC's durability and resistance to environmental factors made it a candidate. However, its weight and the complexity in shaping and joining were points of consideration.

Fiberglass: Similar to carbon fiber in some respects, fiberglass was considered for its strength and lower cost compared to carbon fiber. However, concerns about its weight and the labor-intensive process of shaping and finishing were noted.

Light Thin Project Paneling (Wood): This material was primarily considered for internal structural components. Its lightweight and ease of manipulation were positive aspects, but concerns about its strength and durability under flight conditions were raised.

3D Printed Parts: The flexibility in design, rapid prototyping, and the ability to produce complex shapes made 3D printing an attractive option for specific components of the rocket.

6.2. Material Analysis

In this section, we delve into a comprehensive analysis of the materials considered for the construction of the rocket, evaluating them based on their strengths, weaknesses, and suitability for various components.

Cardboard was initially considered due to its lightweight nature and cost-effectiveness, making it an appealing choice for rapid prototyping. Its ease of shaping and cutting added to its practicality. However, its susceptibility to moisture and environmental factors, coupled with limited durability and strength, raised concerns about its viability, especially for high-stress components.

Carbon Fiber stood out as a strong contender, renowned for its exceptional strength-to-weight ratio and high durability. This material was ideal for load-bearing structures due to its resistance to environmental stresses. Despite these advantages, the higher costs associated with carbon fiber, alongside the need for specialized equipment and a complex manufacturing process, presented significant challenges.

PVC (Polyvinyl Chloride) was another material under consideration. Its durability and resistance to environmental factors like moisture and corrosion made it a robust choice. While PVC is relatively easy to work with, its heavier weight compared to cardboard and carbon fiber, along with challenges in bonding and shaping complex structures, were seen as drawbacks.

Fiberglass offered a good balance with its strength-to-weight ratio and stood out as a cost-effective alternative to carbon fiber. It was fairly easy to mold and shape, fitting for various design requirements. However, the labor-intensive process required for finishing, alongside the



lessened strength and rigidity compared to carbon fiber, and potential health hazards during processing, were points of concern.

Light Thin Project Paneling, typically made of wood, was considered for its lightweight attributes and the ease with which it could be cut and shaped. It provided a certain degree of structural strength, which was advantageous. However, the variability in strength, potential for environmental damage, and limited durability under high stress made it less ideal for certain components.

Finally, 3D Printed Parts were evaluated for their ability to create complex geometries with precision. The rapid prototyping capabilities and flexibility in design modifications that 3D printing offered were significant advantages. Nonetheless, issues such as variability in material strength, potential challenges with dimensional accuracy, and dependency on the quality of the 3D printer and material, necessitated careful consideration.

6.3. Process Selection

In the construction of the rocket, specific processes were selected for different components based on their effectiveness, cost-efficiency, and suitability to the material characteristics.

For the nose cone, the decision was made to utilize 3D printing. This choice was driven by the ease and low cost associated with the 3D printing process. 3D printing allows for precise control over the shape and dimensions of the nose cone, ensuring an aerodynamically efficient design. Additionally, the flexibility to quickly iterate designs in response to testing outcomes made 3D printing an attractive option for the nose cone.

The rocket body, on the other hand, was chosen to be constructed from cardboard. The primary reasons for this selection were its lightweight nature and durability, which are critical in rocketry for achieving the desired altitude and maintaining structural integrity during flight. Moreover, cardboard stands out for its lower cost compared to other materials, making it a budget-friendly option for the rocket body. This choice aligns with the project's objective of balancing performance and cost-effectiveness.

6.4. Component Manufacturing

For this section, the manufacturing of the rocket will be shown. That being 3D designed files for 3D prints as well as shop work to make things such as fins and the battery casing. An image will be shown and a description of the work will be made.



3D Print

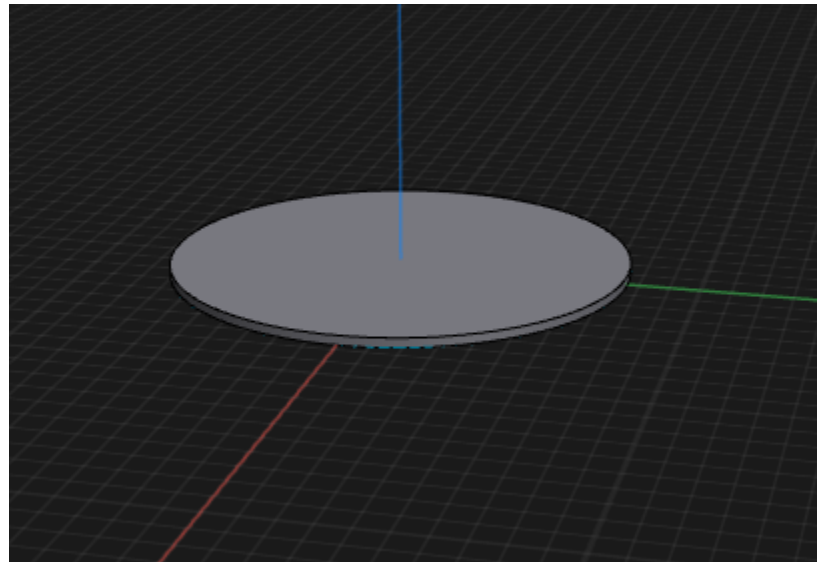


Figure (O): Plate Design

The plate design is very simple. It is the internal diameter of the rocket which is six inches and a thickness of an eighth of an inch. Six of these were printed.

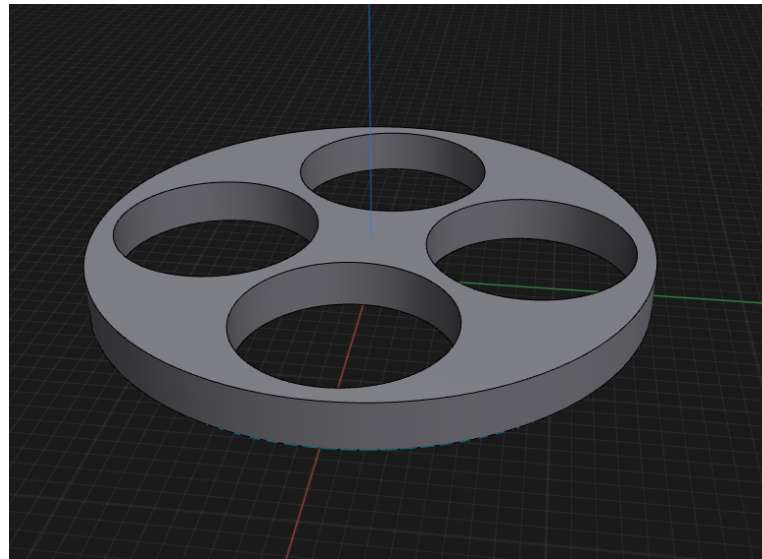


Figure (AR): Motor guide design

The motor guides were made to be a half an inch thick with cylindrical holes measuring 56 millimeters in diameter. This is to make sure that there is a little extra room for the rocket motors to fit in them to ensure that further machining is unnecessary. Two sets of three of these were printed due to an initial error in printing.

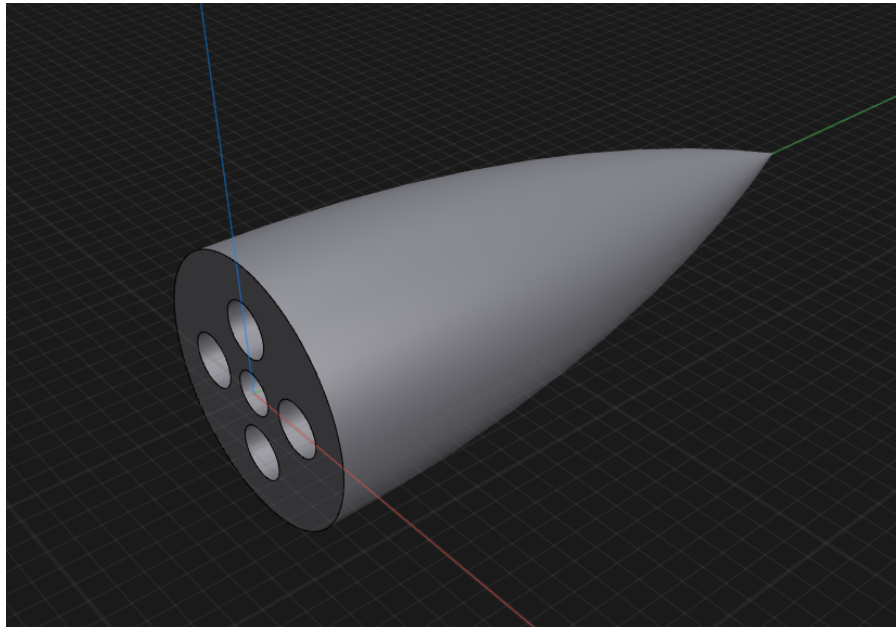


Figure (P): Nose cone design

The nose cone was designed using an arch to create the necessary curve of the cone and then revolved around the green axis. The holds in the bottom were made using subtractions with the center hole being smaller than the 4 holes used to hold the rocket motors which are meant to eject the cone. One of these was made.

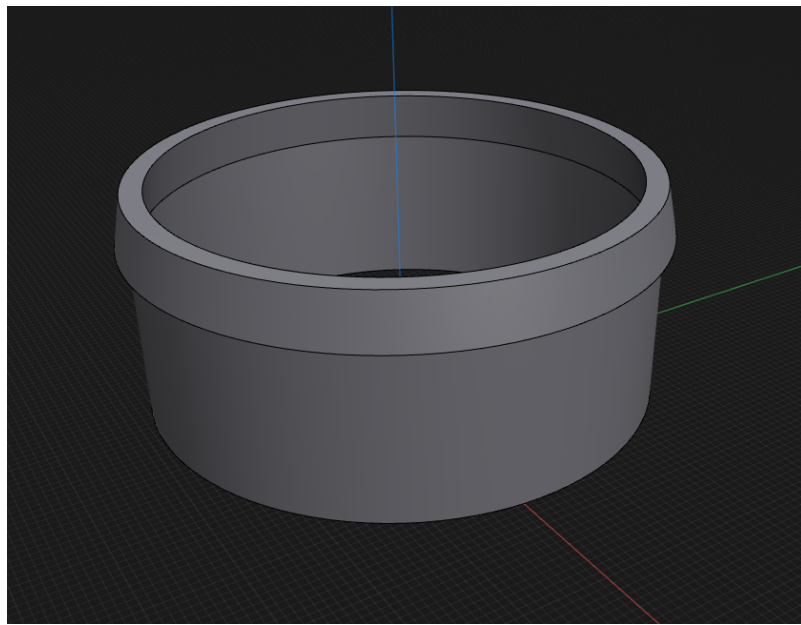


Figure (AS): Nose cone shoulder design

The nose cone shoulder was made to ensure that the nose cone stayed secured on the rocket during flight by the bottom cylinder shown slid internally into the top body of the rocket. Two of these had to be made due to an error in printing.

Shop Work and Assembly

The images shown below are multiple stages in the building process. Descriptions are made below each image.



Figure (Q): Rocket body tubes

The rocket body tubes were purchased as custom orders through a milling shop. Two sets were purchased to prepare for possible damages or errors made in the build process. The cardboard tubes were painted red to make it so in flight the rocket would remain to be clearly observed. So if a malfunction were to occur and the parachute were to be made not to deploy, on descent the rocket could be seen and safety precautions could be taken. The tubes Are six inch internal diameter with an eighth inch thickness.





Figure (R): Nose cone, plates, motor guides, and shoulder results

The figure above shows the successful 3D prints of the rocket components, that being the nose cone, nose cone shoulder, motor guides, plates, as well as a red center ring that will be made to join the top and bottom bodies of the rocket together. The piece of project board in front of these prints is being used to create the fins of the rocket. The fin design was drawn onto the project board to then be cut out using a jigsaw. The corners of the fins would then be rounded and sanded down for smoothness.



Figure (S): Fin manufacturing and assembly

In this portion of the manufacturing process, the plates are being fitted to be placed into the rocket in their designated spots. Further machining with drills and routers were used here to make it so the rocket fins wouldn't detach from the rocket mid-flight. The nose cone was also glued to the nose cone shoulder to make them into one piece.



Figure (T): Final rocket build

Shown above is an image of the rocket after being fully built. It stands at a height of 97 inches or 8.08 feet. The Main motors are not present due to being unavailable so the rocket may be planned to launch at a later date.



6.5. Cost Breakdown

Since this project was not sponsored, the budget for the rocket build was limited only by what the team was willing to spend. Table 7 shows the cost of all components of the rocket.

Component	Cost	Quantity	Total
Nose cone Motors	27.99	1	1
Main Motors (Not Purchased)	200.00	4	4
USB Conversion	9.99	1	1
Battery	39.99	1	1
Motor Driver	14.05	1	1
Pressure Sensor	8.00	1	1
Temp Sensor	2.75	1	1
Accelerometer	10.90	1	1
Temp+Humi+Pressure Sensor	22.20	1	1
Dynamixel	29.00	1	1
Gyroscope	16.00	1	1
Parachute	33.08	1	1
3D Software	300.00	1	1
Body Tubing	405.00	1	1
PLA	155.00	1	1
Materials+Other	115.00	1	1
Total			\$1188.94

Table 7: Rocket costs



6.6. Milestone Chart

The manufacturing of the different rocket components were organized in a milestone chart which is shown in table 8. The planned times are shown in black and the actual times are shown in horizontal gold bars. Most of the deviation from the planned times was the results of errors in the manufacturing process or shipping times of components being delayed.

Rocket Construction																
				Planned Duration												
Activity	9/1	9/8	9/15	9/22	9/29	10/6	10/13	10/20	10/27	11/3	11/10	11/17	11/24	12/1	12/8	12/15
Body																
Nose																
Plates																
Fins																

Table 8: Rocket construction milestone chart

7. Testing Plan

7.1. Testing Objectives

As far as objective for testing goes, they are as follows:

- Successful ignition of all main rocket motors.
- Rocket maintains a vertical flight path up until apogee mimicking OpenRocket flight testing.
- Stability is maintained throughout flight with zero tumbling.



- Successful ignition of all nose cone rocket motors.
- Successful launch of nose cone off rocket.
- Successful ejection of glider being pulled by nose cone.
- Successful deployment of parachute from rocket.
- Successful rocket landing with no major damage.

7.2. Testing Schedule

The schedule for testing fully resides on the availability of the main rocket motors. Currently there is no way to predict when the stock of motors will return. But as far as other factors go, the launch will also be heavily dependent on weather conditions. Preferably a low pressure, clear day so the line of sight with the rocket can be maintained. Partial cloud coverage is acceptable, it all depends on the ceiling. Wind would preferably be under 5 kts but up to 10 kts would be acceptable. The last factor that influences the testing schedule is the availability of a person with level 2 rocket certification to be a witness and guide to the launch. This is to maintain safety and accountability with federal law.



AIRCRAFT DESIGN

1. Conceptual Design

The conceptual design phase of the aircraft was used to analyze the project goals and translate them into design parameters. Using these parameters, a figure of merit table was constructed to weigh various solutions against each other to determine the best possible configuration for the aircraft. This resulted in a single engine, pusher prop, mid-wing design, with retractable wings and horizontal stabilizer.

1.1. Aircraft goals

Since the objective of this project was to determine the feasibility of launching an aircraft out of a rocket, the airplane had to be capable of recording flight data, and fit inside the rocket. In addition, it was decided the aircraft should be able to carry a payload of various weather data collecting devices, which would be capable of being switched out at a moments notice. The aircraft also had to follow all rules specified by the Federal Aviation Administration (FAA).

1.2. General Requirements

General aircraft requirements stemmed from the rules set out by the FAA. A summary of this can be found below in table 9.

FAA rules for recreational flyers	
General	Fly only for recreational purposes
	Follow the safety guidelines of an FAA-recognized community based organisation
	Keep the aircraft in visual line of sight
	Give way and do not interfere with other aircraft
	Fly at or below FAA- authorized altitudes in controlled airspace (Class B, C, D, and surface Class E)
	Fly at or below 400 feet in class G airspace
	Have taken the Recreational UAS Safety Test and carry proof
Sizing	Weigh less than 0.55 pounds or be registered and weigh less than 55 pounds
	Fly no faster than 100 miles per hour

Table 9: FAA rules for recreational flyers

Since we could not fly the aircraft over 400 feet and had to fly within visual line of sight, the original plan for the aircraft to be a glider was changed to make an aircraft with glider-like properties with a small motor. Even with a part 107 license it would almost be impossible to get a waiver to fly over 400 feet as manned aircraft fly at a minimum of 500 feet above ground level (AGL).



1.3. Aircraft Requirements

Since our project was not sponsored, aircraft requirements were set by our design team and faculty mentor. A summary of these requirements can be found in table 10 below.

Aircraft Requirements	
General	The aircraft should have glider-like characteristics
Sizing	Maximum diameter of 6 inches Maximum length of 34 inches
Avionics	Capable of autonomous and remote flight
Propulsion	Motor must be commercially available and either brushed or brushless May be direct drive or have a gear reduction Must use a single motor
Electronics	Must have video recording capabilities Must be able to record in flight data like G-load Must be able to record weather data like temperature and pressure
Deployment	Must be able to recover from spin after rocket deployment Must automatically deploy wings and horizontal stabilizer

Table 10: Aircraft Requirements

1.4. Configurations Considered, Concept Weighting , and Selection Process

The following section outlines configurations considered for the aircraft design. Tail design, wing position, wing configuration, and propulsion placement are discussed. To evaluate each of these concepts, and identify the optimal aircraft configuration, a figure of merit analysis was conducted.

Wing Position

The first thing analyzed was the wing position. The most important factor when determining where the wing would be placed was the wing loading of the aircraft. Since the aircraft had to fit inside a rocket, the maximum wing chord would be slightly less than the diameter of the rocket if the wing was in the center. If the wing was placed in the high or low position it would have to have a significantly smaller wing chord to fit in the rocket. Since the aircraft was supposed to have glider-like characteristics it was important to have the wing area as large as possible to keep wing loading down. Wing configurations that would help minimize the wing loading were given high scores.

The stability of each wing configuration position was analyzed next. Since the aircraft would be flying out of a rocket it was important to design an aircraft that could be as stable as



possible to help recover from spin and turbulent wind coming out of the rocket. Although low wings are more stable than mid wings, when running tests, it was found in the initial aircraft design the difference was negligible. Wing configurations with good stability characteristics were given higher scores.

An important characteristic of the airplane was its glide ratio. During steady level unpowered flight, the glide ratio and lift over drag ratio are equivalent. To get the maximum range of the aircraft it was desirable to have this value as high as possible. High wings usually have the best L/D ratio due to the placement of the wings over the fuselage which helps reduce drag. Low wing designs help reduce interference drag which is the drag when two or more aerodynamic surfaces interact with each other. The interaction disturbs the airflow making it turbulent and increasing drag. The mid wing offers a balance between each design. Wing positions with high L/D ratios were given a higher score.

Finally the structural efficiency of the aircraft was evaluated. High and low wing configurations would require additional structure to support them and thus increase the aircraft's weight. Positions with a high structural efficiency were given a higher score.

All of this information was compiled into table 11 below. From the table it was clear the mid wing was the best option for the design as it had the highest score.

Figure of Merit	Factor	Low Wing	Mid Wing	High Wing
Stability	0.3	4	4	5
Structural Efficiency	0.1	4	5	4
Wing Loading	0.4	3	5	3
L/D Ratio	0.2	3	4	5
Total		1	3.4	4.5
				4.1

Table 11: Wing position FOM

Tail Design

The next aspect of the aircraft analyzed was the tail configuration. Three different variants were considered, conventional, T-tail, and V-tail. The most important part of the tail design was the compatibility or the ability to fit inside of the rocket. With limited working space, a V-tail aircraft would not be very compatible with the rocket as without a complex folding mechanism it would be very hard to achieve the required tail volume. A T-tail aircraft could have a simple folding mechanism to allow for more volume but a smaller wing chord as it would be closer to the outer diameter of the rocket. The convention tail would be located close to the center of the aircraft allowing the chord size to be maximized so a smaller span would be



required. It would also only require a simple folding mechanism. Tail configurations that allowed for large tail volumes with simple folding mechanisms were awarded a higher score.

The next factor looked at was the maneuverability and stability contributions of the tail components. Since the aircraft would not have any ailerons the tail would contain all of the control surfaces. With low pitch and yaw stability in addition to the poor coupling moments due to the high dihedral of the V-tail, this configuration was not favorable for our design. The T-tail gave excellent yaw stability as the horizontal stabilizer acted as a cap and would allow for a smaller vertical stabilizer to be used. The conventional tail provided a similar stability to the T-tail. Tails that offered good stability and high maneuverability were awarded high scores.

The next thing examined was the drag of each configuration. With this design being an iterative process this value changed a lot with motor placement. After eventually determining a high pusher prop configuration would be best, the T-tail would produce a lot of drag as it would be in turbulent wind from the motor. A V-tail configuration would keep the stabilizer out of the turbulent flow of the propeller and its smaller required volume would also cause less drag. The conventional tail would also be out of the prop wash, however its large comparative size to the V-tail would cause more drag. Configurations that produced a low drag were awarded a higher value.

Finally the structural efficiency was examined. If a V-tail could be made with no folding mechanism this would be the best option as weight would be greatly reduced. A high T-tail would require additional support and thus have more weight than a conventional tail. Tail configurations with a low weight were awarded a high score.

All of this information was compiled into table 12 below. From the table it was clear the conventional tail was the best option for the design as it had the highest score.

Figure of Merit	Factor	Conventional	T-tail	V-tail
Maneuverability	0.25	4	4	3
Structural Efficiency	0.25	4	3	5
Drag	0.1	4	3	5
Compatibility	0.4	5	4	2
Total		1	4.4	3.65
				3.3

Table 12: Tail configuration FOM

Motor Placement

Another feature examined was the motor placement. Two different configurations were considered a tractor or pusher prop. Since only two configurations were considered, a figure of



merit analysis was not completed and instead the pros and cons of each configuration was evaluated.

For a tractor configuration

Advantages:

- Helps move the center of gravity forward which is important when having a heavy tail
- The propeller runs in an undisturbed free stream
- Better engine cooling

Disadvantages:

- Lower quality airflow over the wings
- Increases skin friction over the fuselage

For a high pusher prop configuration

Advantages:

- High quality flow over wings and fuselage
- Better view for the video camera
- Keeps propeller away from ground when landing

Disadvantage:

- Disturbed incoming airflow to propeller
- Engine cooling issues
- Pushed the center of gravity back

Because the motor was operating at a low power, heat was not a major concern when considering which placement would be best. Some of the most important factors were the CG location, propeller durability, and having an undisturbed incoming flow. By placing the pusher configuration in the center of the aircraft near the top, it would eliminate the negative effect of the CG contribution and the propeller sticking out from behind the fuselage would experience a clean flow. Additionally a high pusher prop would save the propeller from hitting the ground since there would be no landing gear. With all these considerations in mind it was determined the pusher prop would be the best configuration.

Wing Configuration

Although not as thoroughly examined as other features of the aircraft, wing configuration was also considered. To achieve the lowest possible wing loading a rectangular wing was the best choice as opposed to a tapered, or elliptical wing. A delta wing was considered as fabric



could span from the wing to the fuselage as this would greatly reduce wing loading. This idea was quickly dismissed since the ejection charges from the rocket could potentially melt holes in the wings leading to poor aircraft performance. This would also not allow the wing to have a rigid airfoil shape so it would be hard to calculate the lift produced. To help further reduce wing loading, a slif=ding mechanism would be implemented to extend the wing.

1.5. Final Conceptual Design

From the figure of merit tables and analysis conducted it was decided the best aircraft configuration would be a mid, straight winged, pusher prop, conventional tailed aircraft. From this information the first conceptual sketches could be made. Figure (U) shows a side view of the approximate aircraft shape with the wings not extended. Figure (V) shows a top view of the expected designs with the wings extended. The red and blue box represent the folded back wing and tail respectively. The small brown box on the back of the fuselage represents the motor. The orange box represents the camera, and the green and pink box represent the aircraft avionics and attached sensors respectively. The purple parallel lines represent the rocket body.



Figure (U): Aircraft conceptual sketch side view

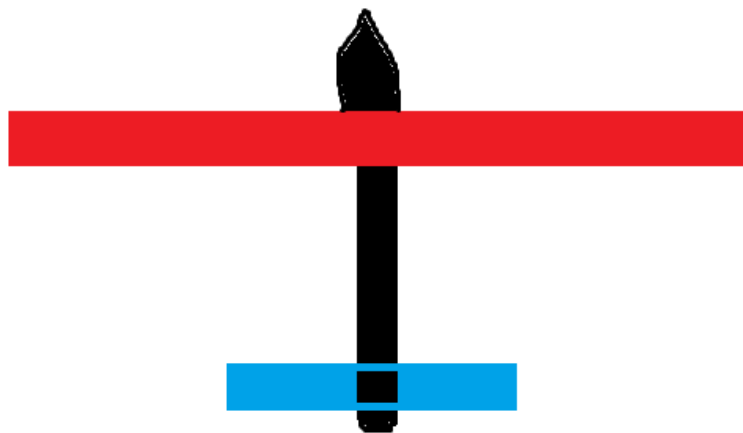


Figure (V): Aircraft conceptual sketch top view

2. Preliminary Design

Once the configuration trade studies were complete, the team began analyzing the selected configuration. A combination of analysis and testing was used in an iterative process to complete the preliminary design. This phase included trade studies, building and breaking components, and analyzing data. These results were used to make the decisions in the final detailed design.

2.1. Design Methodology

The design methodology used was based on the team's past experience with building model aircraft, and advice from Western Michigan University's Design BUild Fly Team. A flow chart of this process can be seen in figure (W) below. Design analysis of multiple prototype parts lead to further iterations to make an aircraft with better performance. This was done with XFLR5 and structural tests.

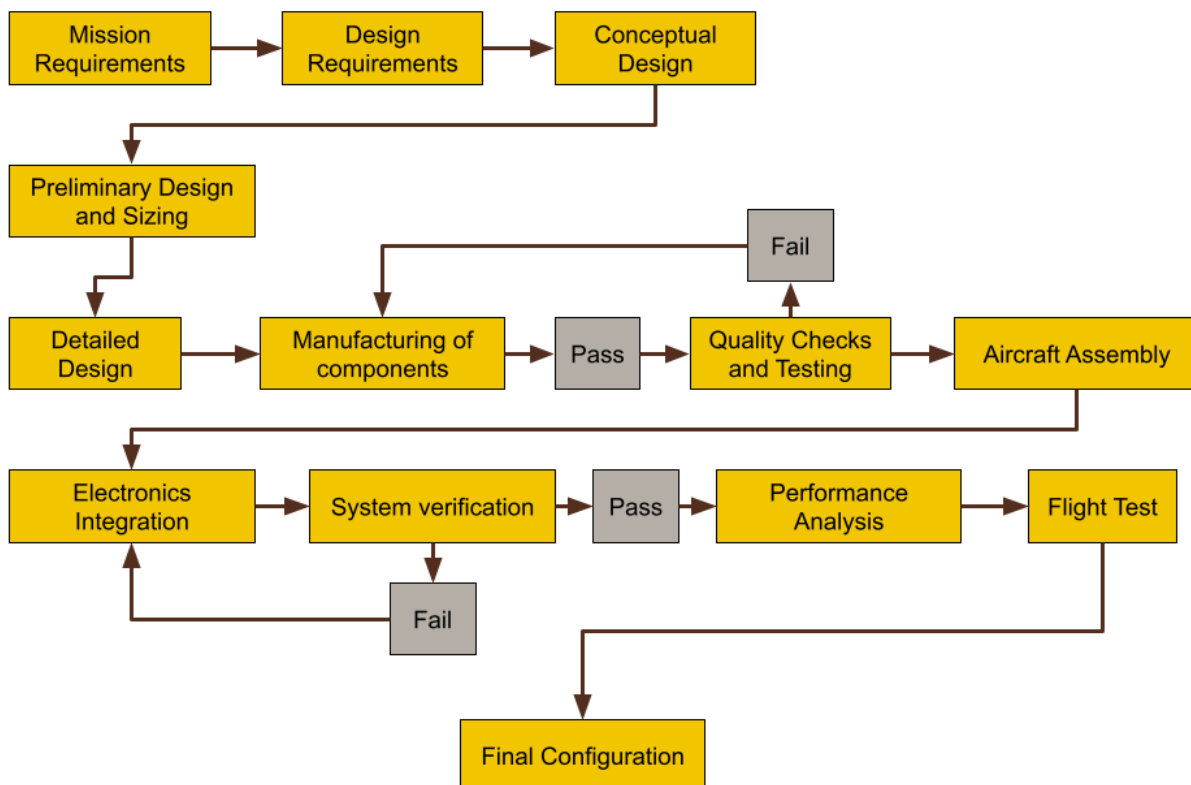


Figure (W): Aircraft design process

2.2. Fuselage Sizing

Fuselage size was dependent on the dimensions of the required avionics and sensors. Other than that there were no other mandatory sizing restrictions. It was important that the aircraft had the smallest cross section as possible to help minimize drag and empty weight. The initial cross sectional shape was an ellipse however after several iterations it moved to an ovate ellipse, to a cross between the split ellipse and what David Rodriguez described in a paper on preliminary aircraft design as a general fuselage shape. These fuselage cross section shapes described by Rodrigues can be seen in figure (X) below. Using a laser cutter and bass wood, this shape would be easy to manufacture, would provide ample space for the payload, and minimize cross sectional area compared to a standard ellipse.

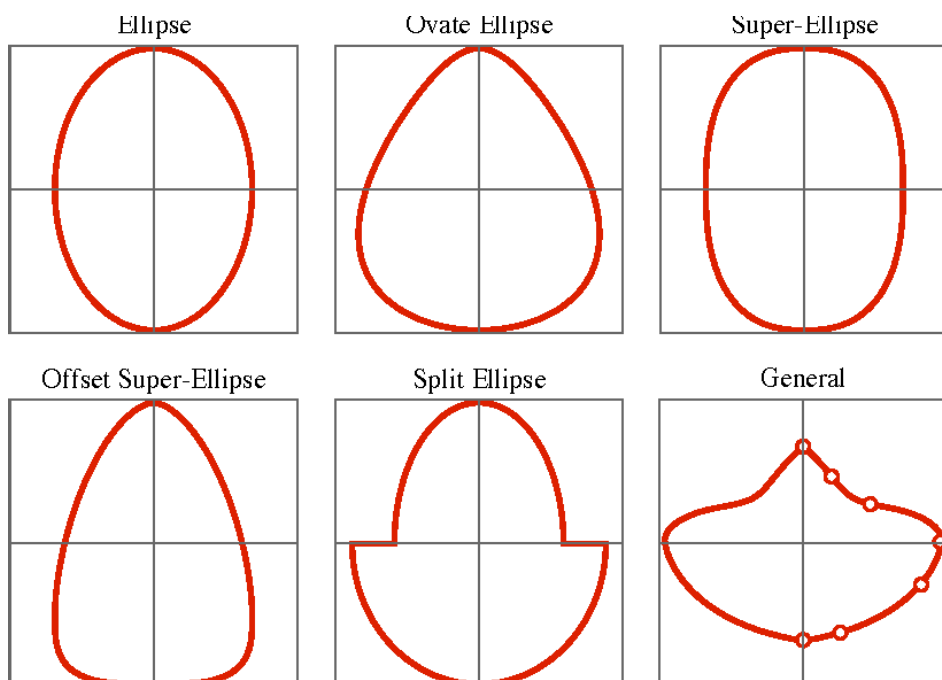


Figure (X): Fuselage cross section shapes

To keep the center of gravity in the right location in the rocket and to prevent the rocket from becoming massive the aircraft's maximum length had to be less than 36 inches. The maximum width and height of the aircraft had to be less than 6 inches to fit in the rocket. This led to a fuselage height and width of 5.5 inches and a total length of 30.25 inches. This length of the fuselage allowed for ample distance between the mean aerodynamic center of the wing and tail to provide good pitch stability. This distance was measured to be 16.75 inches. Figure (Y) and (Z) show a front cross sectional view and side cross sectional view of the aircraft respectively. In the side view it can be seen there is plenty of room for avionics and sensors. In the side view the wings are in the folded collapsed position.



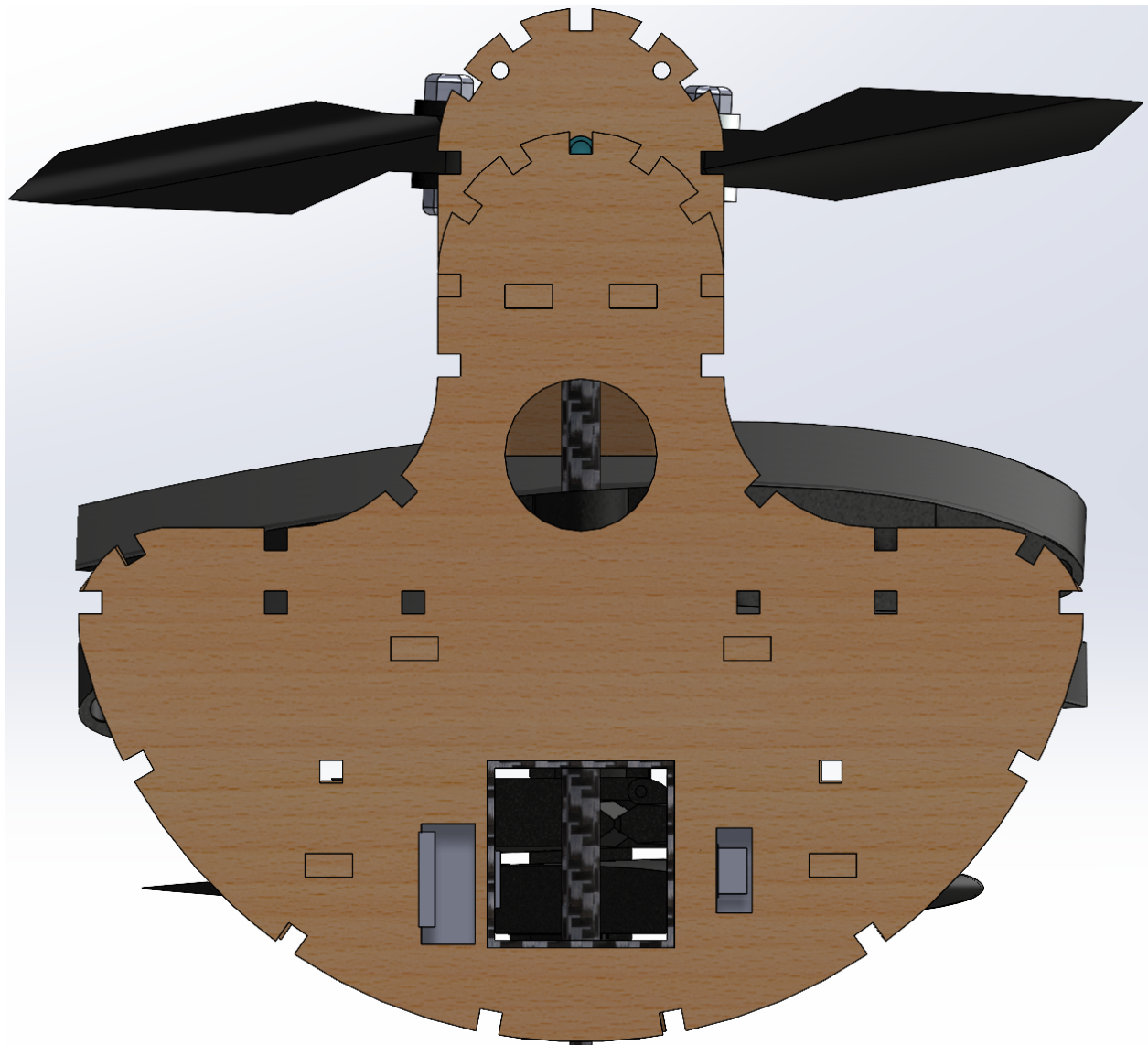


Figure (Y): Front cross sectional view

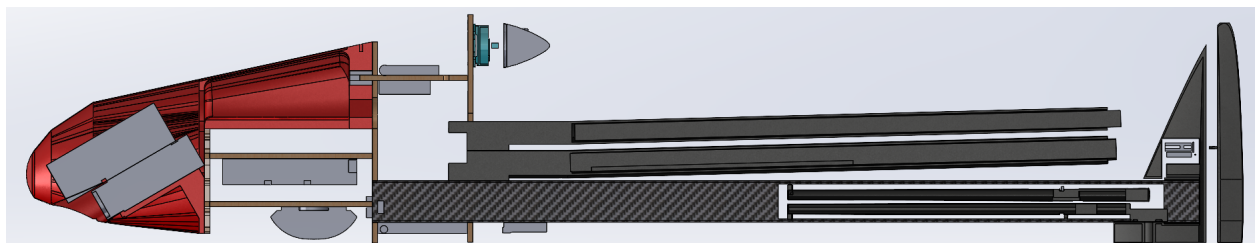


Figure (Z): Side cross sectional view

2.3. Wing Design and Sizing

The chord length of the main wing section was set to 5.3 inches which was the maximum size possible to fit in a 5.5 inch diameter tube. The chord length of the outer section was set to 4.1 inches as it was the largest possible size to slide inside the main wing without too much resistance. The span of the main section of the wing was limited to the distance from the pivot point of the wing to the rudder of the aircraft. This can be seen in figure (Z) above. The shape of the main wing section of the right wing can be seen in figure (AA) below.



Figure (AA): Main wing section

The span of the outer wing section had to fit inside the main wing section. The cut from the leading edge of the main wing section was where the wing made contact with the aircraft fuselage so the wing could fold forward so no wing sweep would be present. At the end of this cut is where the dihedral of the wing started. Since the wing was given dihedral part way through the maximum wingspan of the outer section was limited to 13.5 inches. A 1.5 inch overlap was required to keep the wings rigidly attached to each other so the effective span of the outer section was 12 inches and the total span of the entire aircraft was 55 inches. The resulting average wing chord was 4.77 inches with an aspect ratio of 11.52.

$$AR = \frac{55^2}{262.7} = 11.515$$

A dihedral of 1.5 degrees and an incidence angle of negative 0.424 degrees was used which will be later discussed in the stability analysis in section 5.

2.4. Tail Design and Sizing

Raymer's method outlined in Aircraft Design a Conceptual Approach was used to determine the required area of the aircraft's tail. This method uses volume coefficients for the horizontal and vertical tail (c_{HT} , and c_{VT}) which were determined based on analyzing historical aircraft in different categories such as single engine, twin engine, and sailplanes. For sailplanes these coefficients are 0.5 and 0.02 respectively. If using a full or near full all moving tail such that the entire stabilizer acts as a control surface the volume coefficient can be reduced by 5 to 15 percent. Since the rudder was near the full size of the horizontal stabilizer the new vertical tail coefficient was reduced to 0.018. Using the equations below the area (S) of each stabilizer could be calculated using the length (L) from the mean aerodynamic center of the wing (W) to the mean aerodynamic center of the stabilizer, the aircraft's wing mean chord C and the wingspan b.

$$S_{Vt} = \frac{c_{Vt} b_w S_w}{L_{Vt}} \quad S_{Ht} = \frac{c_{Ht} C_w S_w}{L_{Ht}}$$

Using the above formulas the suggested tail area size was calculated. Values used can be found in table 13 below.

Selected tail volume coefficient	
Horizontal	vertical
0.5	0.018
Horizontal moment tail arm (in)	vertical moment tail arm (in)
16.75	16.75
chord of main wing (in)	span of main wing (in)
4.9	55
Area of main wing (in ²)	Area of main wing (in ²)
263.23	263.23
Required area of horizontal tail (in ²)	Required area of vertical tail (in ²)
38.50229851	15.55807164

Table 13: Required aircraft tail area

The final aircraft's tail area was approximately 55 in² for the horizontal stabilizer and 16 in² for the vertical stabilizer. The horizontal stabilizer was made extra large because if the aircraft were to have a sudden nose down pitching moment and start speeding into the ground the springs in the wings would not be able to hold the wings all the way open pushing the mean aerodynamic center of the wingback. This would in turn decrease the length of the horizontal moment tail arm making the tail too small and incapable of recovering the aircraft from the dive. With a larger tail size it would still be able to recover.



2.5. Control surface sizing

Due to the sliding wing mechanism no ailerons would be present on the aircraft. To allow the aircraft to still perform roll maneuvers the coupling of the wing dihedral and rudder deflection would be used. To help decrease the size of the required vertical stabilizer instead of using the traditional 25-50% of the stabilizer chord for the rudder the rudder was 72% of the chord size and ran the full span. The elevator size was 43% of the chord length. Dimensions for all features can be found in the detailed design section.

2.6. Airfoil Selection

The tail airfoils were designed to be symmetrical to achieve several objectives: minimizing drag, reducing complexity, and ensuring no moment contribution at zero angle of attack. The airfoil thickness was carefully chosen to be as thin as possible while still accommodating the servos embedded within. Consequently, the vertical stabilizer employed a NACA 0015 airfoil, while the horizontal stabilizer utilized a NACA 0008 airfoil.

The objective of selecting the airfoils for the main wing sections was to have a high lift and low drag to maximize the glide ratio. Over 30 different airfoil wing combinations were tested including using different airfoils for the inner and outer sections. These were evaluated with a calculated Reynolds number of 150,000 at a speed of 40 miles per hour. Since lift was dependent on airfoil camber the coefficient of lift was kept constant when the moment of the aircraft was 0 or what the aircraft would experience in steady level flight. This was done by adjusting the incidence angle for each wing combination. Lift calculations and a coefficient of moment vs coefficient of lift graph can be seen in table 14 and figure (AB) respectively below.

Required Lift Calculation	
density (kg/m ³)	1.225
viscosity (kg/m*s)	0.0000181
characteristic length (m)	0.124460249
Speed m/s	18
Reynolds number	151621.4635
Mach number	0.052894505
Coefficient of lift	0.443795905

Table 14: Required coefficient of lift

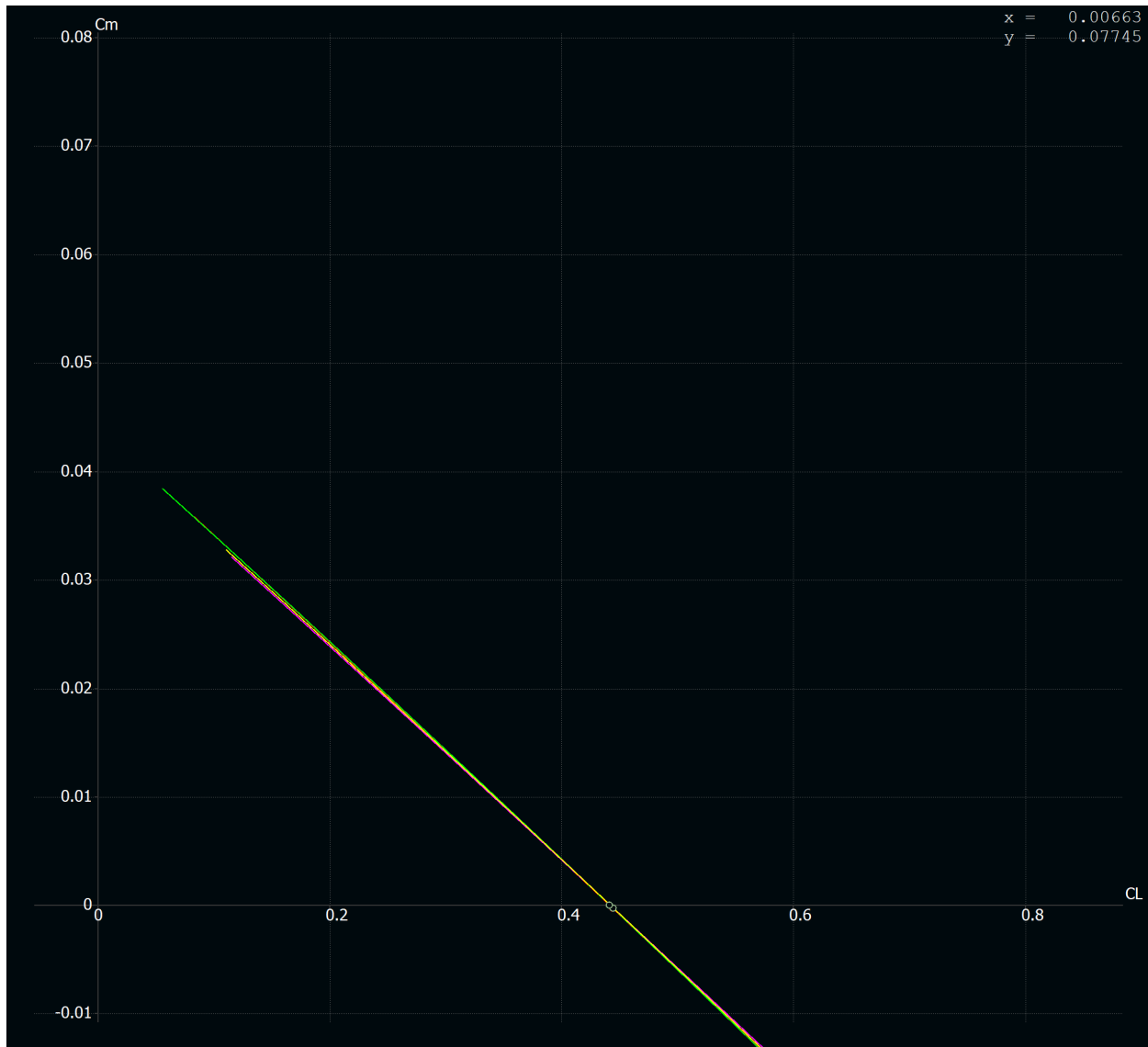


Figure (AB): Coefficient of moment vs coefficient of lift

After the incident angles were set the coefficient of lift divided by the coefficient of drag vs the coefficient of moment was evaluated (CL/CD vs C_m). This graph would show the glide ratio at steady level flight. From the graph it was apparent the pink line had the best glide ratio at steady level flight however based on the coefficient of moment vs alpha graph a significantly higher angle of attack would be required for steady level flight. Therefore the airfoil corresponding to the yellow line was selected. The two graphs mentioned can be found in figure (AC) and (AD) below.

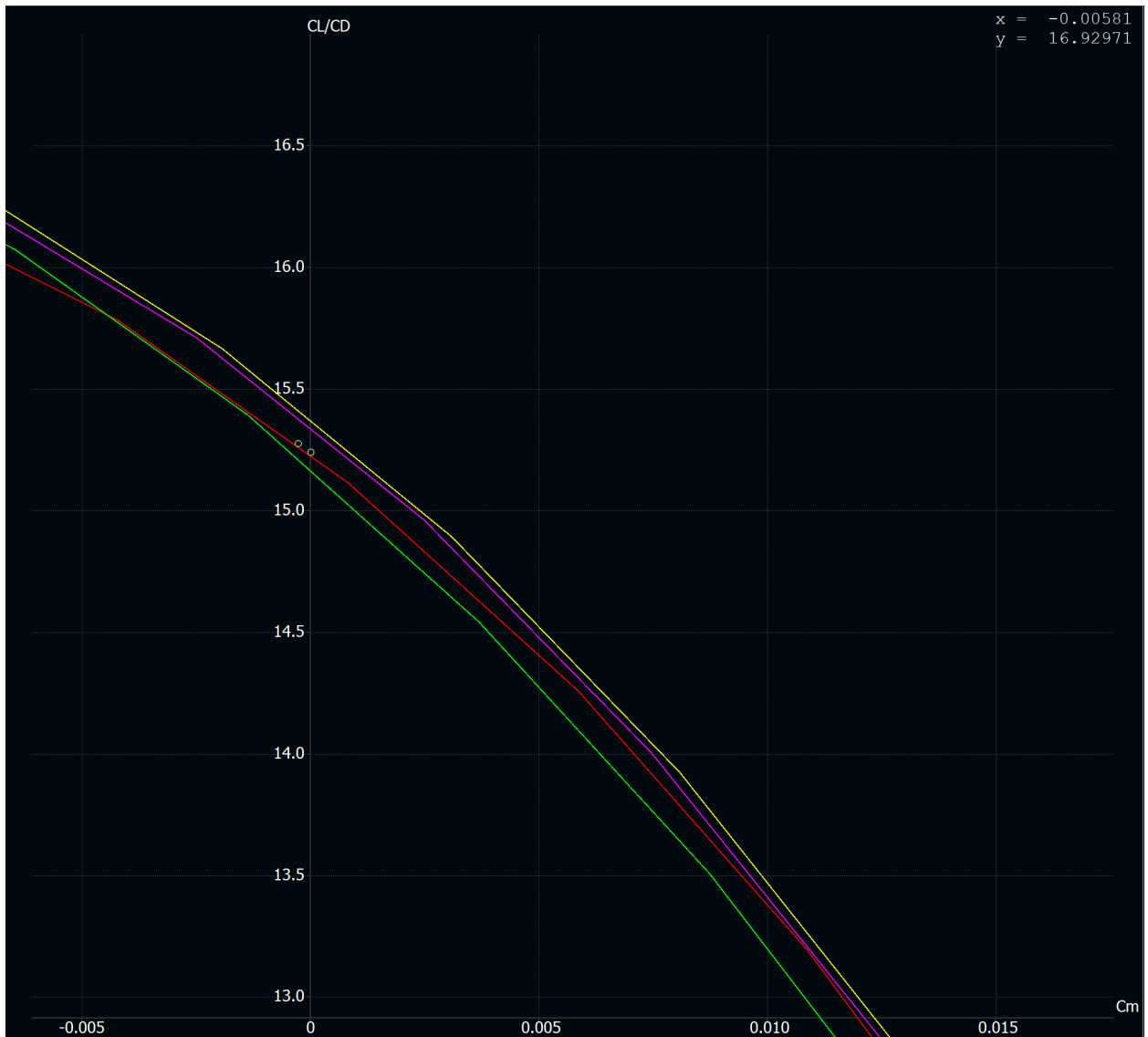


Figure (AC): Coefficient of lift/ coefficient of drag vs coefficient of moment

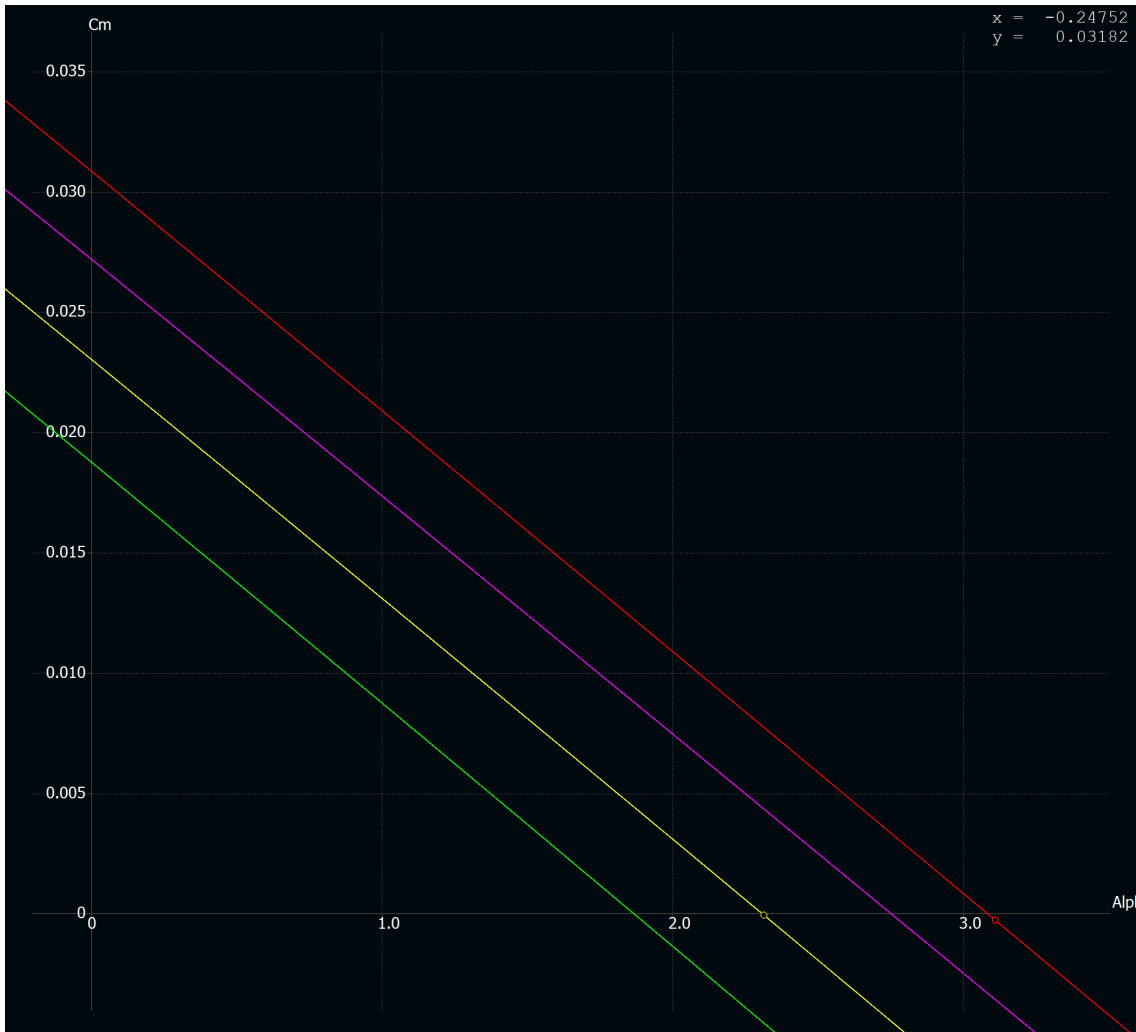


Figure (AD): Coefficient of moment vs angle of attack

A table of the 4 wing designs with their corresponding airfoils can be found below in table 15. The wing design corresponding to the yellow line was selected based on the above discussion.

Line color	Airfoil Inner Wing	Airfoil Outer Wing	Incident Angle	CL @ Cm = 0	CL/CD vs Cm	Alpha @ Cm = 0
Yellow	NACA 3412	NACA 3412	-0.424	0.4415	15.315	2.3
Pink	NACA 2412	NACA 2412	0.008	0.4415	15.334	2.75
Red	NACA 2412	NACA 1412	0.011	0.4415	15.224	3.08
Green	NACA 4412	NACA 4412	-0.861	0.4415	15.161	1.86

Table 15: Wing configurations with airfoils



3. Detailed Design

3.1. Dimensional Parameters

Wing dimensional parameters can be found in table 16 below.

	Wing Section 1	Wing Section 2	Horizontal Stabilizer	Verticle stabiliser
Airfoil	NACA 3412	NACA 3412	NACA 0008	NACA 0015
Tip Chord	5.3 in	4.1 in	3 in	2 in
Root Chord	5.3 in	4.1 in	4 in	4.17 in
Span	15.55 in	12 in	17.2 in	5.2 in
AR	11.52		7.78	1.73
LE Sweep	0 deg	0 deg	6.98 deg	24 deg

Table 16: Aircraft wing dimensions

3.2. Drawing Package

The drawing package is attached to the next 4 pages. Hardware such as nuts and bolts were left out to make the drawings more clear. For more detail on these parts see appendix B containing aircraft assembly instructions



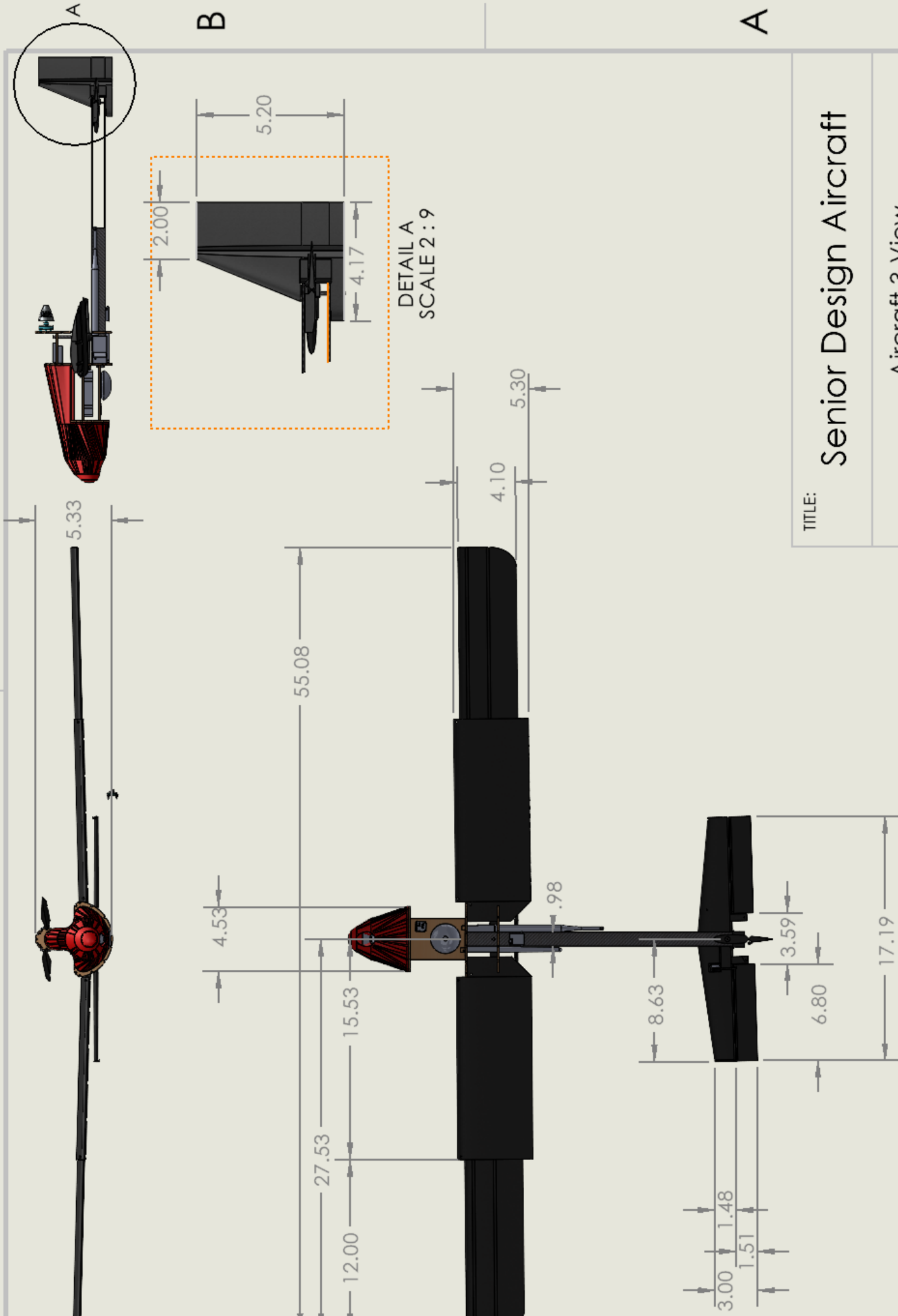
Senior Design Aircraft

Aircraft 3-View

SCALE: 1:16 SHEET 1 OF 4

1

2

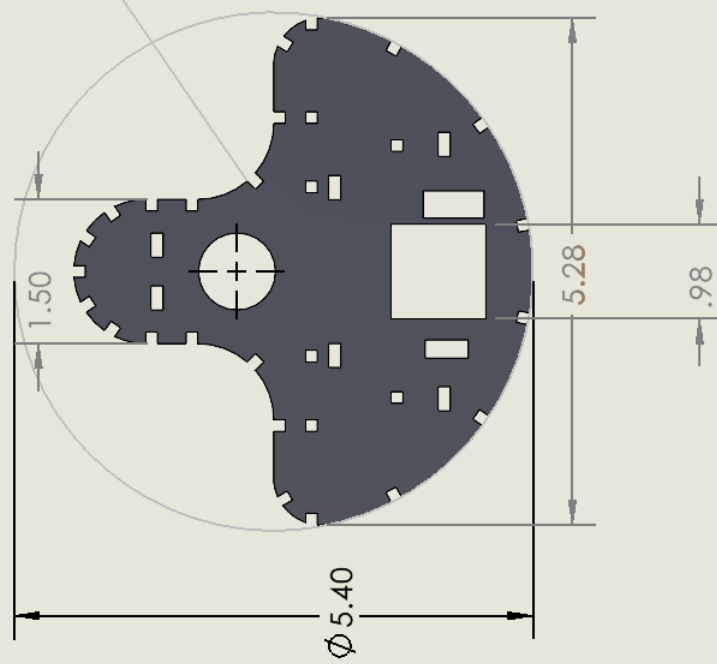
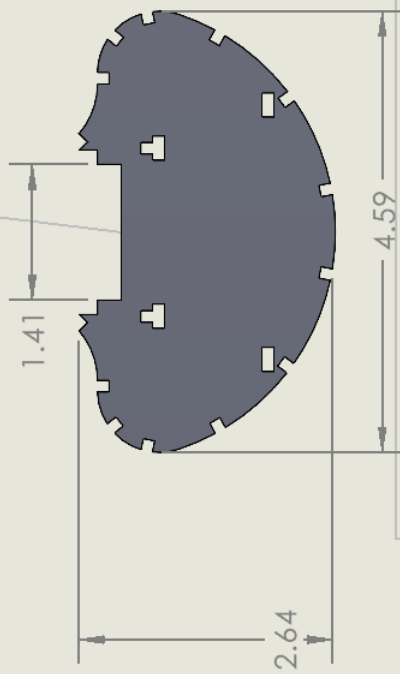
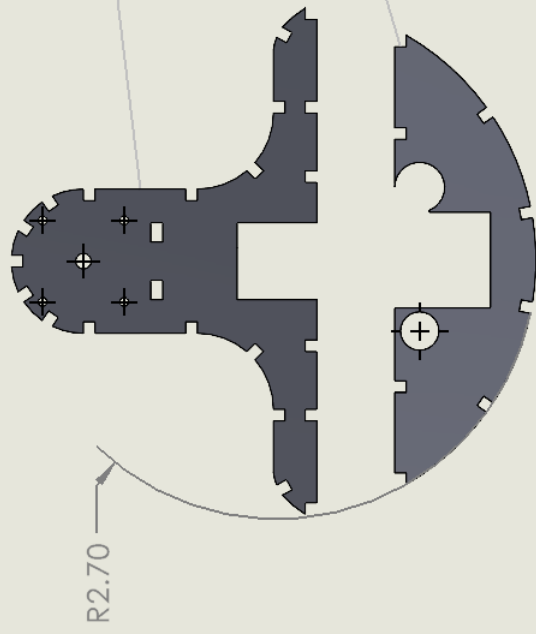
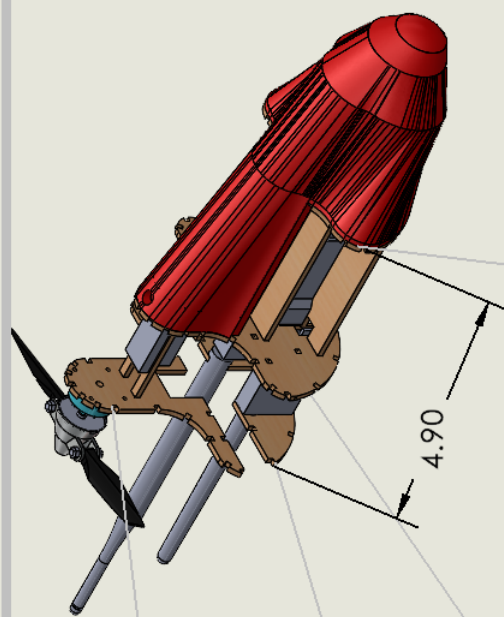


B

A

B

A



B

A

Senior Design Aircraft

Fuselage Breakdown

SCALE: 1:2 SHEET 2 OF 4

1

2

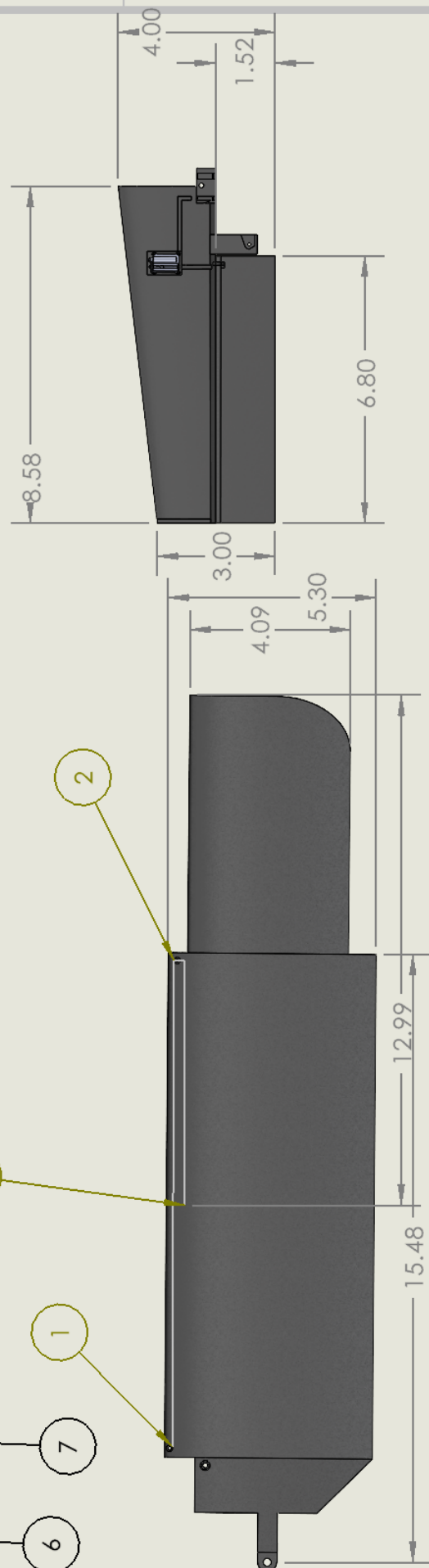
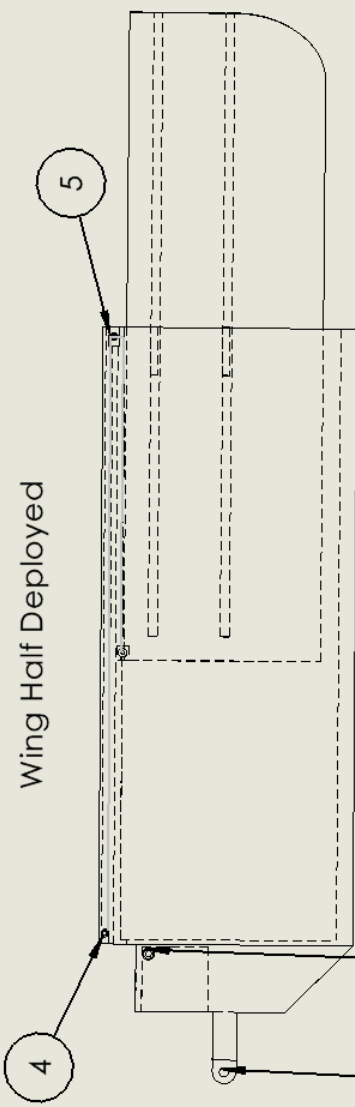
A

A

B

B

Horizontal stabilizer



TITLE:

Senior Design Aircraft

Wing & Tail Design

SCALE: 1:4

SHEET 3 OF 4

2

1

A

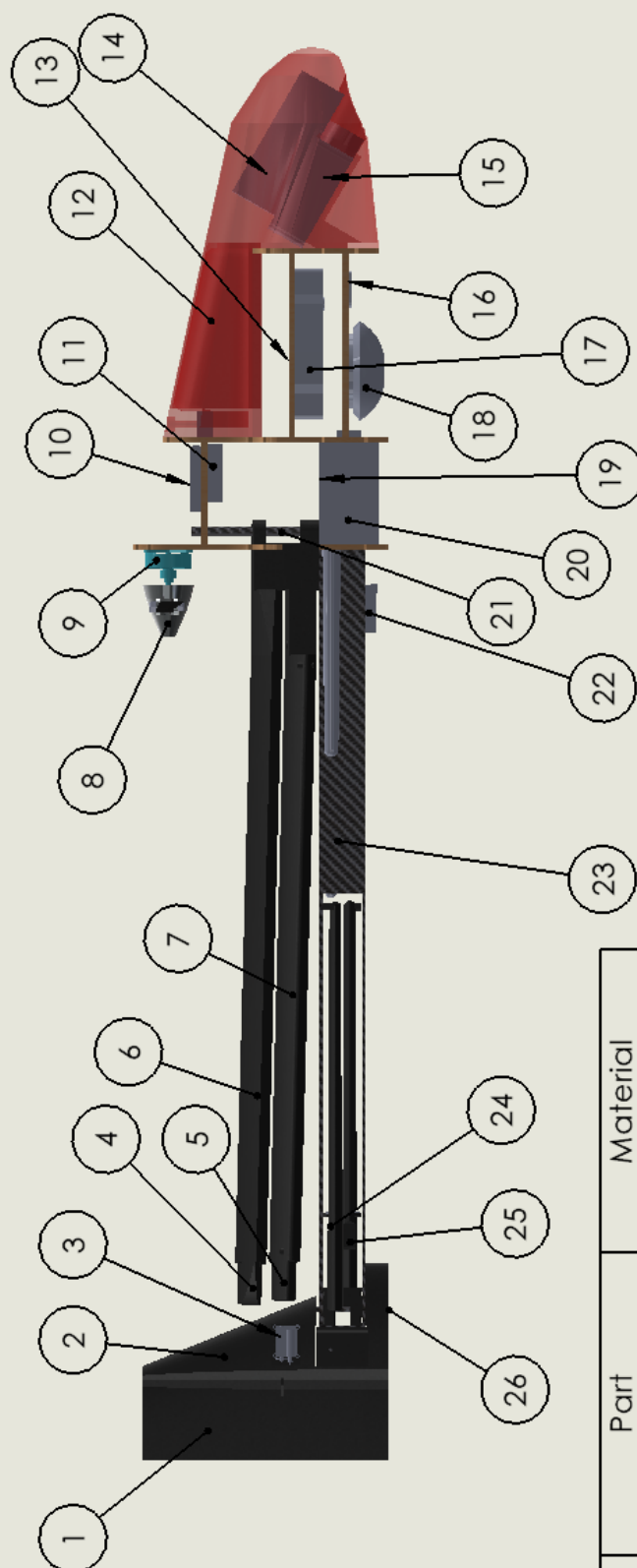
B

1

2

B

A



#	Part	Material	
1	Rudder	PLA	
2	Vertical Stabilizer	PLA	
3	Servo	Electronics	
4	Right Wing B	PLA	
5	Left Wing B	PLA	
6	Right Wing A	PLA	
7	Left Wing A	PLA	
8	Propeller	Plastic	
9	Motor	N/A	
10	ESC	Electronics	
11	Power Module	Electronics	
12	Canopy	PLA	
13	Paylaod Space	N/A	
14	Battery	Electronics	
15	Camera	Electronics	
16	Pressure Sensor	Electronics	
17	PixHawk	Electronics	

TITLE:

Senior Design Aircraft

Detailed Side View

SCALE: 1:4

SHEET 4 OF 4

1

2

4. Electronic Components

The following section outlines the electronic components of the aircraft. This section does not contain information regarding the propulsion system as that is later discussed in section 7.

4.1. Video Transmission

All video footage captured by the aircraft was done with a RunCAM 2. Table 17 below shows the manufacturers specifications on the camera. Although the field of view was 120 degrees the final aircraft had a much smaller one as the camera had to be fitted inside the aircraft and angled downward for better ground surveillance. The high input voltage allowed for the camera to be plugged into the same 3 cell lithium polymer battery as the video transmitter without the need of a Buck converter.

RunCam 2 Specification	
Field of View	120 degrees
Sensor Resolution	4 megapixels
Video Resolution	1920*1440@30fps / 1080p@60fps / 720p@120fps
Video File Format	MOV
Interface	Micro USB
Max Micro SD Card Supported	64 G
Dimension	66mm*38mm*21mm
Battery Capacity	850 mAh
USB Power Input	DC 5-17V
Working Current	<600 mA
Weight	49g with battery 35g without
Battery Life	60-90 minutes

Table 17: RunCam 2 specifications

After video footage was captured, it was stored internally on its micro SD card and transmitted to the ground station using the TS832 48 channel video transmitter module. Specifications for the video transmitter can be found in table 18 below. The video transmitter takes the video signal from the camera and converts it into a radio frequency (RF) signal which can be sent wirelessly through the air. The transmitted RF signal was then sent to the SoloGood

FPV monitor with a built-in video receiver. Specifications for the video receiver can be found in table 19 below.

TS832 (Video Transmitter) Specification	
Power	600 mW
Range	5 km
Input Voltage	DC 7-16V
Working Current	220 mA
Size	54mm*32mm*10mm
Weight	22g
Frequency Band	A, B, E, F, R, D
Antenna	RP-SMA

Table 18: Video transmitter specifications

SoloGood FPV Monitor (Video Reciever) Specification	
Screen Size	4.3 inches
Display Ratio	16:9
Resolution	800*480 ips
Brightness	500 cd/m^2
Frequency Band	A, B, E, F, R
Video File Format	AVI
Power Supply	AC to DC 5v/2A
Internal Battery	1200 mAh
Battery life	2.5 hours
External Battery	DC 5-23V
Antenna	2*RP-SMA
Size	146*80*13mm
Weight	159g

Table 19: Video receiver specifications

As long as the video transmitter and receiver have an overlapping frequency the video can be sent. The video transmitter sends its data on A, B, E, F, R, and D frequency bands and the receiver can pick up A, B, E, F, and R frequency bands. Since there are overlapping



frequency bands the transmitter and receiver are compatible. The frequency table for both the video transmitter and receiver can be found in table 20 below.

Channel / Band	Video Frequency								Video Receiver							
	CH 1	CH 2	CH 3	CH 4	CH 5	CH 6	CH 7	CH 8	CH 1	CH 2	CH 3	CH 4	CH 5	CH 6	CH 7	CH 8
A	5865	5845	5825	5805	5785	5765	5745	5725	5865	5845	5825	5805	5785	5765	5745	5725
B	5733	5752	5771	5790	5809	5828	5847	5866	5733	5752	5771	5790	5809	5828	5847	5866
E	5705	5685	5665	5645	5885	5905	5925	5945	5705	5685	5665	5645	5885	5905	5925	5945
F	5740	5760	5780	5800	5820	5840	5960	5880	5740	5760	5780	5800	5820	5840	5960	5880
R	5658	5695	5732	5769	5806	5843	5880	5917	5658	5695	5732	5769	5806	5843	5880	5917
D	5362	5399	5436	5473	5510	5547	5584	5621								

Table 20: Video frequency chart

The biggest factor in determining the video transmission range is the power of the video transmitter. Most small transmitters operate between 25 mW and 800 mW. The higher the power the higher the range. The downside of a high powered transmitter is they have a higher current draw and use battery capacity much quicker. High powered units can heat up quickly and without proper cooling could malfunction and in severe cases even get damaged. Another factor affecting the range is obstructions. RF signals do not travel through materials such as carbon fiber (aircrafts tail), metal (aircraft battery), or buildings and trees. The manufacturer's suggested transmission range is optimistic at best.

A wiring diagram of the video transmission system can be found in figure (AE) below.

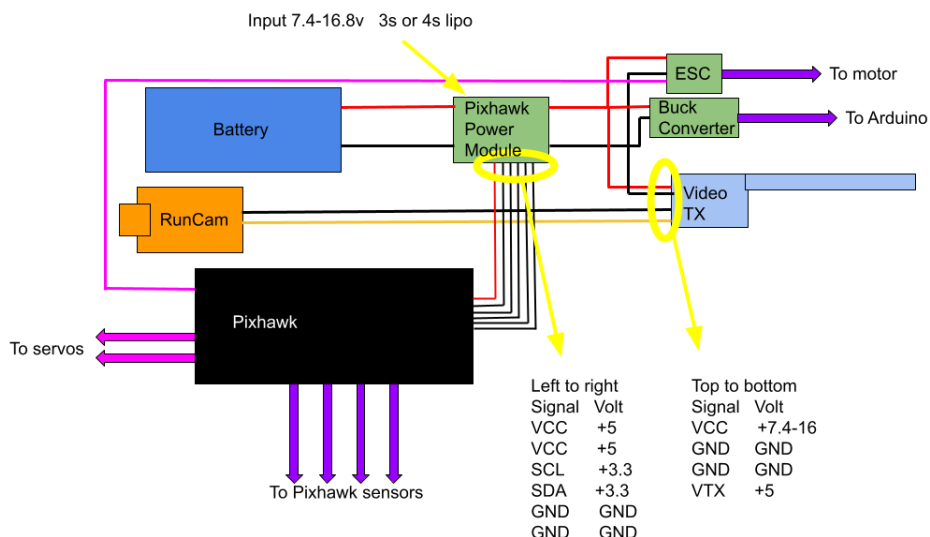


Figure (AE): Video transmission wiring diagram

4.2. Pixhawk

The Pixhawk is a flight controller or system of hardware, that is used with the open source software ArduPilot. The pixhawk is equipped with a large number of sensors that collect data about an aircraft such as orientation, speed, and altitude. A list of the sensors can be found below in table 21. ArduPilot then uses this information to calculate the vehicle's current state and determine the necessary control input required to complete a designated task such as flying to a user specified waypoint. This information is passed on to the servos and motor causing the aircraft's position and orientation to change and the loop then repeats itself. Additionally advanced tasks can be made such as obstacle avoidance precision landing.

PixHawk Sensors	
Gyroscope	Measure vehicle angular rotation rates
Accelerometer	Measure linear acceleration
Magnetometer	Measure heading angle
Barometer	Measure air pressure to determine altitude
Global Positioning Sensor	Provide accurate positioning information
Airspeed Sensor	Determine the aircraft's speed in flight
Current Sensors	Determine current by the battery for motor efficiency
Voltage sensors	Ensure safe operating range and prevent over discharge of battery

Table 21: Pixhawk Sensors

4.3. Digital Spectrum Modulation Transmitter and Receiver

In addition to the pixhawk, if manual control of the aircraft by remote is required, a digital spectrum modulation (DSM) transmitter was required. Since the aircraft had a large carbon fiber spar the DSMX Carbon Fiber Remote Receiver (SPM9746) was selected. This module was selected because it was specifically designed to be used inside carbon fiber aircraft. The carbon fiber creates a radio frequency interference (RFI) and significantly reduces the aircraft's range. The added antennas of the module help overcome RF issues by allowing the antennas to be placed outside the aircraft away from carbon fiber.

DSMX is very similar to DSM as they both work in the 2.4GHz spectrum, however DSMX uses a more advanced frequency hopping algorithm. According to Spektrum, the designing company of the module each transmitter has its own unique frequency shift pattern which is calculated using its own globally unique identifier. Each pattern uses 23 channels in the 2.4 GHz spectrum. The added agility of the frequency shifts in addition to the interference resistant wideband signal, the DSMX transmitter has very good on-channel interference protection with quick reconnection times even in noisy 2.4 GHz environments.



4.4. Glider Data Gathering Components

Arduino Nano

At the heart of the data gathering system is the Arduino Nano. This microcontroller is designed to operate at a voltage of 5V, which is the standard for most microcontrollers to ensure low power consumption while maintaining efficient processing power. The Nano is capable of interfacing with a multitude of sensors due to its multiple input/output pins: 14 digital pins that can read or write binary signals (0V or 5V), and 8 analog pins capable of interpreting voltage levels anywhere from 0V up to 5V, allowing for fine-grained readings from sensors.

MPL3115A2 Pressure and Temperature Sensor

The MPL3115A2 sensor measures atmospheric pressure within a range of 20 to 110 kilopascals (kPa), which can be translated into altitude data. This range allows for precise measurement of altitude changes, as the sensor can detect pressure variations as small as 0.3 Pa, equivalent to an altitude change of less than 30 cm at sea level. The sensor's high range capability ensures that it can accurately report pressure from below sea level up to the stratosphere, making it highly suitable for the vast changes in altitude the glider will experience.

LIS3DH Triple-Axis Accelerometer

The LIS3DH is a versatile accelerometer capable of measuring acceleration in three axes: X, Y, and Z. It provides a dynamic range that can be selected from ± 2 g up to ± 16 g. The lower end of the scale provides higher resolution for slow movements, while the higher end allows the accelerometer to detect and measure rapid or forceful movements without saturating the sensor. At 16 bits of resolution, the sensor offers precise measurement of acceleration, with the ability to detect even minute changes in motion, which is crucial for capturing the nuances of the glider's flight dynamics.

MPM3610 Buck Converter

The MPM3610 buck converter's primary role is to manage the input voltage from the glider's onboard battery, which is typically 12.6V when fully charged. The converter steps this voltage down to a stable 5V with high efficiency, providing a safe and regulated power supply for the Arduino Nano and other 5V components. The use of a buck converter is necessary because the 12.6V from the battery would otherwise be too high and could damage the 5V components, leading to potential system failure. By converting this higher voltage down to 5V before it reaches the Arduino, the system is protected against overvoltage scenarios.



MicroSD Card Breakout Board

The breakout board interfaces with a MicroSD card, which stores the voluminous data generated during flight. This storage solution is capable of handling up to 32 gigabytes (GB) of data, which is more than sufficient for storing the high-resolution data captured by the sensors. The SPI (Serial Peripheral Interface) communication protocol employed by the breakout board allows for high-speed data transfer to the MicroSD card, which is critical for ensuring that data is written quickly and efficiently, preventing data loss during periods of high sensor activity.

In summary, these components work in unison, each with its specific input voltage and sensor range carefully selected to ensure that the glider's flight data is captured comprehensively, accurately, and reliably. The system's design accounts for the wide range of conditions expected during flight, guaranteeing that the sensors operate within their optimal ranges to provide detailed and actionable flight data.

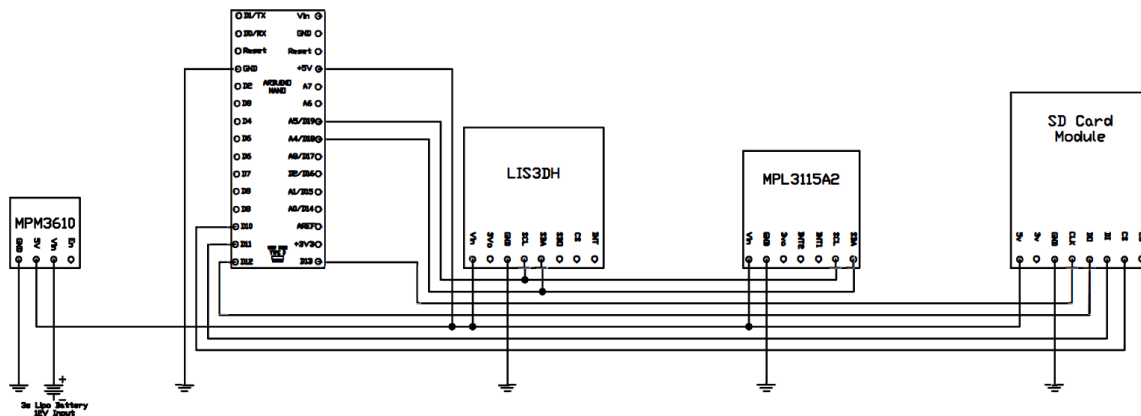


Figure (AQ): Data Gathering Wiring Diagram

5. Performance Characteristics

The following section outlines some aircraft performance characteristics.

5.1. Stability Analysis

The second most important characteristic of the glider, the first being it fit in the rocket, was that it would be statically and dynamically stable. To show that it was statically stable the coefficient of moment vs angle of attack graph was examined. For the aircraft to be stable this graph had to be balanced with a positive stiffness. This means the graph mentioned above had to have a negative slope and intersect the x-axis at a positive value. Any aircraft could have a positive stiffness if the center of gravity was far enough forward. To ensure the center of gravity was not too far forward, the neutral point of the aircraft had to be evaluated. The neutral point of the aircraft can be determined by adjusting the center of gravity until the pitching moment does not vary with angle of attack. The neutral point of the aircraft was located 83 millimeters or 3.267 inches back from the leading edge of the wing. The green line in figure (AF) shows the neutral point where the yellow line shows the aircraft with a balanced and positive stiffness.

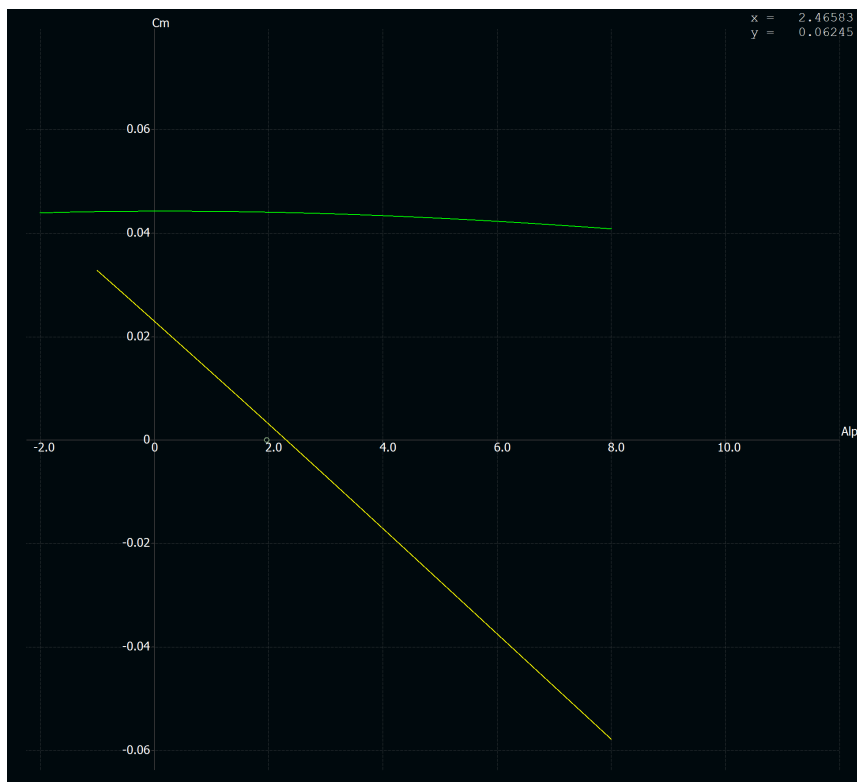


Figure (AF): Coefficient of moment vs alpha graph

The static margin of the aircraft is the distance between the actual center of gravity location and the neutral point. This value is divided by the mean aerodynamic chord and given as a percentage. The mean aerodynamic center was calculated by XFLR5 to be 124.336 mm from the leading edge or 4.89 inches. For aircraft, the static margin is usually between 5 to 15 percent. If the aircraft is too stable it may be unable to pitch and if it is not stable enough it may get tossed about by the wind and have a hard time recovering. For this aircraft a static margin of 10% was used. This meant the payload of the aircraft had to be adjusted so the center of gravity would be located 70.56 mm from the leading edge or 2.778 inches.

With the required stability requirements met, the aircraft's stability could now be analyzed. Using XFLR5 the root locus plots were generated for the lateral and longitudinal stability, these can be found in figure AG and AH below.

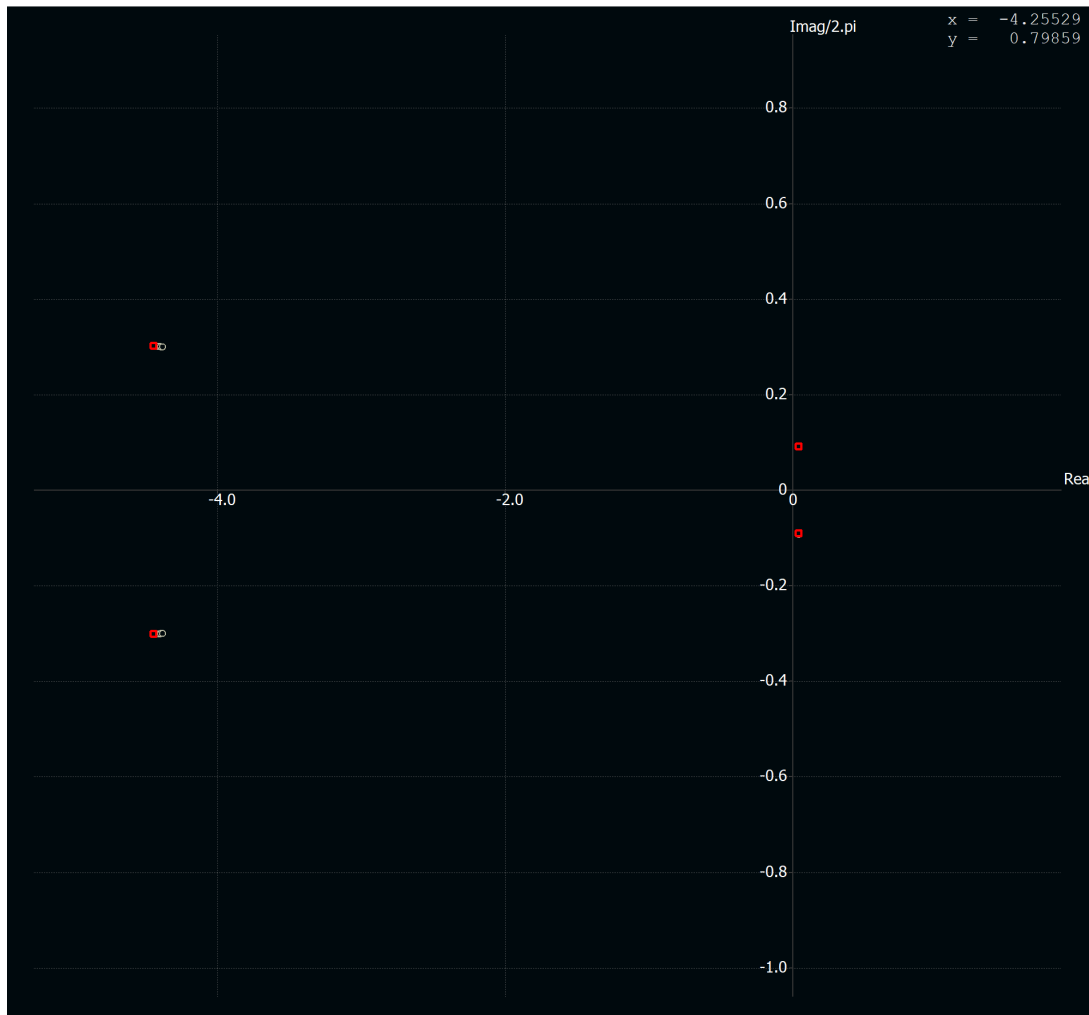


Figure (AG): Longitudinal root locus plot

From figure (AG) It can be seen from the short period mode, the high frequency damped oscillation in pitch that occurs when the aircraft is disturbed, has a high frequency and is heavily damped. This is important as it is almost impossible to determine how the aircraft will interact with the air as it is ejected from the rocket. This graph also displays the phugoid mode. It can be seen that in this mode the aircraft is very lightly damped and has a low frequency. Which means the oscillation persists for several cycles before dying out.

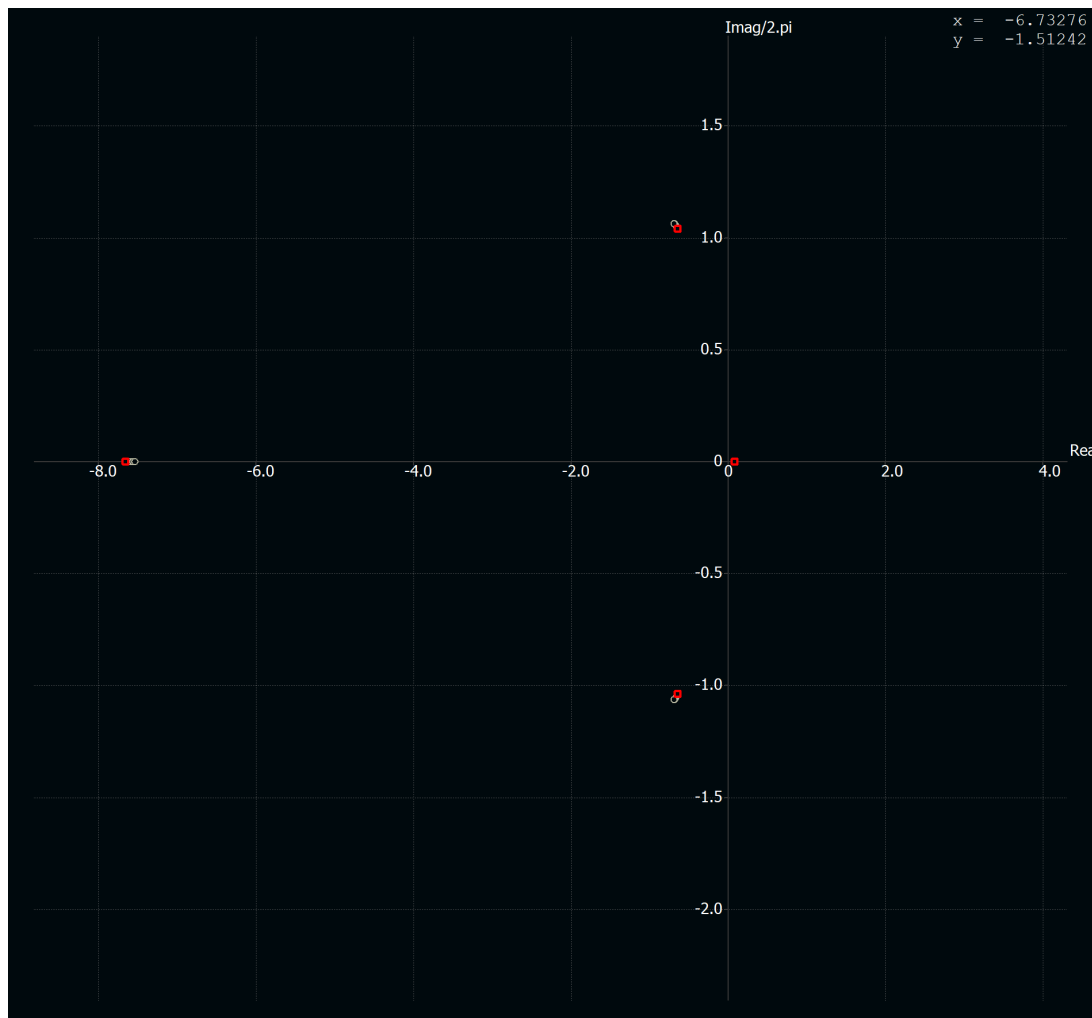


Figure (AH): Lateral root locus plot

From figure (AH) above, it can be seen the roll is heavily damped. This was due to the aircraft's large wingspan and dihedral wings. The doctoral modes corresponding to the dutch roll (phugoid-like oscillation in roll and yaw) is seen to have a high frequency and light damping. The spiral mode is non damped and non oscillating which needs to be taken in mind while flying. This mode can be triggered by stall so it is important to maintain adequate airspeed to prevent this from happening. Redesigning the aircraft's tail and making it bigger could help enhance the spiral mode damping.

5.2. Estimated drag

The lift and drag characteristics were evaluated using OpenVSP. The parasite drag solver used linear inviscid models to calculate the drag over each aircraft component and

summed them together. These results were not very accurate especially at high angles of attack due to flow separation. The greatest source of drag came from the wetted surface area of the wing. The total drag coefficient was estimated to be 0.022.

5.3. Turn Radius

Since the aircraft was supposed to loiter over an area and collect video footage, it was important to know the turn radius of the aircraft. This could be calculated using the aircraft's speed and bank angle or speed and load factor. Before this could be determined it was important to know whether the aircraft could bank at all given it only had rudder and elevator control. To determine if the aircraft would roll, the roll rate was calculated using the equation below.

$$\omega = L_R / I_x$$

In the above equation L_R is the rolling moment and I_x is the aircraft's inertia. The inertia was found in solidworks and the rolling moment coefficient was found using the equation below.

$$L_R = 0.5 * \rho * V^2 * S * b * CL_R * \delta_R$$

CL_R is the non dimensional rolling coefficient due to rudder deflection and δ_R is the rudder deflection angle in radians. Simulating a 3 degree rudder deflection in xflr5 CL_R could be calculated by the program. This value was found to be 0.11332. Plugging all variables into the above equation the rolling rate was found to be 1.88 rad/s. Wingspan and wing area were converted from inches to m.

$$\omega = (.5 * 1.225 * 17.34^2 * 1.698 * 1.397 * .11332 * .05) / 0.137 = 1.88 \text{ rad/s or } 107 \text{ deg/s}$$

With this information it was evident the aircraft was very capable of rolling with rudder deflection. The turn radius could then be calculated using the equation below.

$$R = \frac{V^2}{g \tan \phi} = \frac{V^2}{g \sqrt{n^2 - 1}}$$

Since the aircraft was capable of achieving any roll angle its turn radius was limited only by the load factor n . To prevent the wings from snapping in flight the aircraft would be kept with a maximum load of 2g. This allowed for a maximum bank angle of 60 degrees resulting in a turn radius of 19.16 meters or 62 ft. The turn rate could then be calculated using the equation below.

$$\dot{\psi} = V/R = 18/19.16 = 0.9394 \text{ rad/s or } 54 \text{ deg/s}$$



This means the aircraft would take approximately 3.34 seconds to make a 180 degree turn or 6.68 second to do a full 360.

5.4. Stall speed

The Stall speed was calculated using the formula below

$$V_{stall} = \sqrt{2w/\rho S C_l_{max}}$$

C_l_{max} is the maximum coefficient of lift that the aircraft can achieve. For this aircraft this value was 1 achieved at an 8 degree angle of attack. This gave a stall speed of 3.69 m/s or 8.25 mph.



6. Manufacturing Plan

The following sections outline the manufacturing of the aircraft.

6.1. Materials Considered

Many different materials were analyzed for the manufacturing of the airplane. The materials considered are listed below.

- **Expanded Polystyrene (EPS) Foam:** EPS was initially seen as an appealing building material due to its relatively low cost and ease of use. The team also has extensive experience with cutting EPS to form wings and various fuselage components. Using a hot wire, exact wings could be cut for each iteration of the design. This material was ultimately decided against as the resulting tolerances of the manufacturing process were too large and this method did not allow for stiff complex geometries.
- **Carbon Fiber:** Carbon fiber was considered due to its high strength-to-weight ratio and ability to carry large bending moments. This material was used for the aircraft's tail as it had to be hollow to allow room for the folding horizontal stabilizer but still remain rigid under aircraft pitch and yaw maneuvers.
- **Wood:** Balsa wood was considered for its outstanding strength to weight ratio, its ability to absorb shock and vibration, the ease of cutting with simple hand tools and for a simple assembly process. This was the material chosen for the aircraft's longerons. Bass wood was considered for its high strength and tight wood grain. Although it weighs approximately 3.6 times as much by volume as balsa wood, it is a lot stiffer as it is a healthier wood. This made it a perfect choice for the frame of the aircraft. In addition, the use of a laser cutter allowed for tolerances up to the nearest thousandths of an inch which made the material easy to work with.
- **MonoKote:** MonoKote is a thin protective film used to cover the aircraft frame. When heat is applied the back becomes sticky and it adheres to the aircraft's longerons and stringers forming the aircraft's skin. This material was used only for the fuselage because there was a concern that the ejection charge from the rocket could melt a hole through it.
- **Polylactic Acid (PLA):** This material was considered because using a 3d printer it is capable of making strong, complex shapes, with tight tolerances and is relatively cheap. The only downside to this material is weight. For ease of manufacturing and prototyping, weight was not a main concern for this project. Future design iterations could use lighter materials so the aircraft could carry a heavier payload with similar wing loading. This material was also a good choice because it does not soften until 60 degrees celsius meaning the brief heat from the ejection charge would not melt through it. Lightweight



pla was briefly experimented with but it was difficult to achieve consistent tolerances so the material went unused for the final aircraft design. If more time was available this would have been the better option.

- **Glue:** Wood glue was considered for this project because it is less dense than epoxy meaning it is slightly lighter and creates strong wood on wood bonds. This material was used to connect the longerons to the frame. Hot glue was used as a means to connect some electronics to the aircraft as it allowed for variable depth unlike the use of double sided sticky tape. Epoxy was used to attach wood on carbon fiber surfaces and to help reinforce some PLA components.

6.2. Material Analysis

Materials were analyzed based on multiple things such as strength, cost, and weight. Each of these categories were then weighted based on their importance to the project. This breakdown can be found below.

- **Tolerance (30):** The most important material property for this project was its ability to have tight tolerances. If parts were too big they may rub and not fit together or in the case of holes, cause too much slop in the movement of mechanical parts. If parts are too small they may not come in contact with their desired parts and could flop around or in the case of holes, not allow bolts to fit. If the parts were not the correct size they would not fit together and the entire aircraft would suffer. Materials that have tighter tolerances are scored higher.
- **Strength (25):** The aircraft was expected to have high g-loads and needed to be strong enough to deploy from the rocket without ripping itself apart. THis category represents the material ability to withstand various flight conditions. Materials that are stronger are scored higher.
- **Weight (20):**The aircraft was designed to have glider like characteristics so it was important to keep the weight low to minimize wing loading. Since the goal of this project was to determine the feasibility of putting an aircraft in a rocket future iterations could decrease structural weigh for a lighter plane or use the saved weight for a larger payload. For these reasons weight was not a primary concern.
- **Cost (15):** Since this entire project is self funded it is desirable to keep costs as low as possible. For the aircraft it was decided it was more important to have high quality parts that function properly then get low quality parts and have a potential safety hazard.

- **Ease of Manufacturing (10):** The knowledge and skill involved in working with each material was evaluated. A higher score indicates either a low skill manufacturing process or one that a team member had sufficient experience with.

Material selection was based on table 22 below.

Figure of Merit	Scoring Weight	EPS Foam	Balsa Wood	Bass Wood	PLA	Lightweight PLA	Carbon Fiber	MonoKote
Tolerance	0.3	3	5	5	5	3	5	5
Strength	0.25	1	2	3	4	4	5	1
Weight	0.2	5	4	3	1	3	4	5
Cost	0.15	5	5	4	4	3	2	5
Manufacturing Ease	0.1	4	5	5	5	3	4	5
Total	1	3.3	4.05	3.95	3.8	3.25	4.25	4

Table 22: Material Selection Figure of Merit

Different materials were more appropriate for different portions of the aircraft. From this figure of merit chart it is evident EPS foam and lightweight PLA are both poor choices for the manufacturing of the aircraft and should be avoided if possible.

6.3. Process selection

The manufacturing process of a build-up plane was selected as opposed to a foam construction due to the need of a high strength structure. The largest loads on the aircraft's structure will come from exiting the rocket, the pusher-prop propeller configuration, and the moment produced by the aircraft's tail. Using a build up design, different areas of the aircraft could be designed to take specific loads. This building process, although significantly harder than making a foam core and cutting out spots for components, would provide the required strength for the aircraft.

6.4. Component Manufacturing Process

Due to the large number of steps required to build this aircraft, detailed instructions involving the assembly can be found in the appendix.

Laser Cut Parts

Laser cutting proved to be the fastest, most economical, and most efficient method for fabricating intricate bulkheads and formers. Employing an OmTech 40-watt CO₂ laser cutter, numerous components were expertly crafted in under two minutes. However, a potential drawback of laser cutting was the illusion of absolute precision. If the machine was not calibrated with utmost care, significant errors could arise.



To combat these potential inaccuracies, parts were rigorously inspected using calipers and protractors, ensuring that all 90-degree angles were indeed right angles and that all dimensions aligned with the specifications outlined in the CAD designs. In the event of any discrepancies, the affected components were promptly reprinted.

Warping in basswood sheets presented a particularly challenging issue, as it prevented them from lying perfectly flat within the laser cutter. To address this warping, the sheets were carefully sprayed with water and placed between two weighted glass plates, maintaining their flatness. As the water evaporated, the wood retained its flattened state. Before being imported into LightBurn software for cutting, all design files were diligently saved in DXF format.

3D Printing

3D printing played a significant role in the fabrication of various aircraft components. While not as structurally efficient as balsawood construction, 3D printing enabled the production of intricate 3D shapes without the laborious process of manual assembly. Additionally, parts could be printed for several hours without requiring constant supervision. This methodology also facilitated mass production whenever necessary.

A crucial aspect of 3D printing aerodynamic surfaces was its ability to withstand brief exposure to heat without melting. This was particularly important for components located near the rocket's ejection charge. Moreover, 3D printing of the wings contributed to size reduction, as no additional support structures were required to maintain the airfoil's shape when using a 3-layer thick shell. This design allowed the outer wing section to seamlessly integrate with the section mounted to the aircraft's fuselage.

3D printing also offered flexibility in structural and weight management. Component thicknesses and infill densities could be manipulated within the slicing software to achieve either enhanced strength or reduced weight. A noteworthy feature of this slicing software was the ability to utilize horizontal expansion to thicken shells that were inadvertently designed too thin in SolidWorks files. Ultimaker Cura and Superslicer served as the primary tools for converting STL files into G-code, which could then be executed on one of the three available printers: Creality Ender3, Voron 2.4, or FLSun V400.



6.5. Cost Breakdown

Since this project was not sponsored, the budget for the aircraft was limited only by what the team was willing to spend. Table 23 shows the cost of all components of the aircraft.

Component	Cost	Quantity	Total
Carbon Fiber	28.22	1	28.22
PLA	19.99	3	59.97
Motor	16.99	1	16.99
ESC	17.99	1	17.99
Propeller	11.5	2	23
Bass Wood	21.99	1	21.99
Balsa Wood	15.99	1	15.99
Nuts, Bolts, and Springs	85	1	85
Pixhawk	279.99	1	279.99
Runcam	99.99	1	99.99
DSM RX	39.99	1	39.99
Battery	36.99	1	36.99
FPV Monitor	62.99	1	62.99
FPV TX	19.99	1	19.99
Epoxy	19.99	1	19.99
Arduino	12.99	1	12.99
Arduino sensors	25.99	1	25.99
Servos	32.99	2	65.98
Telemetry TX/RX	70.99	1	70.99
Other	28.14	1	28.14
Total			\$ 1033.17

Table 23: Aircraft cost breakdown

The total cost of the aircraft was around \$1033.17. Important to note in Table 23 above is the cost of the nuts, bolts, and sprigs is approximate as many were bought and some went unused.

6.6. Milestone Chart

The manufacturing of different aircraft components were organized in a milestone chart which is shown in table 24. The planned times are shown in black and the actual times are shown in horizontal gold bars. Most of the deviation from the planned times was the result of redesigning parts when testing data came back with less than satisfactory results. The red box represents the current week.

Aircraft Construction															
ACTIVITY	Plan Duration							Actual Duration							
	9/1	9/8	9/15	9/22	9/29	10/6	10/13	10/20	10/27	11/3	11/10	11/17	11/24	12/1	12/8
Tail															
Fuselage															
Canopy															
Wings															

Table 24: Aircraft construction milestone chart

7. Testing Plan

The following section outlines the testing of aircraft components.

7.1. Testing Objectives

Testing each aircraft component was vital in ensuring the aircraft would function as intended. A testing plan was created to evaluate the performance of the main components of the aircraft. These components include the propulsion system, springs for wing deployment, structural rigidity, and flight testing. Testing occurred as parts arrived and continued through the build of the project. This process was done iteratively until desired results were obtained. The testing process can be seen in figure (AI).

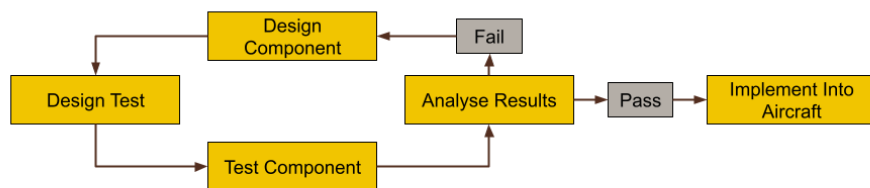


Figure (AI): Testing Process

7.2. Testing Schedule

The general testing schedule is shown below in table 25. The planned times are shown in black and the actual times are shown in horizontal gold bars. Most of the deviation from the planned times was the result of waiting for new parts when testing data came back with less than satisfactory results. The red box represents the current week.

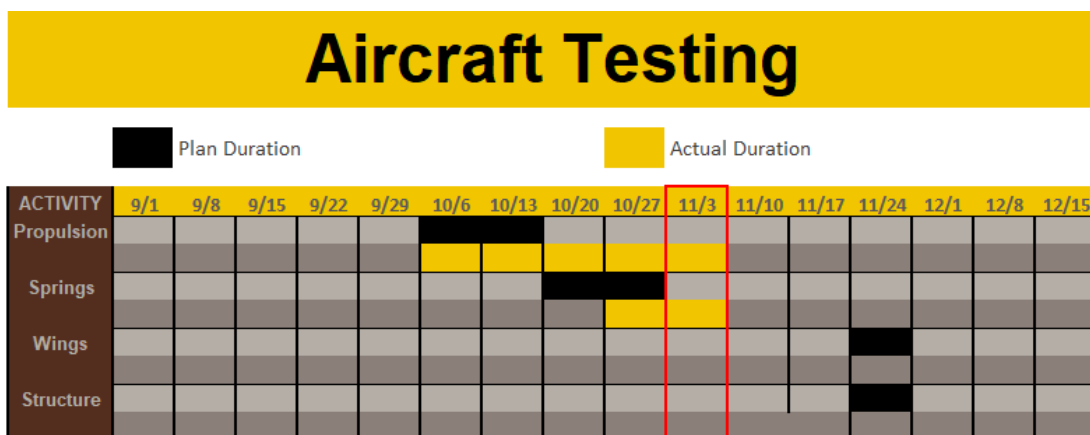


Table 25: Aircraft testing milestone chart

7.3. Propulsion Testing

The selection of the aircraft motor began by using ecalc, a physics and mathematical model which can simulate flight characteristics of aircraft by imputing aircraft components such as battery size and capacity, motor, speed controller size, and propeller size, as well as aircraft characteristics like weight, and wingspan. It uses this data to calculate the aircraft's partial motor loads, and estimated aircraft speeds. The data ran through this program, and the results can be seen in figure (AJ) below.

General	Model Weight: 1400 g incl. Drive 49.4 oz	# of Motors: 1 (on same Battery)	Wingspan: 1397 mm 55 inch	Wing Area: 16.97 dm ² 263 in ²	Drag: coefficient 0.022 Cd	Field Elevation: 500 m.ASL 1640 ft.ASL	Air Temperature: 25 °C 77 °F	Pressure (QNH): 1013 hPa 29.91 inHg																																																																																																																																																																																																																										
Battery Cell	Type (Cont. / max. C) - charge state: LiPo 2200mAh - 35/50C	Configuration: 3 S 1 P	Cell Capacity: 2200 mAh	max. discharge: 85% ▾	Resistance: 0.0073 Ohm	Voltage: 3.7 V	C-Rate: 35 C cont. 50 C max	Weight: 57 g 2 oz																																																																																																																																																																																																																										
Controller	Type - Timing: max 20A	Current: 20 A cont. 20 A max	Resistance: 0.01 Ohm	Weight: 25 g 0.9 oz	Battery extension Wire: AWG10=5.27mm ²	Length: 0 mm 0 inch	Motor extension Wire: AWG10=5.27mm ²	Length: 0 mm 0 inch																																																																																																																																																																																																																										
Motor	Manufacturer - Type (Kv) - Cooling: (t = discontinued) SunnySky - X2304-1800 V3 (1800)	KV (w/o torque): 1800 rpm/V	no-load Current: 0.5 A @ 10 V	Limit (up to 15s): 160 W	Resistance: 0.113 Ohm	Case Length: 19 mm 0.75 inch	# mag. Poles: 14	Weight: 21 g 0.7 oz																																																																																																																																																																																																																										
Propeller	Type - yoke twist: custom	Diameter: 6 inch 152.4 mm	Pitch: 4 inch 101.6 mm	# Blades: 2	PConst / TConst: 1.20 / 1.0	Gear Ratio: 1 : 1	Flight Speed: 0 km/h 0 mph	calculate																																																																																																																																																																																																																										
Remarks: <table border="1"> <tbody> <tr> <td>Battery</td> <td>Motor @ Optimum Efficiency</td> <td>Motor @ Maximum</td> <td>Propeller</td> <td>Total Drive</td> <td>Airplane</td> </tr> <tr> <td>Load: 5.34 C</td> <td>Current: 6.51 A</td> <td>Current: 11.74 A</td> <td>Static Thrust: 600 g</td> <td>Drive Weight: 239 g</td> <td>All-up Weight: 1400 g</td> </tr> <tr> <td>Voltage: 10.84 V</td> <td>Voltage: 10.89 V</td> <td>Voltage: 10.73 V</td> <td>21.2 oz</td> <td>8.4 oz</td> <td>49.4 oz</td> </tr> <tr> <td>Rated Voltage: 11.10 V</td> <td>Revolutions*: 17541 rpm</td> <td>Revolutions*: 16062 rpm</td> <td>Revolutions*: 16062 rpm</td> <td>Power-Weight: 93 W/kg</td> <td>82.5 g/dm²</td> </tr> <tr> <td>Energy: 24.42 Wh</td> <td>electric Power: 70.9 W</td> <td>electric Power: 125.9 W</td> <td>Stall Thrust: - g</td> <td>42 W/lb</td> <td>27 oz/ft²</td> </tr> <tr> <td>Total Capacity: 2200 mAh</td> <td>mech. Power: 60.3 W</td> <td>mech. Power: 103.7 W</td> <td>- oz</td> <td>Thrust-Weight: 0.43 : 1</td> <td>Cubic Wing Load: 20.0</td> </tr> <tr> <td>Used Capacity: 1870 mAh</td> <td>Efficiency: 85.1 %</td> <td>Efficiency: 82.4 %</td> <td>avail.Thrust @ 0 km/h: 600 g</td> <td>Current @ max: 11.74 A</td> <td>est. Stall Speed: 43 km/h</td> </tr> <tr> <td>min. Flight Time: 9.6 min</td> <td>est. Temperature: 47 °C</td> <td>est. Temperature: 117 °F</td> <td>avail.Thrust @ 0 mph: 21.2 oz</td> <td>P(in) @ max: 130.3 W</td> <td>27 mph</td> </tr> <tr> <td>Mixed Flight Time: 9.8 min</td> <td></td> <td></td> <td>Pitch Speed: 98 km/h</td> <td>P(out) @ max: 103.7 W</td> <td>est. Speed (level): 81 km/h</td> </tr> <tr> <td>Weight: 171 g</td> <td></td> <td></td> <td>Tip Speed: 61 mph</td> <td>Efficiency @ max: 79.6 %</td> <td>50 mph</td> </tr> <tr> <td>6 oz</td> <td></td> <td></td> <td>Specific Thrust: 4.61 g/W</td> <td>0.06 Nm</td> <td>est. Speed (vertical): - km/h</td> </tr> <tr> <td></td> <td></td> <td></td> <td>Power: 127.3 W</td> <td>286 mph</td> <td>- mph</td> </tr> <tr> <td></td> <td></td> <td></td> <td></td> <td>Climb Capacity: 2692 m</td> <td>est. rate of climb: 4.7 m/s</td> </tr> <tr> <td></td> <td></td> <td></td> <td></td> <td>0.16 oz/W</td> <td>(~20...25°) 924 ft/min</td> </tr> </tbody> </table>									Battery	Motor @ Optimum Efficiency	Motor @ Maximum	Propeller	Total Drive	Airplane	Load: 5.34 C	Current: 6.51 A	Current: 11.74 A	Static Thrust: 600 g	Drive Weight: 239 g	All-up Weight: 1400 g	Voltage: 10.84 V	Voltage: 10.89 V	Voltage: 10.73 V	21.2 oz	8.4 oz	49.4 oz	Rated Voltage: 11.10 V	Revolutions*: 17541 rpm	Revolutions*: 16062 rpm	Revolutions*: 16062 rpm	Power-Weight: 93 W/kg	82.5 g/dm ²	Energy: 24.42 Wh	electric Power: 70.9 W	electric Power: 125.9 W	Stall Thrust: - g	42 W/lb	27 oz/ft ²	Total Capacity: 2200 mAh	mech. Power: 60.3 W	mech. Power: 103.7 W	- oz	Thrust-Weight: 0.43 : 1	Cubic Wing Load: 20.0	Used Capacity: 1870 mAh	Efficiency: 85.1 %	Efficiency: 82.4 %	avail.Thrust @ 0 km/h: 600 g	Current @ max: 11.74 A	est. Stall Speed: 43 km/h	min. Flight Time: 9.6 min	est. Temperature: 47 °C	est. Temperature: 117 °F	avail.Thrust @ 0 mph: 21.2 oz	P(in) @ max: 130.3 W	27 mph	Mixed Flight Time: 9.8 min			Pitch Speed: 98 km/h	P(out) @ max: 103.7 W	est. Speed (level): 81 km/h	Weight: 171 g			Tip Speed: 61 mph	Efficiency @ max: 79.6 %	50 mph	6 oz			Specific Thrust: 4.61 g/W	0.06 Nm	est. Speed (vertical): - km/h				Power: 127.3 W	286 mph	- mph					Climb Capacity: 2692 m	est. rate of climb: 4.7 m/s					0.16 oz/W	(~20...25°) 924 ft/min																																																																																																																																						
Battery	Motor @ Optimum Efficiency	Motor @ Maximum	Propeller	Total Drive	Airplane																																																																																																																																																																																																																													
Load: 5.34 C	Current: 6.51 A	Current: 11.74 A	Static Thrust: 600 g	Drive Weight: 239 g	All-up Weight: 1400 g																																																																																																																																																																																																																													
Voltage: 10.84 V	Voltage: 10.89 V	Voltage: 10.73 V	21.2 oz	8.4 oz	49.4 oz																																																																																																																																																																																																																													
Rated Voltage: 11.10 V	Revolutions*: 17541 rpm	Revolutions*: 16062 rpm	Revolutions*: 16062 rpm	Power-Weight: 93 W/kg	82.5 g/dm ²																																																																																																																																																																																																																													
Energy: 24.42 Wh	electric Power: 70.9 W	electric Power: 125.9 W	Stall Thrust: - g	42 W/lb	27 oz/ft ²																																																																																																																																																																																																																													
Total Capacity: 2200 mAh	mech. Power: 60.3 W	mech. Power: 103.7 W	- oz	Thrust-Weight: 0.43 : 1	Cubic Wing Load: 20.0																																																																																																																																																																																																																													
Used Capacity: 1870 mAh	Efficiency: 85.1 %	Efficiency: 82.4 %	avail.Thrust @ 0 km/h: 600 g	Current @ max: 11.74 A	est. Stall Speed: 43 km/h																																																																																																																																																																																																																													
min. Flight Time: 9.6 min	est. Temperature: 47 °C	est. Temperature: 117 °F	avail.Thrust @ 0 mph: 21.2 oz	P(in) @ max: 130.3 W	27 mph																																																																																																																																																																																																																													
Mixed Flight Time: 9.8 min			Pitch Speed: 98 km/h	P(out) @ max: 103.7 W	est. Speed (level): 81 km/h																																																																																																																																																																																																																													
Weight: 171 g			Tip Speed: 61 mph	Efficiency @ max: 79.6 %	50 mph																																																																																																																																																																																																																													
6 oz			Specific Thrust: 4.61 g/W	0.06 Nm	est. Speed (vertical): - km/h																																																																																																																																																																																																																													
			Power: 127.3 W	286 mph	- mph																																																																																																																																																																																																																													
				Climb Capacity: 2692 m	est. rate of climb: 4.7 m/s																																																																																																																																																																																																																													
				0.16 oz/W	(~20...25°) 924 ft/min																																																																																																																																																																																																																													
<input type="button" value="share"/> <input type="button" value="performanceCalc"/> <input type="button" value="add to >>"/> <input type="button" value="Download.csv (0)"/> <input type="button" value="<< clear"/>																																																																																																																																																																																																																																		
Motor Partial Load <table border="1"> <thead> <tr> <th rowspan="2">Propeller rpm</th> <th rowspan="2">Throttle %</th> <th rowspan="2">Current (DC) A</th> <th rowspan="2">Voltage (DC) V</th> <th rowspan="2">el. Power W</th> <th colspan="2">Efficiency %</th> <th colspan="2">Thrust g</th> <th colspan="2">Spec. Thrust g/W</th> <th colspan="2">Pitch Speed km/h</th> <th colspan="2">Speed (level) mph</th> <th rowspan="2">Motor Run Time (85%) min</th> </tr> <tr> <th>g</th> <th>oz</th> <th>oz/W</th> <th>km/h</th> <th>mph</th> <th>km/h</th> <th>mph</th> </tr> </thead> <tbody> <tr><td>2400</td><td>13</td><td>0.1</td><td>11.1</td><td>0.8</td><td>45.9</td><td>13</td><td>0.5</td><td>17.8</td><td>0.63</td><td>15</td><td>9</td><td>-</td><td>-</td><td>1652.6</td></tr> <tr><td>3600</td><td>20</td><td>0.2</td><td>11.1</td><td>1.8</td><td>64.0</td><td>30</td><td>1.1</td><td>16.6</td><td>0.58</td><td>22</td><td>14</td><td>-</td><td>-</td><td>682.1</td></tr> <tr><td>4800</td><td>26</td><td>0.3</td><td>11.1</td><td>3.7</td><td>73.8</td><td>54</td><td>1.9</td><td>14.3</td><td>0.51</td><td>29</td><td>18</td><td>-</td><td>-</td><td>331.6</td></tr> <tr><td>6000</td><td>33</td><td>0.6</td><td>11.1</td><td>6.8</td><td>79.0</td><td>84</td><td>3.0</td><td>12.3</td><td>0.43</td><td>37</td><td>23</td><td>-</td><td>-</td><td>181.6</td></tr> <tr><td>7200</td><td>40</td><td>1.0</td><td>11.1</td><td>11.4</td><td>81.9</td><td>121</td><td>4.3</td><td>10.6</td><td>0.37</td><td>44</td><td>27</td><td>-</td><td>-</td><td>108.7</td></tr> <tr><td>8400</td><td>48</td><td>1.6</td><td>11.1</td><td>17.7</td><td>83.4</td><td>164</td><td>5.8</td><td>9.3</td><td>0.33</td><td>51</td><td>32</td><td>-</td><td>-</td><td>69.6</td></tr> <tr><td>9600</td><td>55</td><td>2.4</td><td>11.0</td><td>26.2</td><td>84.1</td><td>214</td><td>7.6</td><td>8.2</td><td>0.29</td><td>59</td><td>36</td><td>-</td><td>-</td><td>46.9</td></tr> <tr><td>10800</td><td>63</td><td>3.4</td><td>11.0</td><td>37.3</td><td>84.3</td><td>271</td><td>9.6</td><td>7.3</td><td>0.26</td><td>66</td><td>41</td><td>-</td><td>-</td><td>32.9</td></tr> <tr><td>12000</td><td>71</td><td>4.7</td><td>11.0</td><td>51.2</td><td>84.2</td><td>335</td><td>11.8</td><td>6.5</td><td>0.23</td><td>73</td><td>45</td><td>55</td><td>34</td><td>23.9</td></tr> <tr><td>13200</td><td>79</td><td>6.3</td><td>11.0</td><td>68.3</td><td>84.0</td><td>405</td><td>14.3</td><td>5.9</td><td>0.21</td><td>81</td><td>50</td><td>67</td><td>42</td><td>17.8</td></tr> <tr><td>14400</td><td>88</td><td>8.2</td><td>10.9</td><td>89.1</td><td>83.6</td><td>482</td><td>17.0</td><td>5.4</td><td>0.19</td><td>88</td><td>55</td><td>73</td><td>45</td><td>13.6</td></tr> <tr><td>15600</td><td>96</td><td>10.6</td><td>10.9</td><td>113.9</td><td>83.1</td><td>566</td><td>20.0</td><td>5.0</td><td>0.18</td><td>95</td><td>59</td><td>79</td><td>49</td><td>10.6</td></tr> <tr><td>16062</td><td>100</td><td>11.7</td><td>10.8</td><td>125.9</td><td>82.4</td><td>600</td><td>21.2</td><td>4.8</td><td>0.17</td><td>98</td><td>61</td><td>81</td><td>51</td><td>9.6</td></tr> </tbody> </table>									Propeller rpm	Throttle %	Current (DC) A	Voltage (DC) V	el. Power W	Efficiency %		Thrust g		Spec. Thrust g/W		Pitch Speed km/h		Speed (level) mph		Motor Run Time (85%) min	g	oz	oz/W	km/h	mph	km/h	mph	2400	13	0.1	11.1	0.8	45.9	13	0.5	17.8	0.63	15	9	-	-	1652.6	3600	20	0.2	11.1	1.8	64.0	30	1.1	16.6	0.58	22	14	-	-	682.1	4800	26	0.3	11.1	3.7	73.8	54	1.9	14.3	0.51	29	18	-	-	331.6	6000	33	0.6	11.1	6.8	79.0	84	3.0	12.3	0.43	37	23	-	-	181.6	7200	40	1.0	11.1	11.4	81.9	121	4.3	10.6	0.37	44	27	-	-	108.7	8400	48	1.6	11.1	17.7	83.4	164	5.8	9.3	0.33	51	32	-	-	69.6	9600	55	2.4	11.0	26.2	84.1	214	7.6	8.2	0.29	59	36	-	-	46.9	10800	63	3.4	11.0	37.3	84.3	271	9.6	7.3	0.26	66	41	-	-	32.9	12000	71	4.7	11.0	51.2	84.2	335	11.8	6.5	0.23	73	45	55	34	23.9	13200	79	6.3	11.0	68.3	84.0	405	14.3	5.9	0.21	81	50	67	42	17.8	14400	88	8.2	10.9	89.1	83.6	482	17.0	5.4	0.19	88	55	73	45	13.6	15600	96	10.6	10.9	113.9	83.1	566	20.0	5.0	0.18	95	59	79	49	10.6	16062	100	11.7	10.8	125.9	82.4	600	21.2	4.8	0.17	98	61	81	51	9.6
Propeller rpm	Throttle %	Current (DC) A	Voltage (DC) V	el. Power W	Efficiency %		Thrust g							Spec. Thrust g/W		Pitch Speed km/h		Speed (level) mph		Motor Run Time (85%) min																																																																																																																																																																																																														
					g	oz	oz/W	km/h	mph	km/h	mph																																																																																																																																																																																																																							
2400	13	0.1	11.1	0.8	45.9	13	0.5	17.8	0.63	15	9	-	-	1652.6																																																																																																																																																																																																																				
3600	20	0.2	11.1	1.8	64.0	30	1.1	16.6	0.58	22	14	-	-	682.1																																																																																																																																																																																																																				
4800	26	0.3	11.1	3.7	73.8	54	1.9	14.3	0.51	29	18	-	-	331.6																																																																																																																																																																																																																				
6000	33	0.6	11.1	6.8	79.0	84	3.0	12.3	0.43	37	23	-	-	181.6																																																																																																																																																																																																																				
7200	40	1.0	11.1	11.4	81.9	121	4.3	10.6	0.37	44	27	-	-	108.7																																																																																																																																																																																																																				
8400	48	1.6	11.1	17.7	83.4	164	5.8	9.3	0.33	51	32	-	-	69.6																																																																																																																																																																																																																				
9600	55	2.4	11.0	26.2	84.1	214	7.6	8.2	0.29	59	36	-	-	46.9																																																																																																																																																																																																																				
10800	63	3.4	11.0	37.3	84.3	271	9.6	7.3	0.26	66	41	-	-	32.9																																																																																																																																																																																																																				
12000	71	4.7	11.0	51.2	84.2	335	11.8	6.5	0.23	73	45	55	34	23.9																																																																																																																																																																																																																				
13200	79	6.3	11.0	68.3	84.0	405	14.3	5.9	0.21	81	50	67	42	17.8																																																																																																																																																																																																																				
14400	88	8.2	10.9	89.1	83.6	482	17.0	5.4	0.19	88	55	73	45	13.6																																																																																																																																																																																																																				
15600	96	10.6	10.9	113.9	83.1	566	20.0	5.0	0.18	95	59	79	49	10.6																																																																																																																																																																																																																				
16062	100	11.7	10.8	125.9	82.4	600	21.2	4.8	0.17	98	61	81	51	9.6																																																																																																																																																																																																																				

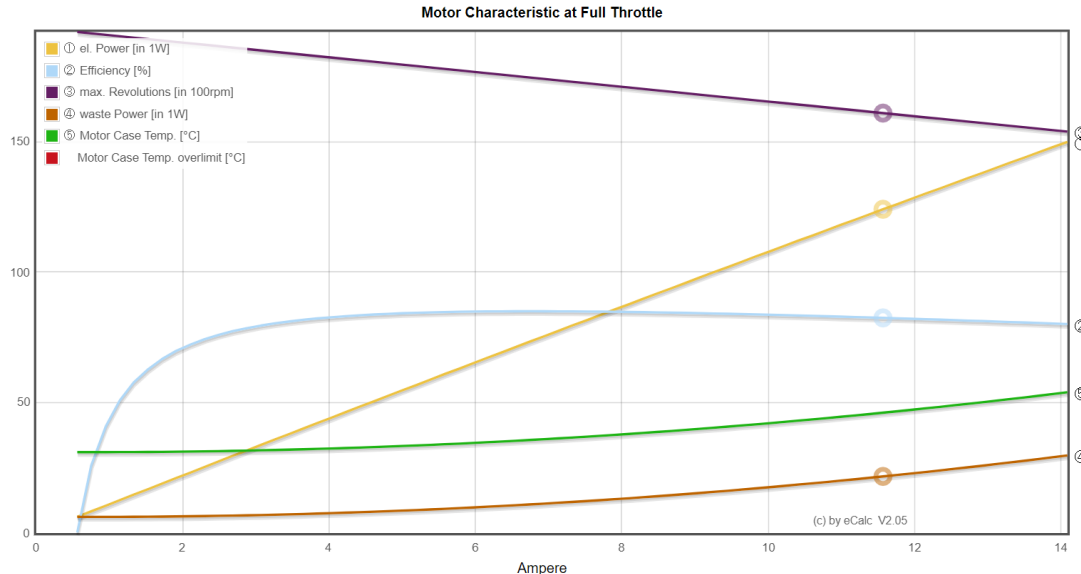


Figure (AJ): ecalc thrust data

A lot of different motors were considered during the iterative design process, and two different motors were tested. The first motor produced significantly less thrust than expected (Sunny Sky x2304-1480 V3) likely due to the low prop efficiency, and inability of the wires to carry the required current demand of the motor. As the test continued in the high current ranges of the speed controller the battery and wires warmed up creating more resistance and the static thrust decreased. To help resolve this issue a larger esc with a bigger gauge wire was selected. To help increase the thrust from the low propeller efficiency a higher KV motor was selected.

The selected motor for the final design of the aircraft was the Sunny Sky x2304-1800 V3. This motor had the exact same diameter and depth as the first motor but produced more thrust due to the higher KV value. This motor spun at an additional 320 RPM per volt compared to the original selected motor. To measure the thrust of the selected motor, the Hyperion 48mm Thrust Measuring Stand Tester was used. This is shown below in figure (AK). The collected thrust data was reported in table 26.



Figure (AK): Thrust testing setup

Propulsion Test Data		
Throttle %	Current (A)	Thrust (g)
0	0	0
10	N/A	8
20	0.21	25
30	0.52	58
40	1	110
50	1.73	172
60	3.21	226
70	4.65	280
80	6.32	334
90	11.4	378
100	11.4	378

Table 26: Thrust data

The collected thrust data was still significantly lower than what was suggested by the ecalc simulation. One potential reason this could be the case is the thrust stand was not properly calibrated. This thrust stand is old and was discontinued after a lot of reported inconsistent thrust data. Another potential reason the trust data was off was because the thrust stand was measuring static thrust not dynamic thrust. Small propeller diameters have a significantly smaller static thrust than dynamic thrust. Additionally higher pitched propellers have a higher dynamic thrust then static thrust. With this in mind the selected motor was deemed adequate for the aircraft. With an estimated stall speed of 29 miles per hour the motor was run at 8.2 amps (predicted speed of 40 MPH) with all other electronics connected and lasted 9 minutes and 50 seconds with 15% capacity remaining for reserve.

7.4. Spring Testing

Since the main wings of the aircraft folded backward when being stored in the rocket, it was important to know if the spring force would be sufficient to keep the wings out during flight. Using xflr5 the main wing could be isolated and the force of drag over just that part could be calculated. The drag force in newtons over the entire main wing in newtons is shown in figure (AL) below. This force was plotted against the coefficient of moment so at steady level flight when the coefficient of moment is zero the drag could be determined. This value was found to be 1.118 newtons.

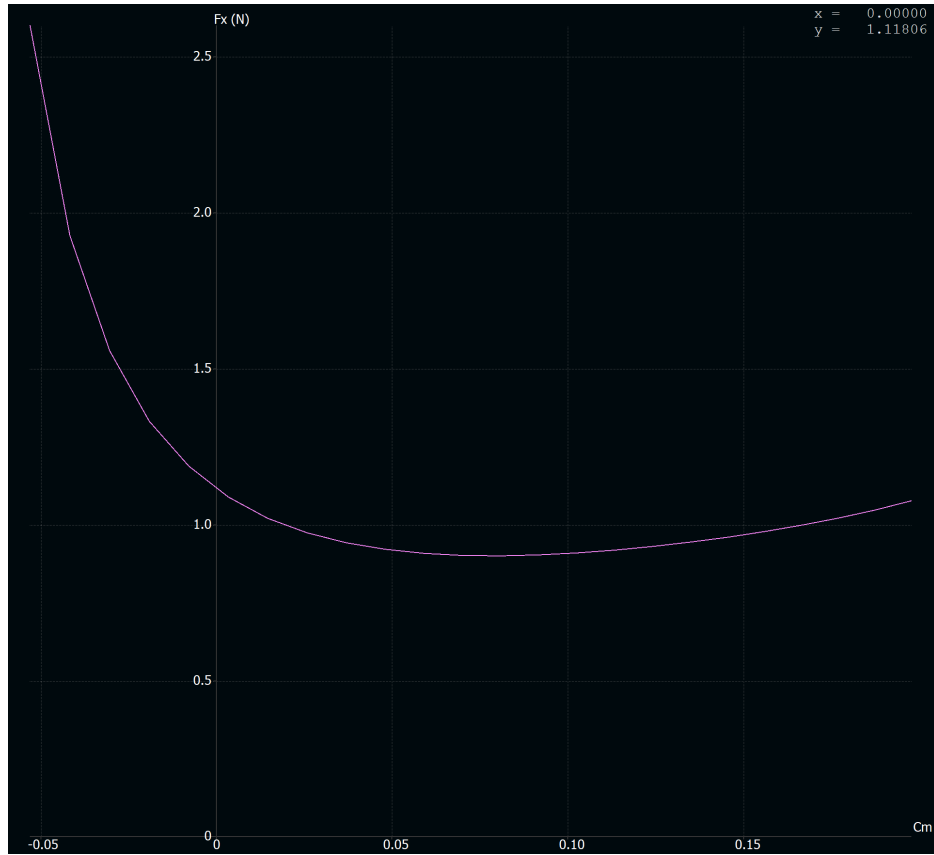


Figure (AL): Main wing drag force vs coefficient of moment

By dividing this force by 2 we are able to find the equivalent point force applied at the center of one wing which is approximately 27 inches long. Multiplying these numbers together we can find the moment of each wing in steady level flight. In the equation below the half wingspan is converted to meters from inches to get the units of newton-meters.

$$\frac{1.118 \text{ Newton}}{2} * \frac{27 \text{ Inch}}{2} * \frac{1 \text{ Meter}}{39.37 \text{ Inch}} = 0.19168 \text{ newton - meters}$$

The moment arm between the spring and the fuselage was designed to be 1.5 inch or 0.0254 inches. This meant the required force to keep the wings out would need to be 4.7188 newtons or higher.

To find how long the spring needed to be stretched to get this force, weights were hung from the spring and the deflection was measured. In figure (AM) below 510 grams of weight were applied to the spring and a deflection of 1.5 inches was measured. Mass was converted to newtons and length was converted to meters so the spring constant k could be found.

$$k = (510 \text{ grams} * \frac{0.0098 \text{ newtons}}{\text{gram}}) / (1.5 \text{ inches} * \frac{0.0254 \text{ meters}}{\text{inch}}) = 131.1811 \text{ newton/meter}$$



This resulted in a spring constant of 131.1811 newtons per meter. With the known force and spring constant, the required deflection to keep the wings out could be calculated.

$$\Delta x = \frac{4.7188}{131.1811} = 0.03835 \text{ meters} = 1.416 \text{ inches}$$



Figure (AM): Spring testing

With this information the wings could be designed with the required spring deflection of 1.416 inches to keep the wings open during steady level flight. The spring used was also tested to find its plastic deformation and the team found it became permanently deformed after stretching from 3.5 to 7.5 inches.

7.5. Structural Testing

To help with the material selection process, multiple material tests were attempted. The tailboom of the aircraft was constructed out of a square carbon fiber spar. After fixing one end to a table weights were applied until significant deformation occurred. Figure (AN) below shows this test taking place. In the first test it was discovered significant deflection occurred after applying 240g at the end of the spar. The results showed a redesign of the tail would need to be made as the tail components weighed over 120g and the airflow going over the control surfaces would cause deformation. A material yield strength test was attempted to determine the

maximum stress the material could endure before becoming permanently deformed. After applying over 1.4 kg of weight, the spar sprung back to its original shape and the team decided no additional testing was required in this area.

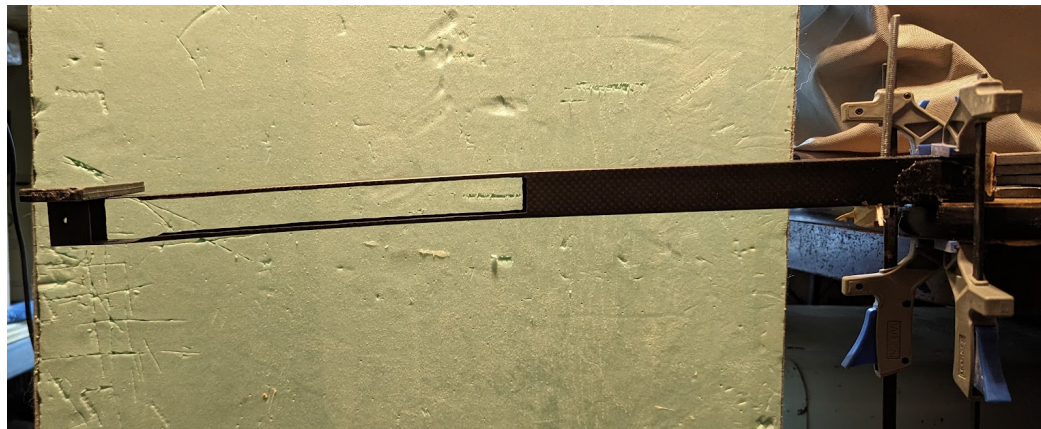


Figure (AN): Carbon fiber spar testing

Similar tests were performed for 3-D printed components of the aircraft and the results from test to test were so inconsistent no meaningful material property data could be deduced. Parts were redesigned and reprinted when it was determined they could not withstand the forces they would experience in flight.

Being too expensive to run further material tests, no additional analysis was conducted. Since the carbon fiber manufacturer had no material properties for their spars a full structural analysis of the aircraft could not be completed. Tests were also done on the basswood and balsa wood components of the aircraft. These parts were so small any deformities in the wood caused significant deviation from published material property tables, thus no structural analysis was done on those parts either.

7.6. Video Transmission Testing

The video system was tested in an open field. The video signal transmitted half a mile before the transmitter was no longer in line of sight and went behind a building. The signal instantly dropped off and this was to be expected because RF signals will not pass through objects. The field of view of the camera can be found in figure (AO) below.



Figure (AO): Camera field of view

7.7. Arduino Testing

The purpose of this section is to describe the testing procedures and results for the Arduino-based data gathering system integrated into the Rocket Launched Aircraft. This system is critical for collecting in-flight data, including acceleration, atmospheric pressure, temperature, and altitude, which are essential for evaluating the aircraft's performance and validating its design.

Testing Setup

The Arduino testing involved using an Arduino Nano, coupled with various sensors like the Adafruit LIS3DH (a 3-axis accelerometer), the Adafruit MPL3115A2 (a pressure and temperature sensor), and a MicroSD Card Breakout Board for data storage. These components

were connected as per the circuit diagram provided in figure AE, ensuring proper communication and power supply.

Procedure

Sensor Calibration: Before the actual flight tests, each sensor was calibrated individually in a controlled environment to ensure accuracy. The accelerometer was calibrated for its sensitivity to detect even minor changes in acceleration, and the pressure sensor was tested against known atmospheric conditions.

Data Logging: A crucial aspect of the testing was to verify the data logging functionality. This involved running the Arduino code (as detailed in Appendix F) to collect data from the sensors and store it on the MicroSD card at regular intervals.

Integration Testing: The Arduino setup was then integrated with the aircraft. This involved ensuring that the sensors and the Arduino Nano were securely mounted within the aircraft, and that they didn't interfere with the aircraft's balance or aerodynamics.

Ground Testing: Preliminary tests were conducted on the ground. These tests included powering up the Arduino system, initiating the data logging code, and then manually moving the aircraft to simulate various flight conditions, such as tilting and shaking, to record the sensor responses.

Flight Testing: The final phase of Arduino testing will be conducted during the flight testing that is outlined below.

Challenges and Resolutions

A key challenge was enhancing the resolution of data readings. This issue was addressed by identifying and resolving bugs in the data logging code, which improved the accuracy and reliability of the data collected.

Another issue of having the sensors store the acquired data at the necessary speed required to have good readings during the small flight time of the launch was another challenge. This was resolved by allowing the file storage to not be opened and closed in between readings. This increased the risk of data loss but allowed the frequency of reading to be increased.

Conclusion

The Arduino-based data gathering system is anticipated to be an effective tool for capturing critical flight data. The testing process emphasizes the importance of rigorous calibration, integration, and real-time data logging in dynamic flight conditions. The data



gathered will be crucial for assessing the aircraft's performance and informing future design improvements.

7.8. Flight Testing

Flight testing of the aircraft was planned to take place before thanksgiving break however the carbon fiber spar for the tail was on backorder and did not ship until after thanksgiving. Without time to fly prior to the presentation, a new flight test was scheduled over christmas break with the help of a nationally ranked pilot.

Results

Using the MATLAB code in Appendix G, we were able to calculate an ejection velocity of 1.5761 m/s with an ejection max acceleration of 31.0236 m/s² which results in the glider experiencing a maximum force of 3.1808 g's. Graphs of these results can be seen in figure (AP) below. We believe that our glider should be able to survive this force being maintained for less than a tenth of a second and the maximum velocity being much lower than the plane's flight speed. Due to all of this, we believe this to be a successful designed mechanism to eject our glider from the rocket body.

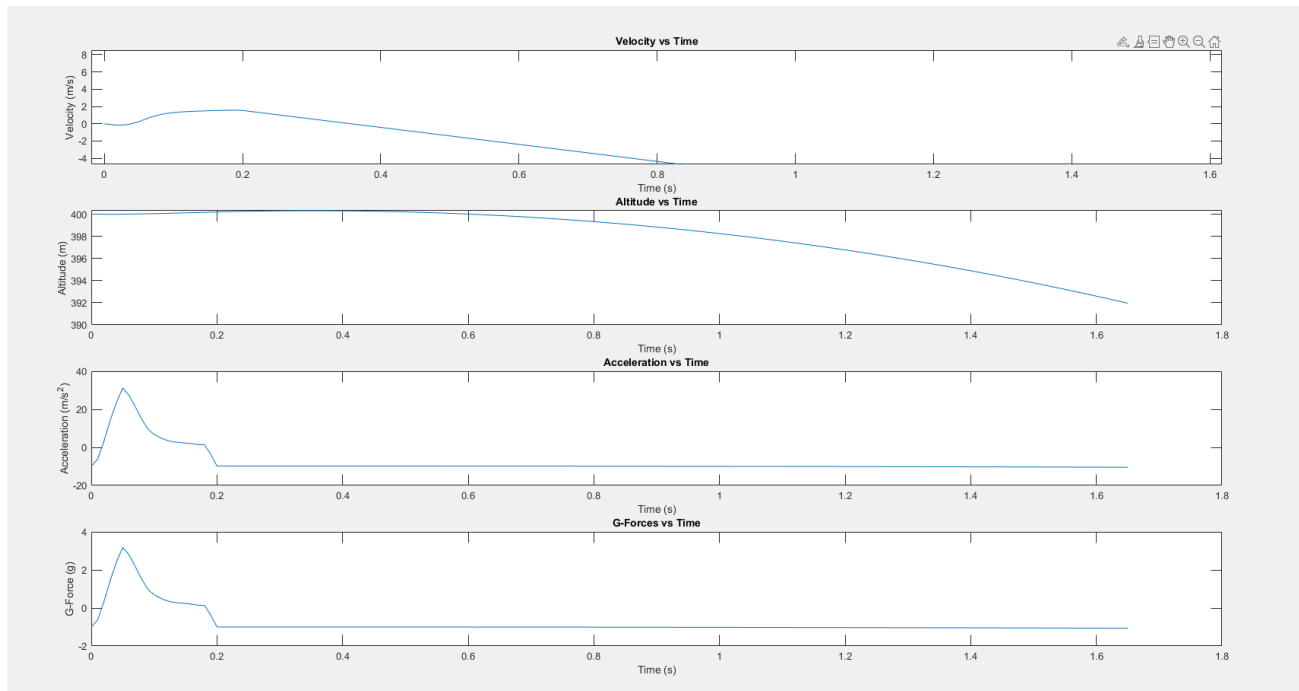


Figure (AP)

Conclusions

Although it is theoretically possible to put a remote controlled aircraft inside a rocket there is no practical recreational application. With an expected g load of 4.56 on ejection, the aircraft would likely not survive the deployment phase. In addition to that this project was not economically efficient. It would be more cost effective to go to the location of interest and launch a typical quadcopter. A lot of barriers were encountered in this project such as rocket motors being out of stock for months. To use this design to its full potential multiple licenses would need to be obtained such as a level 2 rocket license and a part 107 remote pilot license.

There are plans to launch the rocket in the future as soon as motors become available. Graduate students from Michigan State University and undergrad students from Marshall University have reached out to the team to help continue the development of the project. The Students at Michigan State want to further optimize the glider's design and increase its structural rigidity so it can undergo larger forces without breaking up. The students at Marshall University want to optimize the gliders data gathering devices for environmental data collecting at high altitudes. By using an aircraft launched from a rocket, high altitudes can quickly be achieved allowing more time for data gathering before the battery is depleted.



References

- [1] Anderson, J. D. (1999). *Aircraft Performance and Design*.
- [2] Etkin, B., & Reid, L. D. (1996). *Dynamics of Flight Stability and Control* (3rd ed.).
- [3] Raymer, D. P. (1992). *Aircraft design: A conceptual approach*.
- [4] *Recreational Flyers & community-based organizations*. Recreational Flyers & Community-Based Organizations | Federal Aviation Administration. (n.d.).
https://www.faa.gov/uas/recreational_flyers
- [5] Rodriguez, D. L., & Sturdza, P. (2006, January 9). A rapid geometry engine for preliminary aircraft design - semantic scholar.
<https://www.semanticscholar.org/paper/A-Rapid-Geometry-Engine-for-Preliminary-Aircraft-Rodriguez-Sturdza/a1166d6854d64bef9241e0fb519db2ae52b8eb28>
- [6] *Spektrum DSMX technology: DSMX RC transmitters and receivers*. Spektrum. (n.d.).
<https://www.spektrumrc.com/spm-bs-dsmx.html#:~:text=Spektrum%20leads%20the%20way%20again,advanced%20spread%20spectrum%20RC%20technology>.



Appendix

Appendix A: MATLAB Code To Calculate Launch

```
%% Rocket Velocity Calculation with Changing Air Density, Altitude,
% Acceleration, and G-Force Graph
% Read thrust curve data from file
thrust_curve = readmatrix('K695R_Data.txt');
% Columns: [Thrust, Motor Mass (g), Time]
% Constants
g = 9.81; % Acceleration due to gravity (m/s^2)
pi = 3.14159265359; % Pi
Cd = 0.75; % Drag coefficient typical of model rockets
diameter_in = 6.25; % Diameter of nose cone (inches)
diameter_m = diameter_in / 39.37; % Diameter of nose cone (meters)
A = pi * (diameter_m / 2)^2; % Reference area (m^2)
initial_altitude = 238.963; % Launching altitude (meters)
total_rocket_weight = 4.5; % Total weight of the rocket (kg)
time_step = 0.01; % Time step for simulation (seconds)
% Extract data from thrust curve
thrust = thrust_curve(:, 1); % Thrust in Newtons
motor_mass_g = thrust_curve(:, 2); % Motor mass in grams
time_data = thrust_curve(:, 3); % Time in seconds
% Convert motor mass to kilograms
motor_mass = motor_mass_g / 1000; % Convert grams to kilograms
% Initialize arrays
time = 0:time_step:time_data(end); % Extend time array
velocity = zeros(size(time));
altitude = zeros(size(time));
acceleration = zeros(size(time));
g_force = zeros(size(time)); % Array for G-force
altitude(1) = initial_altitude; % Initial altitude
% Loop to calculate velocity, altitude, and G-force
i = 1;
while i <= length(time)
    if i <= length(time_data)
        current_thrust = thrust(i);
        current_mass = total_rocket_weight - (motor_mass(i) - motor_mass(1));
    else
        current_thrust = 0; % No thrust after burnout
        current_mass = total_rocket_weight - (motor_mass(end) -
motor_mass(1));
    end
    % Calculate air density based on altitude (basic exponential model)
    rho = 1.225 * exp(-altitude(i) / 8500); % Scale height approximation
    % Calculate drag force
```

```

F_drag = 0.5 * rho * velocity(i)^2 * Cd * A;

% Update net force
net_force = current_thrust - current_mass * g - F_drag;

% Calculate acceleration
acceleration(i) = net_force / current_mass;
% Calculate G-force
g_force(i) = acceleration(i) / g;
% Update velocity and altitude for next step
if i < length(time)
    velocity(i+1) = velocity(i) + acceleration(i) * time_step;
    altitude(i+1) = altitude(i) + velocity(i+1) * time_step;
end
i = i + 1;
end

% Trim arrays to actual size
time = time(1:i-1);
velocity = velocity(1:i-1);
altitude = altitude(1:i-1);
acceleration = acceleration(1:i-1);
g_force = g_force(1:i-1);

% Calculate maximum altitude
max_altitude = max(altitude);
% Display maximum altitude
disp(['Maximum Altitude Achieved: ', num2str(max_altitude), ' meters']);
% Calculate maximum G-Force
max_g_force = max(g_force);
% Display maximum G-Force
disp(['Maximum G-Force Experienced: ', num2str(max_g_force)]);
% Plotting the results
figure;
subplot(4,1,1);
plot(time, velocity);
title('Velocity vs Time');
xlabel('Time (s)');
ylabel('Velocity (m/s)');
subplot(4,1,2);
plot(time, altitude);
title('Altitude vs Time');
xlabel('Time (s)');
ylabel('Altitude (m)');
subplot(4,1,3);
plot(time, acceleration);
title('Acceleration vs Time');
xlabel('Time (s)');

```

```
ylabel('Acceleration (m/s^2)');
subplot(4,1,4);
plot(time, g_force);
title('G-Forces vs Time');
xlabel('Time (s)');
ylabel('G-Force (g)');
```



WESTERN MICHIGAN UNIVERSITY

Appendix B: Aircraft Assembly Photos







Appendix C: Aircraft Stability Derivatives With Rudder Deflection of 3 Degrees

Rotating the flap by 3.00°, total angle is 3.00°

Creating the unit RHS vectors...

Creating the influence matrix...

Performing LU Matrix decomposition...

Solving the LU system...

Time for linear system solve: 0.216 s

Searching for zero-moment angle... Alpha=2.34253°

Creating source strengths...

Calculating doublet strength...

Calculating speed to balance the weight... V_{Inf} = 17.30496 m/s

Phi = 60.00° Turn radius = 17.62 Turn rate = 0.98 Roll rate = 0.00

Pitch rate = 0.85 Yaw rate = 0.49

Inertia - Stability Axis - CoG Origin

I_{xx}= 0.1364

I_{yy}= 0.186

I_{zz}= 0.05263

I_{xz}= 0.009451

Calculating the stability derivatives

Creating the RHS translation vectors

LU solving for RHS - longitudinal

Calculating forces and derivatives - lateral

Creating the RHS rotation vectors

LU solving for RHS - lateral

Calculating forces and derivatives - lateral

Calculating the control derivatives

Longitudinal derivatives

X_u= -0.020503 C_{xu}= -0.011478

X_w= 0.53814 C_{xa}= 0.30126

Z_u= -1.5906 C_{zu}= -0.00027498

Z_w= -10.222 C_{La}= 5.7225

Z_q= -0.94546 C_{Lq}= 8.5138

M_u= 6.5219e-09 C_{mu}= 2.9365e-08

M_w= -0.12848 C_{ma}= -0.57849

M_q= -0.27426 C_{mq}= -19.864

Neutral Point position= 0.08338 m



Lateral derivatives

Yv= -0.33045	CYb= -0.18499
Yp= -0.036453	CYp= -0.029757
Yr= 0.15442	CYr= 0.12606
Lv= -0.057655	Clb= -0.023532
Lp= -1.0261	Clp= -0.61068
Lr= 0.19041	Clr= 0.11332
Nv= 0.12331	Cnb= 0.050329
Np= -0.11466	Cnp= -0.068241
Nr= -0.057093	Cnr= -0.033979

Control derivatives

Xde= -0.12529	CXde= -0.0040532
Yde= 4.3264	CYde= 0.13996
Zde= 0.10047	CZde= 0.0032503
Lde= -0.0090614	CLde= -0.00021372
Mde= 0.017286	CMde= 0.0044976
Nde= -1.8224	CNde= -0.042983

State matrices

Longitudinal state matrix

-0.0146189	0.383701	0	-9.81
-1.13413	-7.28844	16.6308	0
3.50639e-08	-0.690763	-1.47454	0
0	0	1	0

Lateral state matrix

-0.235616	-0.0259916	-17.1949	9.81
-0.263692	-7.77214	1.33774	0
2.29549	-3.57423	-0.844544	0
0	1	0	0

Control Matrices

Longitudinal control matrix

-0.0893343
0.07163689
0.09293652
0

Lateral control matrix

3.084764
 -2.497312
 -35.07372
 0

Longitudinal modes

Eigenvalue:	-4.431+	-1.893i		-4.431+	1.893i		0.04235+	-0.5738i	
	0.04235+	0.5738i							

Eigenvector:	1+	0i		1+	0i		1+	0i		1+	0i
	-4.292+	-5.441i		-4.292+	5.441i		-0.07973+	0.01104i			
	-0.07973+	-0.01104i									
	-1.289+	-0.4463i		-1.289+	0.4463i		0.03343+	0.007617i			
	0.03343+	-0.007617i									
	0.2823+	-0.01988i		0.2823+	0.01988i		-0.008926+	0.05892i			
	-0.008926+	-0.05892i									

Lateral modes

Eigenvalue:	-7.63+	0i		-0.6533+	-6.572i		-0.6533+	6.572i	
	0.08395+	0i							

Eigenvector:	1+	0i		1+	0i		1+	0i		1+	0i
	1.274+	0i		-0.05302+	0.02198i		-0.05302+	-0.02198i		0.234+	
	0i										
	0.3328+	0i		0.02294+	0.3774i		0.02294+	-0.3774i		1.571+	
	0i										
	-0.167+	0i		-0.002517+-0.008318i			-0.002517+	0.008318i			
	2.788+	0i									

Calculating aerodynamic coefficients in the far field plane

Calculating point 2.34°....



Computing On-Body Speeds...
Computing Plane for alpha= 2.34°
Calculating aerodynamic coefficients...
Calculating wing...Main Wing
Calculating wing...Elevator
Calculating wing...Fin

Phillips formulae:

Phugoid eigenvalue: 0.04389+ 0.58123i
frequency: 0.093 Hz
damping: -0.076
Dutch-Roll eigenvalue: -0.72444+ 6.54644i
frequency: 1.048 Hz
damping: 0.111

_____Finished operating point calculation for control position 3.00_____



WESTERN MICHIGAN UNIVERSITY

Appendix D: Rocket Assembly



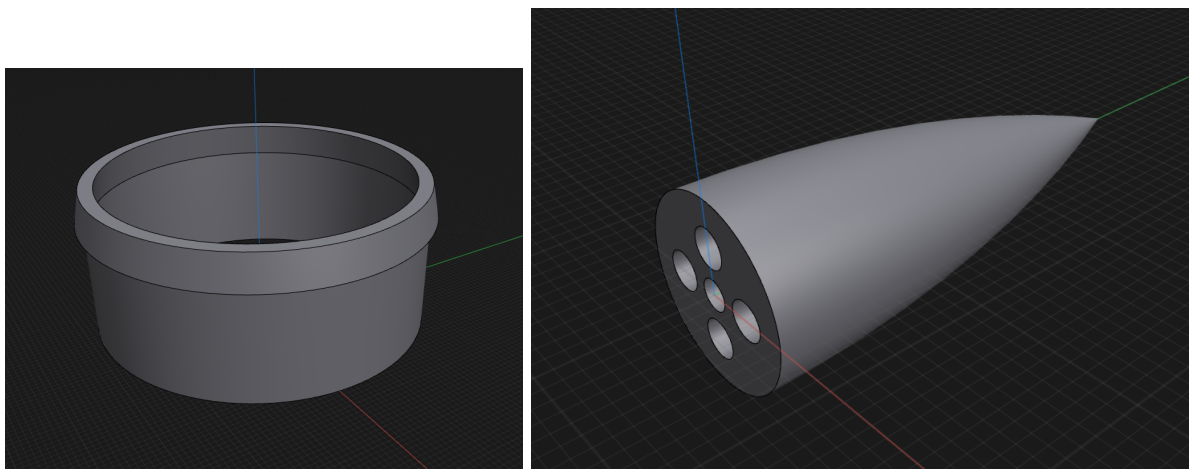
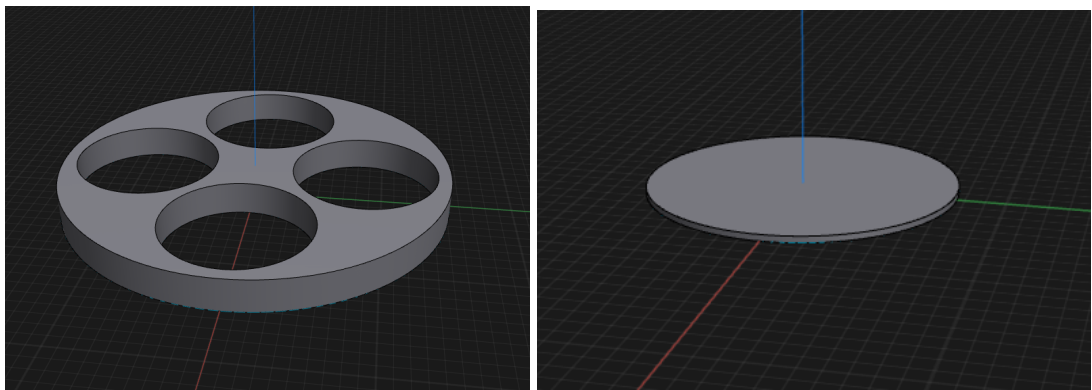




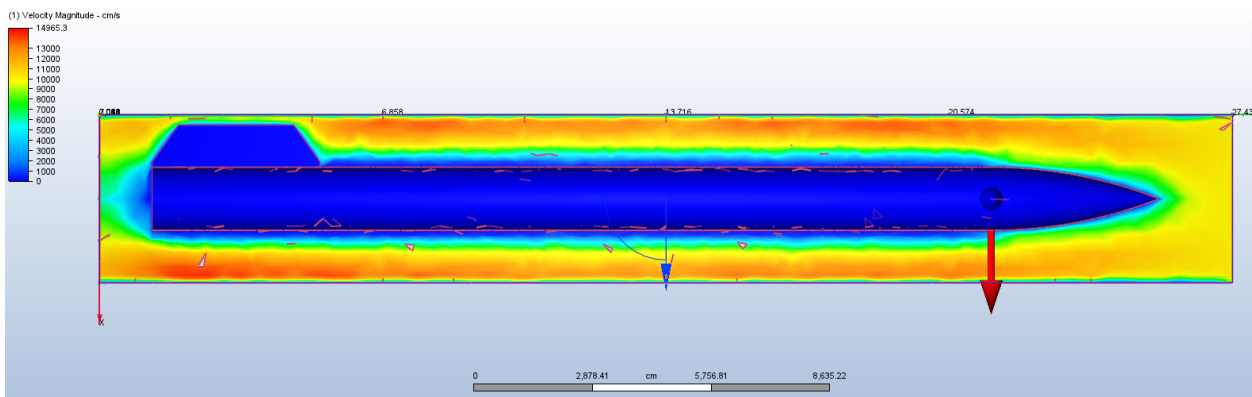
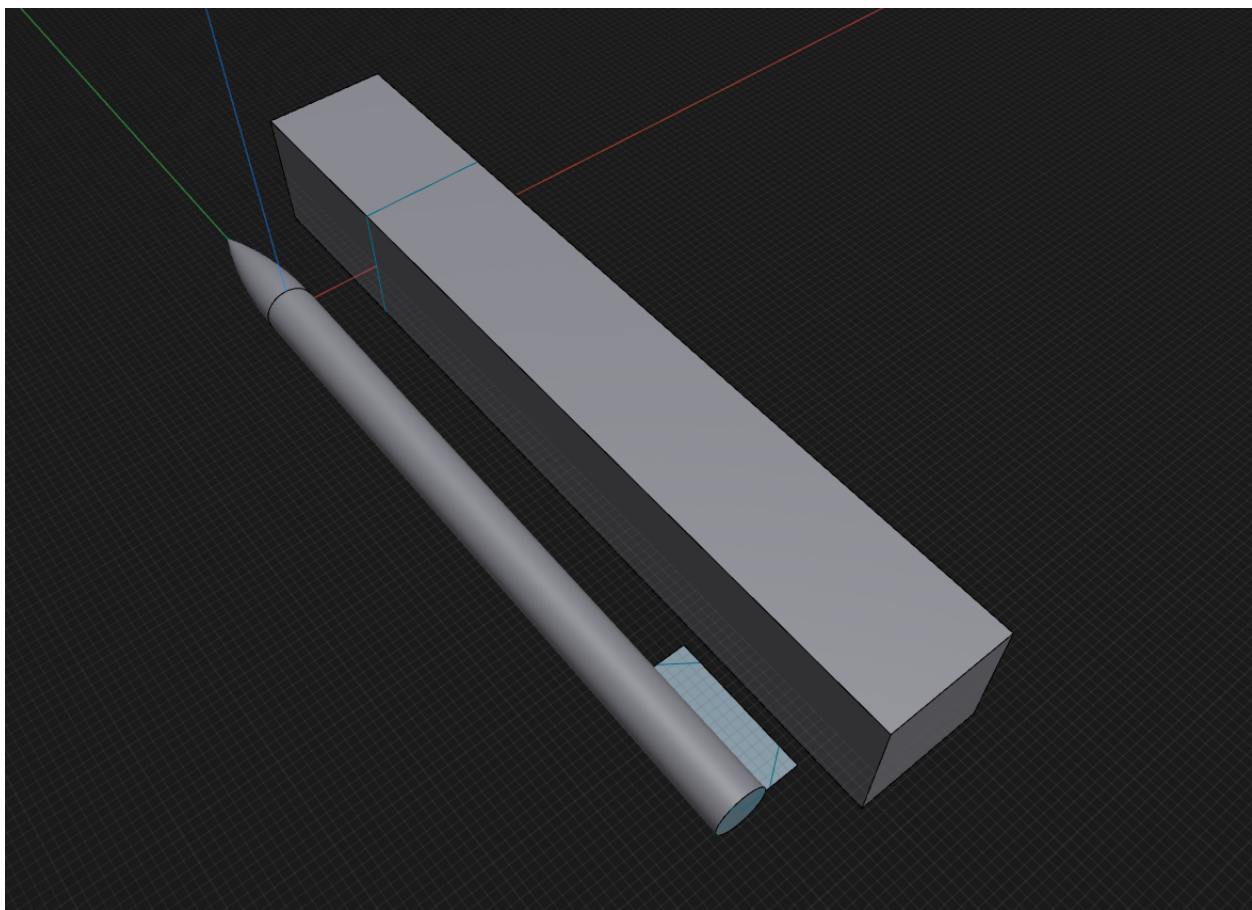


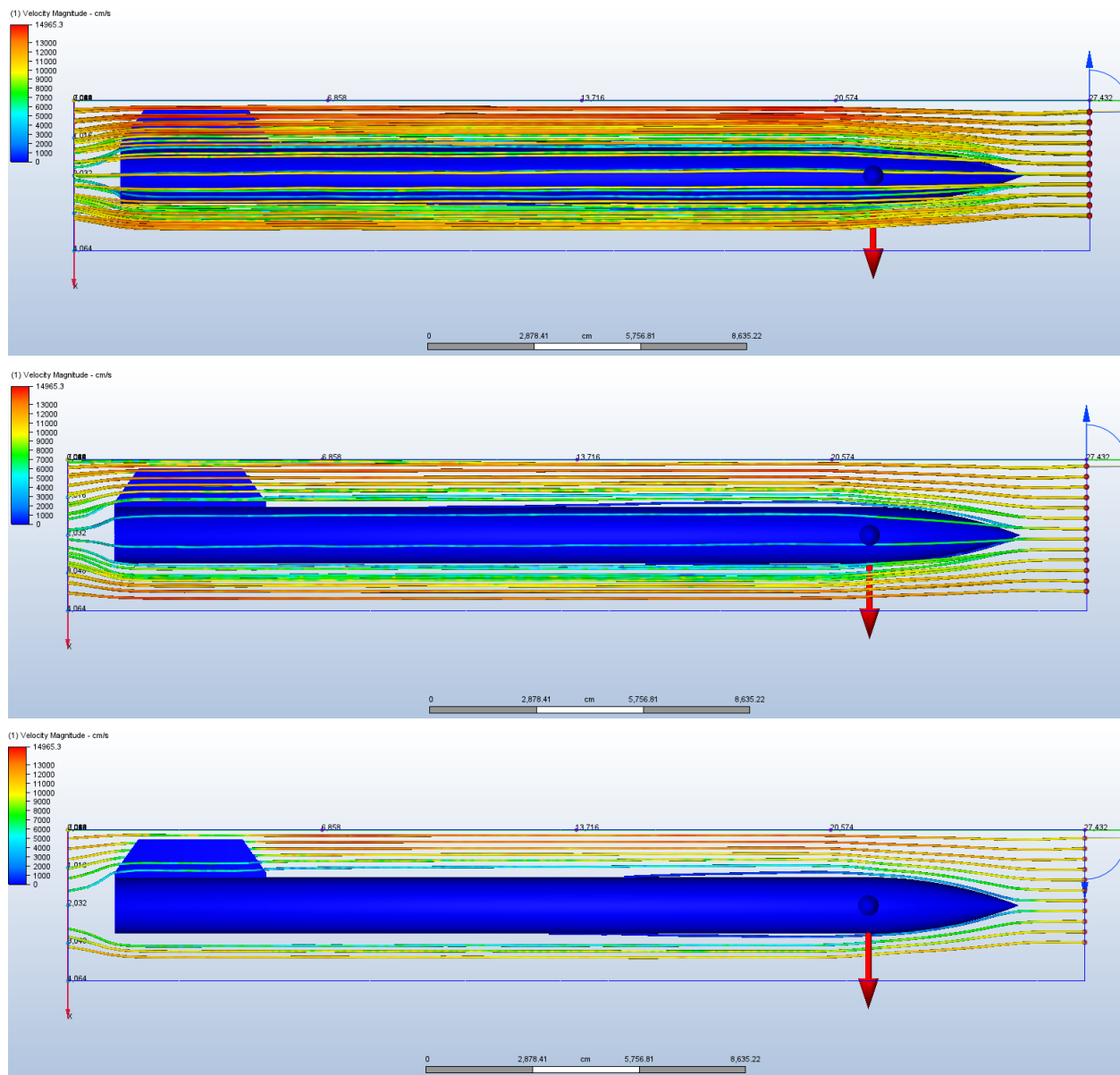
WESTERN MICHIGAN UNIVERSITY

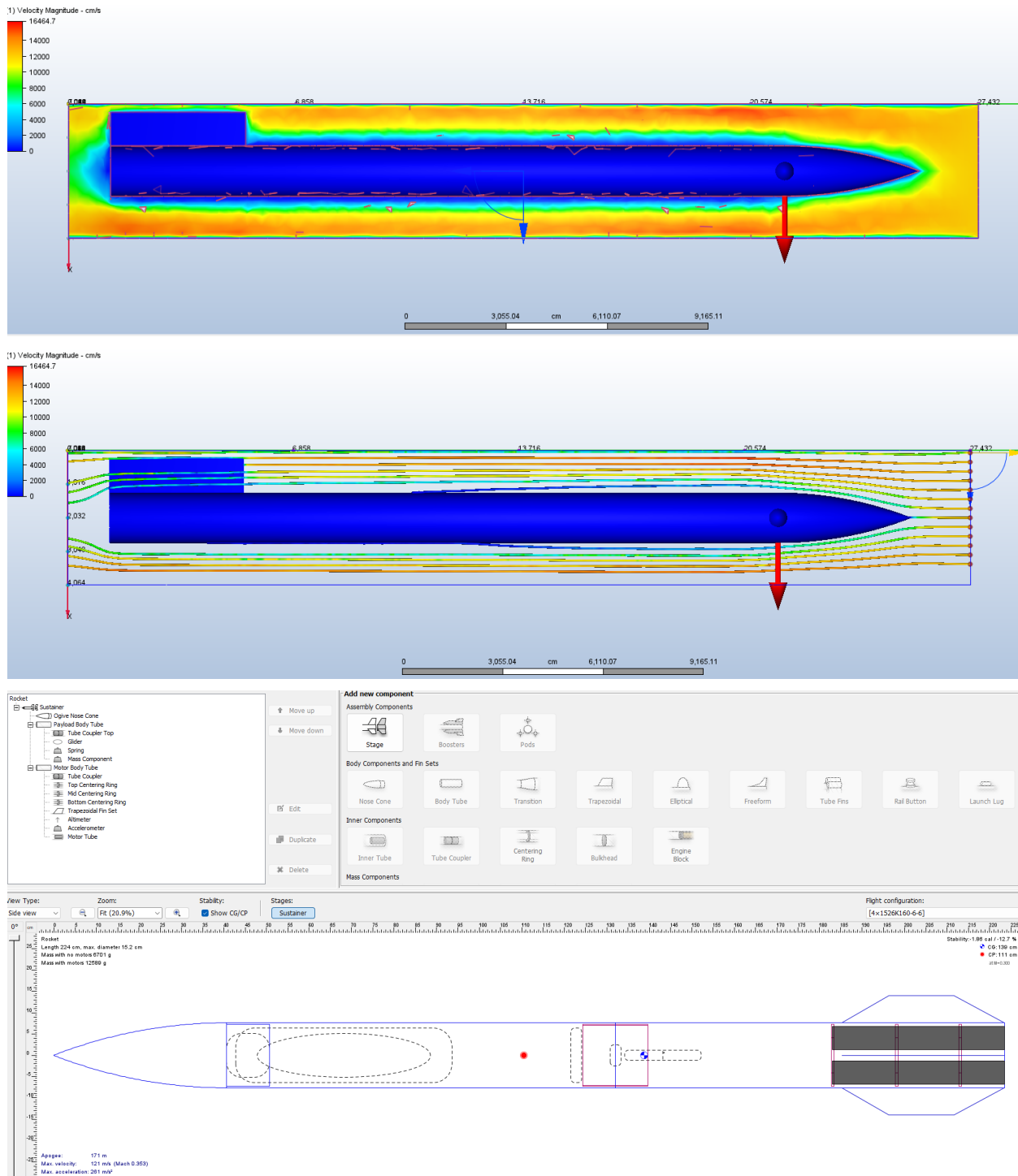




Appendix E: Openrocket Charts and CFD Images

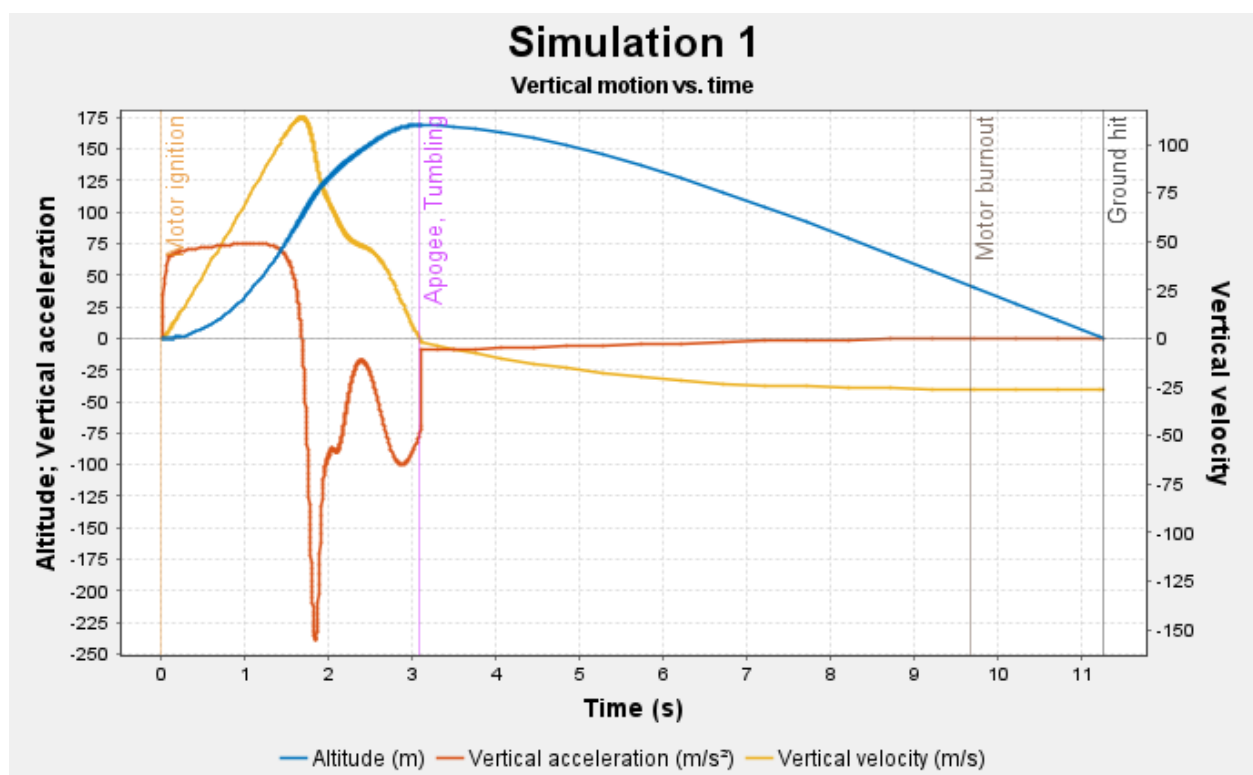






Simulation 1

Vertical motion vs. time



Appendix F: Data Gathering Arduino Code

```
#include <Wire.h>
#include <Adafruit_LIS3DH.h>
#include <Adafruit_Sensor.h>
#include <Adafruit_MPL3115A2.h>
#include <SD.h>

// Initialize sensors
Adafruit_LIS3DH lis = Adafruit_LIS3DH();
Adafruit_MPL3115A2 baro = Adafruit_MPL3115A2();

// Chip select pin for the SD card breakout board
const int chipSelect = 10;

File dataFile;

void setup(void) {
    Serial.begin(9600);

    // Initialize SD card
    if (!SD.begin(chipSelect)) {
        Serial.println("Card failed, or not present");
        // Don't do anything more if the SD isn't working
        while (1)
            ;
    }

    // Initialize LIS3DH
    if (!lis.begin(0x18)) {
        Serial.println("Could not start LIS3DH");
        while (1)
            ;
    }
    lis.setRange(LIS3DH_RANGE_16_G);

    // Initialize MPL3115A2
    if (!baro.begin()) {
```

```

    Serial.println("Could not start MPL3115A2");
    while (1)
        ;
    }
}

void loop() {
    // Read sensor data and store it in variables
    sensors_event_t event;
    lis.getEvent(&event);
    float pressure = baro.getPressure();
    float altitude = baro.getAltitude();
    float temperature = baro.getTemperature();

    // Open the file. note that only one file can be open at a time,
    // so you have to close this one before opening another.
    dataFile = SD.open("datalog.txt", FILE_WRITE);

    // If the file is available, write to it:
    if (dataFile) {
        dataFile.print(event.acceleration.x);
        dataFile.print(event.acceleration.y);
        dataFile.print(event.acceleration.z);
        dataFile.print(pressure);
        dataFile.print(altitude);
        dataFile.println(temperature);
        dataFile.close(); // close the file
    } else {
        // if the file isn't open, pop up an error:
        Serial.println("error opening datalog.txt");
    }

    //delay(1000); // Delay a second between readings.
}

```

Appendix G: MATLAB Code for Glider Ejection

```
%% Rocket Velocity Calculation with Changing Air Density, Altitude,
Acceleration, and G-Force Graph
% Read thrust curve data from file
thrust_curve = readmatrix('D12_Data.txt');
% Columns: [Thrust, Motor Mass (g), Time]
% Constants
g = 9.81; % Acceleration due to gravity (m/s^2)
pi = 3.14159265359; % Pi
Cd = 0.75; % Drag coefficient typical of model rockets
diameter_in = 6.25; % Diameter of nose cone (inches)
diameter_m = diameter_in / 39.37; % Diameter of nose cone (meters)
A = pi * (diameter_m / 2)^2; % Reference area (m^2)
initial_altitude = 400; % Launching altitude (meters)
total_rocket_weight = 2.16078; % Total weight of the rocket (kg)
time_step = 0.01; % Time step for simulation (seconds)
% Extract data from thrust curve
thrust = 3*thrust_curve(:, 1); % Thrust in Newtons
motor_mass_g = 3*thrust_curve(:, 2); % Motor mass in grams
time_data = thrust_curve(:, 3); % Time in seconds
% Convert motor mass to kilograms
motor_mass = motor_mass_g / 1000; % Convert grams to kilograms
% Initialize arrays
time = 0:time_step:time_data(end); % Extend time array
velocity = zeros(size(time));
altitude = zeros(size(time));
acceleration = zeros(size(time));
g_force = zeros(size(time)); % Array for G-force
altitude(1) = initial_altitude; % Initial altitude
% Loop to calculate velocity, altitude, and G-force
i = 1;
while i <= length(time)
    if i <= length(time_data)
        current_thrust = thrust(i);
        current_mass = total_rocket_weight - (motor_mass(i) - motor_mass(1));
    else
        current_thrust = 0; % No thrust after burnout
        current_mass = total_rocket_weight - (motor_mass(end) -
motor_mass(1));
    end
    % Calculate air density based on altitude (basic exponential model)
    rho = 1.225 * exp(-altitude(i) / 8500); % Scale height approximation
    % Calculate drag force
    F_drag = 0.5 * rho * velocity(i)^2 * Cd * A;
```

```

% Update net force
net_force = current_thrust - current_mass * g - F_drag;

% Calculate acceleration
acceleration(i) = net_force / current_mass;
% Calculate G-force
g_force(i) = acceleration(i) / g;
% Update velocity and altitude for next step
if i < length(time)
    velocity(i+1) = velocity(i) + acceleration(i) * time_step;
    altitude(i+1) = altitude(i) + velocity(i+1) * time_step;
end
i = i + 1;
end
% Trim arrays to actual size
time = time(1:i-1);
velocity = velocity(1:i-1);
altitude = altitude(1:i-1);
acceleration = acceleration(1:i-1);
g_force = g_force(1:i-1);
% Calculate maximum altitude
max_altitude = max(altitude);
% Display maximum altitude
disp(['Maximum Altitude Achieved: ', num2str(max_altitude), ' meters']);
% Calculate maximum G-Force
max_g_force = max(g_force);
% Display maximum G-Force
disp(['Maximum G-Force Experienced: ', num2str(max_g_force)]);
% Plotting the results
figure;
subplot(4,1,1);
plot(time, velocity);
title('Velocity vs Time');
xlabel('Time (s)');
ylabel('Velocity (m/s)');
subplot(4,1,2);
plot(time, altitude);
title('Altitude vs Time');
xlabel('Time (s)');
ylabel('Altitude (m)');
subplot(4,1,3);
plot(time, acceleration);
title('Acceleration vs Time');
xlabel('Time (s)');
ylabel('Acceleration (m/s^2)');
subplot(4,1,4);

```

```
plot(time, g_force);
title('G-Forces vs Time');
xlabel('Time (s)');
ylabel('G-Force (g)');
```

Appendix PUT HERE:Resumes



JACK FRIEDE

jackfriedle21@gmail.com | (989)600-4394 | Linwood, MI 48634

EDUCATION

Western Michigan University, Kalamazoo, MI
Bachelor of Science: Aerospace Engineering

EXPECTED IN 12/2023

- Minor: Mathematics
- Senior Project: Rocket Launched Glider, Project is on-going and will be completed by December of 2023
- Aerospace structural Design Project: Single Fuselage Cross-section Design, The goal was to design and test a fuselage cross-section for buckling and fractures when under a pin-point force and combined pressure load using Abaqus

PROFESSIONAL SUMMARY

Soon to be graduated with a Bachelor of Science majoring in Aerospace engineering. I am seeking a long-time career opportunity to gain knowledge on the engineering field to further my abilities as an engineer and increase my usefulness to the field. I have a wide range of technical skills gained from my college experience as well as mechanical skills gained from personal experiences.

SKILLS

- Technical Proficiency
- SolidWorks (CAD)
- Project Leadership
- AutoCAD
- Autodesk Inventor
- Data Entry
- MATLAB Knowledge
- Problem Solving
- Conflict Resolution
- C++ Programming
- Abaqus
- Time Management

PROFESSIONAL EXPERIENCE

Manager | St. Laurent Brothers - Bay City, MI

08/2015 - 12/2020

- Accomplished multiple tasks within established timeframes.
- Cross-trained existing employees to maximize team agility and performance.

Sign Maker | MitchArt - Midland, MI

05/2018 - 12/2018

- Set machines for engraving and laser etching of completed designs.
- Maintained clean and tidy shop space for maximum customer appeal, safety and organization.
- Created custom signs for customers with quality builds and careful installation

Sign Maker | Sign Center - Kalamazoo, MI

10/2017 - 10/2018

- Maintained clean and tidy shop space for maximum customer appeal, safety and organization.
- Set machines for engraving and laser etching of completed designs.
- Created custom signs for customers with quality builds and careful installation

Matthew Guscarr
Milford, MI 48381 | (248) 675 5248 | mattguscarr@gmail.com

Professional Summary

Reliable aerospace engineer seeking an entry level job to expand skills and gain valuable real-world experience. Proficient at leading and coordinating with others on group projects. Dedicated to working until all specifications are completed to the highest standards in a timely manner. Looking to continue my passion and interest for aerospace engineering as I have been flying unmanned aerial vehicles since I was 10.

Education

Bachelor of Applied Science: Aerospace Engineering GPA 3.45 Expected in December 2023

Western Michigan University – Kalamazoo, MI

ABET Accredited

Relevant Coursework Completed:

- Aerodynamics I & II
 - Flight Vehicle Performance
 - Propulsion I & II
 - Aircraft Design
 - Intro to Aerospace Engineering
 - Programming in C for Engineers

Work Experience

Western Michigan University – Kalamazoo, MI

08/2022 to 8/2023

Team Lead for Western Michigan's Design Build Fly Team

- Lead engineer in aircraft design and propulsion who is collaborating with electrical, mechanical, and computer engineer leads to design, build, and fly a RC plane for an international competition
 - Managing a team of 8 students with a budget of \$5000
 - Team supervisor in 2022 gaining valuable technical experiences
 - Competed in 2021-2022 AIAA DBF competition placing 18th out of 97
 - Competed in 2022-2023 AIAA DBF competition placing 77th out of 99

Senior Design Project

01/2023 to Present

- Design and manufacture a rocket launched glider capable of surveillance and data collection.

Ground Crew Worker

06/2021 to 9/2022

Huron Clinton Metroparks = Milford, MI

- Supervisor of waste management with exceptional communication and organizational skills
 - Safely operated heavy equipment

Delivery Helper

07/2020 to 06/2021

DGPP Inc - Lake Orion, MI

- Safely loaded items into delivery vehicle to minimize damage in transit
 - Submitted money received from deliveries at the end of each shift
 - Safely handled explosive and corrosive materials

Volunteer Work

- School Unmanned Aerial Vehicle Lab assistant

Skills

- Problem-solving
 - Critical thinking
 - Leadership
 - Teamwork
 - Communication
 - Organization
 - Project management
 - Experience with
 - MATLAB
 - C++
 - Siemens NX
 - AutoCAD
 - 3D printing
 - SOLIDWORKS